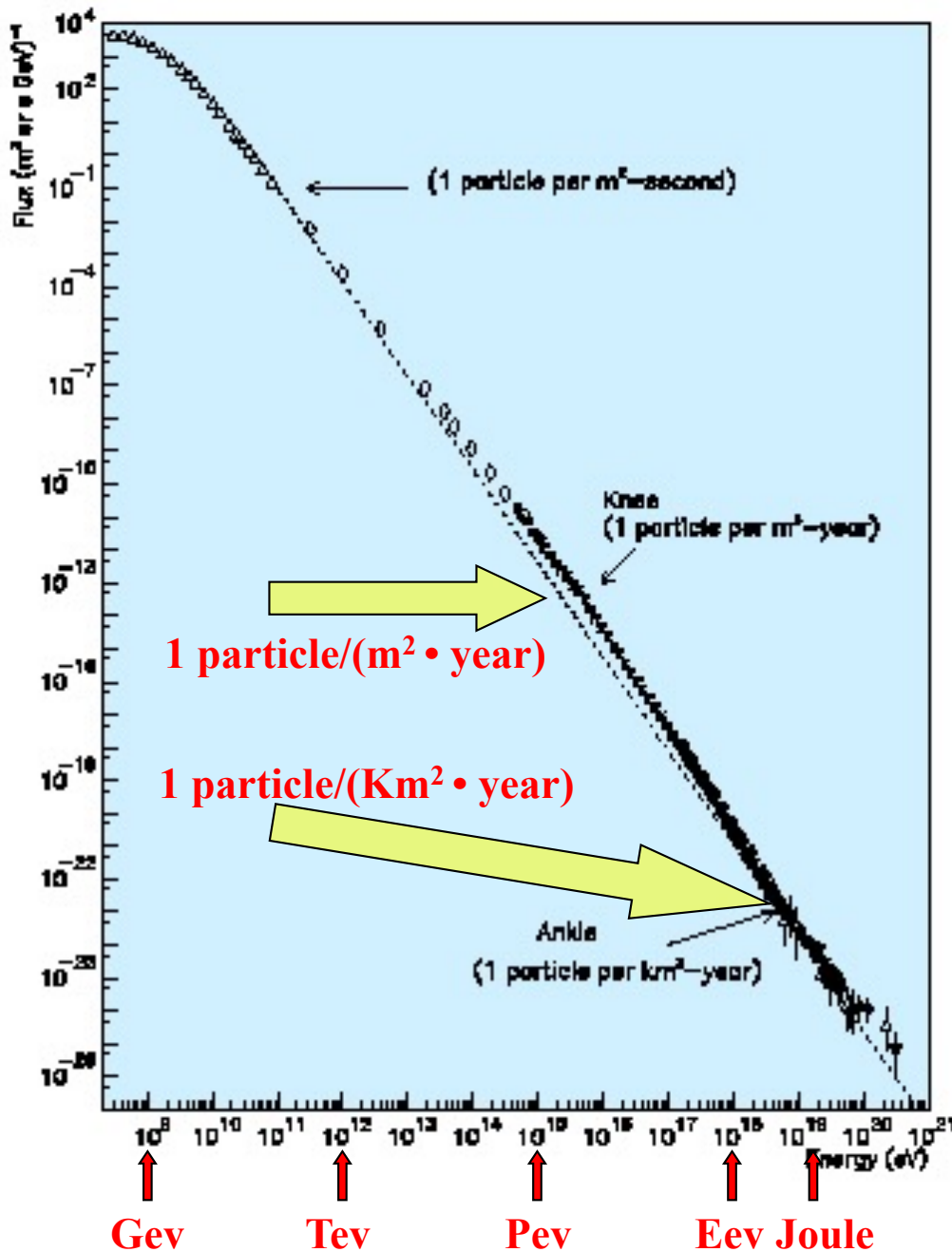


Lessons 9 and 10

- Detection at ground of extensive Air Showers: nature, direction and energy of the primary C.R.
- The KASCADE experiment
- Detection of U.H.E. Cosmic Rays ($E \gg 100$ PeV) (AGASA, ...)
- Detection of charged C.R. with energy $> 10^{17}$ eV
- The GZK expected cut-off
- Feature of UHE Cosmic Rays spectrum for $E > 10^{18}$ eV
- Measurements with hybrid detectors (HIRES, AUGER, Telescope Array)
- Spectrum and composition of C.R. with $E > 10^{17}$ eV
- The "chemical composition" of UHE C.R. as measured by hybrid detectors at ground
- Measurement of the CR anisotropy
- The role of the radio detection technique in the HiRes hybrid detector

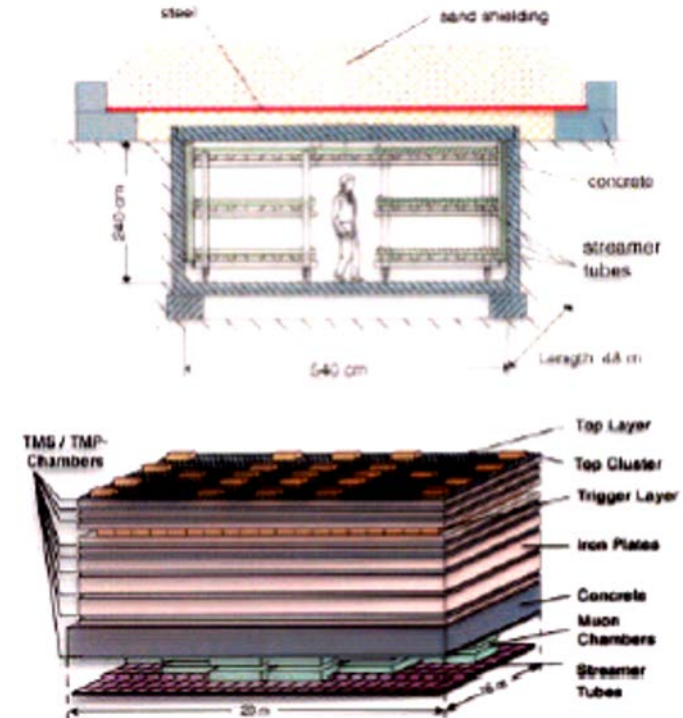
Detection of Very High Energy ($\sim 100\text{TeV}$) charged C.R.



The study of cosmic rays with $E \geq 100\text{TeV}$ requires:

- large equipment (scintillator apparatus, Cherenkov light, tracers, ...)
- on the earth's surface
- Studied the "results" of the interactions of the primary cosmic rays with the atmosphere
- From these measurements go back to E, direction, nature of the "primary"

As an example: the KASCADE detector for C.R.s



Atmospheric showers induced by charged C.R.

Atmospheric Thickness:

1035 g/cm²

≈ 11 λ_I (hadr. interact. lengths)

≈ 27 X₀ (radiation lengths)

Some basics...

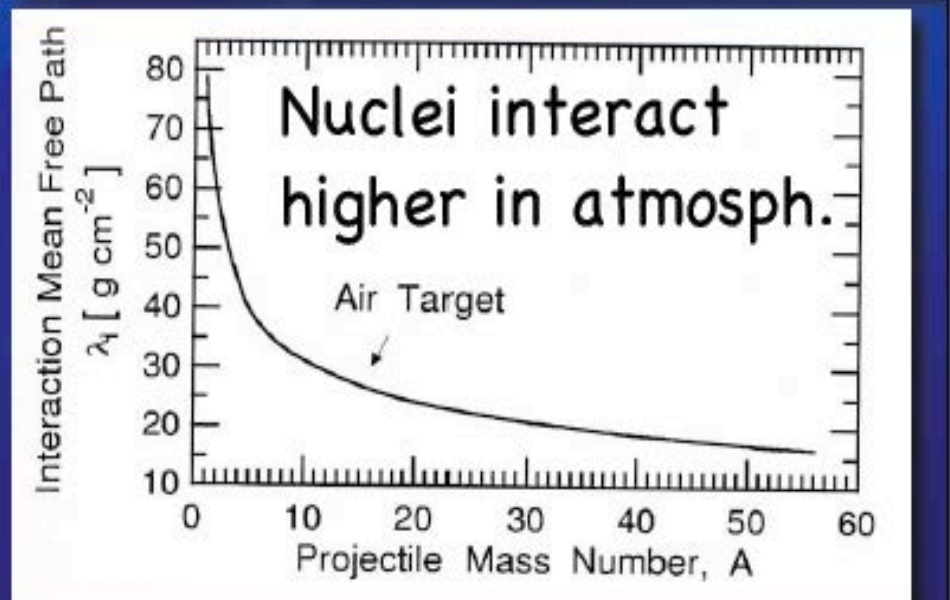
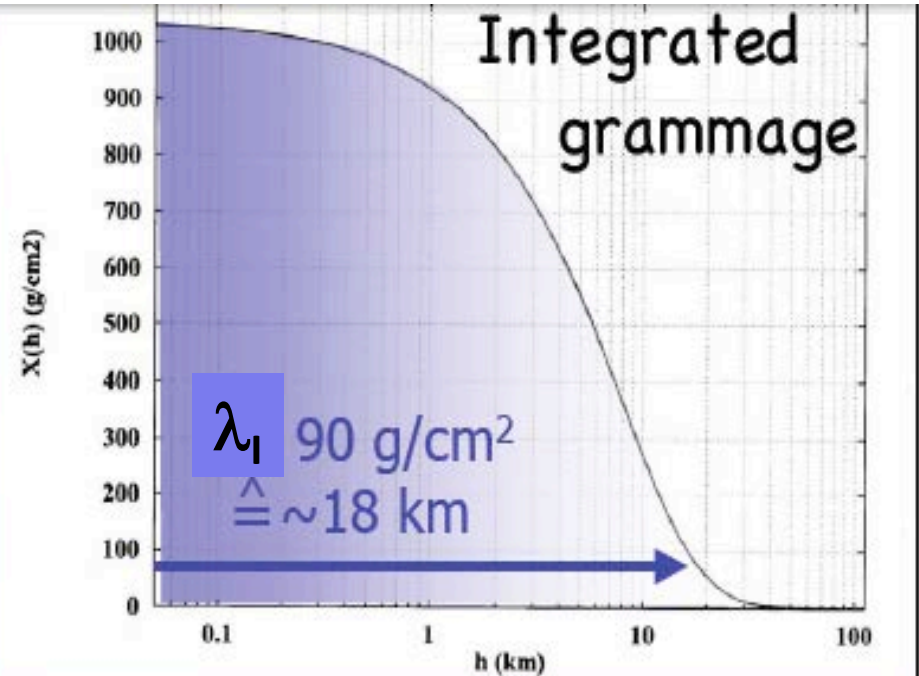
$$\lambda_I = \frac{1}{n \cdot \sigma} \cong 90 \text{ g/cm}^2 \text{ (p-Air)}$$

(n: density of absorber nuclei;
σ: total inelastic X-section)

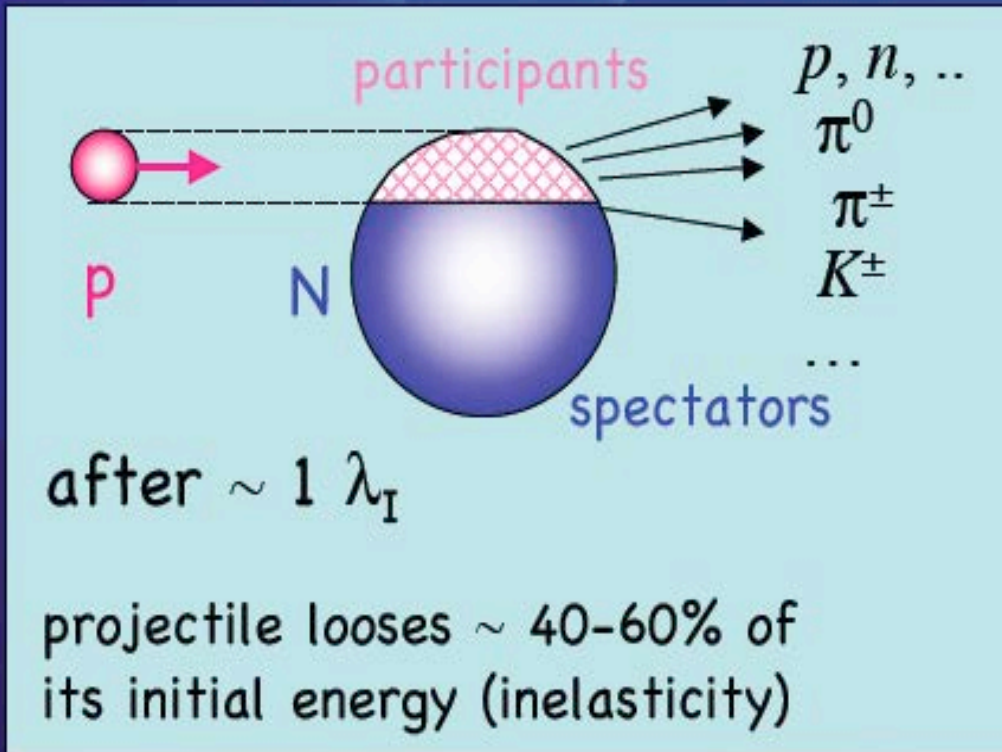
X₀ defined by energy loss of high-energy electrons in media:

$$\langle E_e \rangle \propto e^{-\frac{X}{X_0}}$$

In air: X₀ = 36.66 g/cm²



If the primary C.R. is a proton: p-air interaction



$$\pi^0 \rightarrow \gamma\gamma \quad (\tau_0 = 0.8 \cdot 10^{-16} \text{ s})$$

$$\pi^\pm \rightarrow \mu^\pm + \nu_\mu \quad (\tau_0 = 26 \text{ ns})$$

decay of π^\pm :

$$R_\pi = \gamma \cdot v \cdot \tau_0 \simeq \frac{E_\pi^{tot}}{m_0 c^2} \cdot c \cdot \tau_0$$

$\approx 7.8 \text{ m}$

e.g.: $E_\pi = 14 \text{ GeV} \rightarrow R_\pi = 780 \text{ m}$
 $\approx 1 \lambda_I$ at 5 km height

consequence:

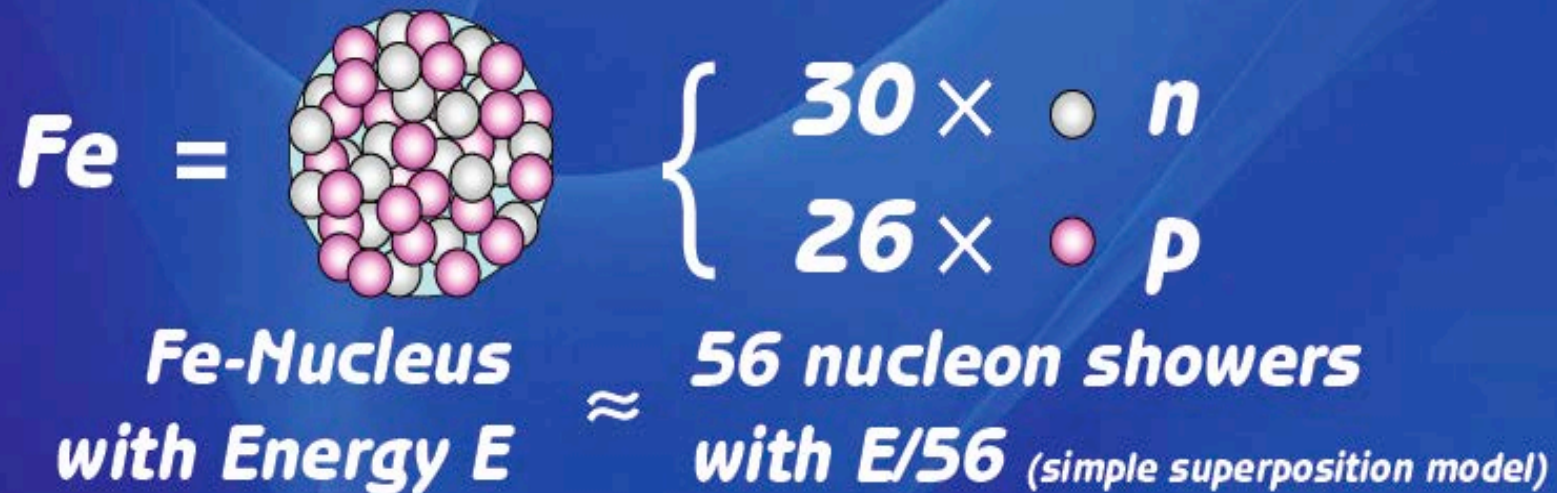
in early shower, the hadronic interaction of π^\pm is more probable than decay into μ and vice versa in late showers

Consequences:

pions are the most abundant hadrons in showers;

μ 's are integrative; decay into e^\pm of no relevance

p vs Fe induced EAS at the same total energy



Fe-Showers:

larger χ -section $\rightarrow \chi_{max}$ develops higher in atmosphere

\rightarrow fewer electrons at ground, flatter $\rho(r)$

56 nucleons with $E/56 \rightarrow$ lower energy secondaries (π, K, \dots)

\rightarrow probability of π, K -decay favoured over interaction

& $n_{\pi} \sim 56 \cdot \log(E/56)$

\rightarrow more muons at ground

& smaller fluctuations than p-showers

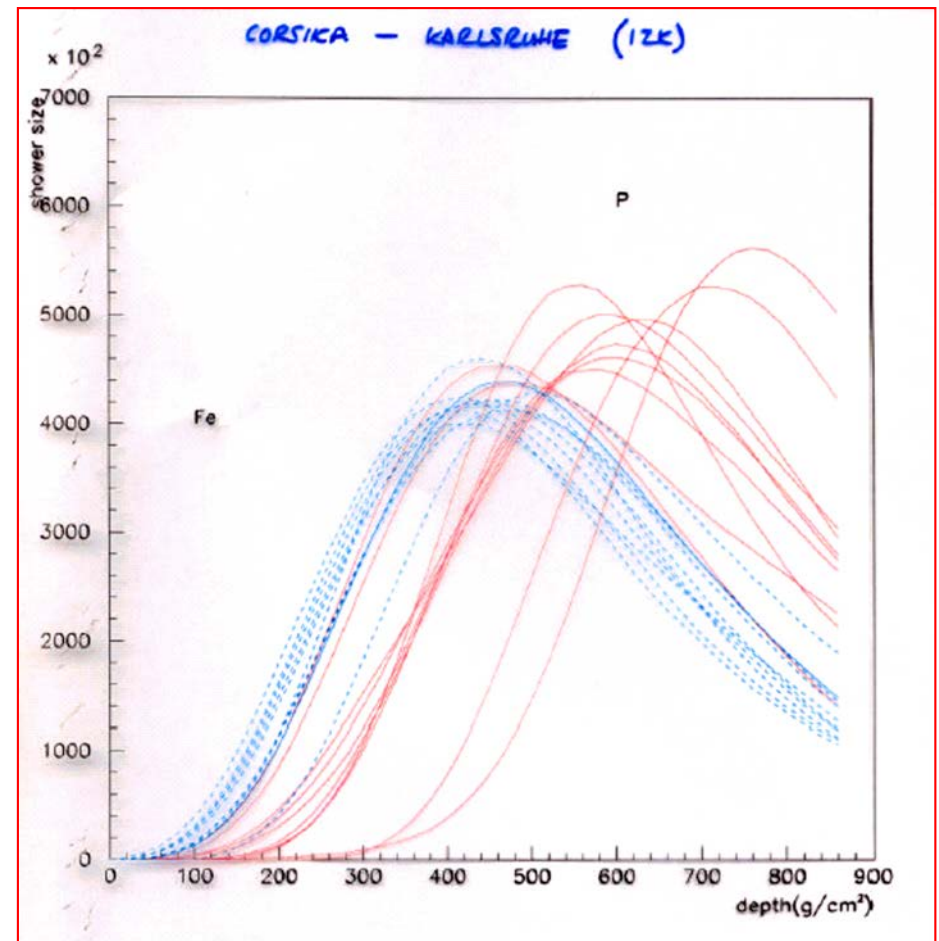
Development of hadronic showers in the atmosphere. C.R. composition: measure of A

A detector for atmospheric air showers is realized with an apparatus, usually composed of different parts, capable of measuring with good resolution the arrival times of the incident particles, in which it is possible to define the "coincidence" time between the signals on different parts of the apparatus itself. A nucleus of mass A and total energy E_0 can be treated as A set of A nucleons each with energy $E = E_0 / A$

□

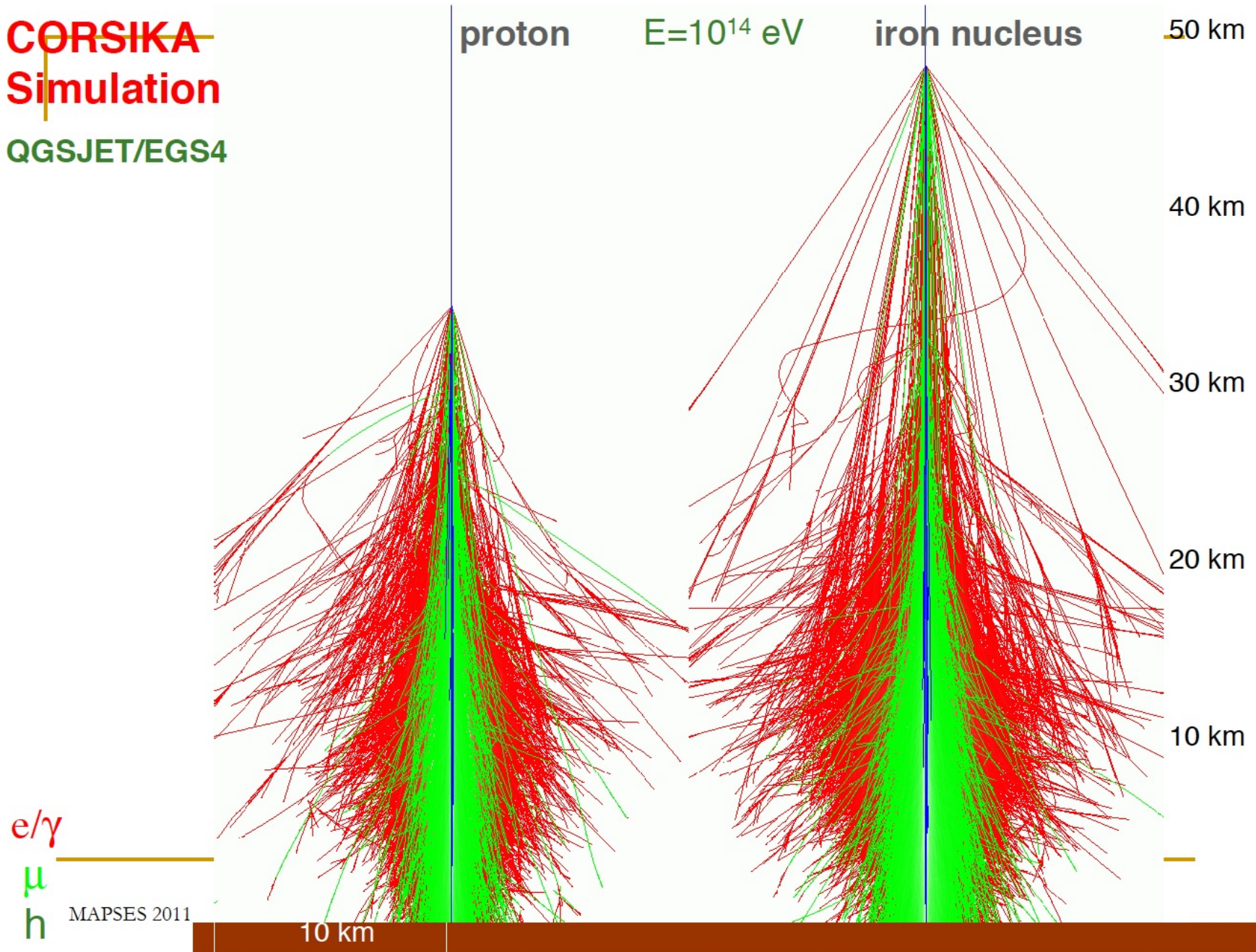
The shower induced by a nucleus with mass A and energy is E similar to A showers induced by protons with E/A energy but:

- For protons $x_{\max} \sim \lambda \cdot \ln(E/E_C)/\ln(2)$
- for nuclei A $x_{\max} \sim \lambda \cdot \ln(E/AE_C)/\ln(2)$



Proton and Iron induced showers (MC simulation)

~~CORSIKA~~
Simulation
QGSJET/EGS4



KASCADE experiment

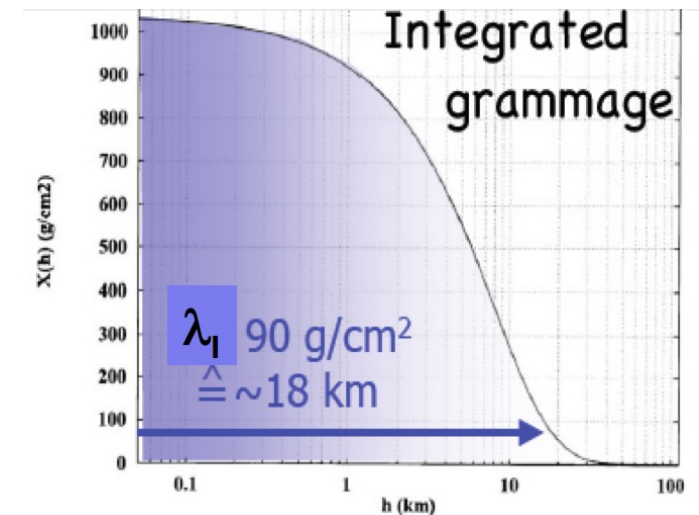
Karlsruhe **S**hower **C**ore and **A**rray **D**etector -Grande is an extensive air shower experiment array to study the cosmic ray primary composition and the hadronic interactions in the energy range $E_0=10^{16}$ - 10^{18} eV.

The experiment was situated near Karlsruhe (Germany) at 110m a.s.l, corresponding to an average atmospheric depth of 1022g/cm^2 .

It measures simultaneously the electromagnetic, muonic and hadronic components of extensive air showers of cosmic rays.

As an extension of the former KASCADE experiment running successfully since 1996, KASCADE-Grande was built by reassembling 37 stations of the former EAS-TOP experiment -basically the electromagnetic detectors- running between 1987 and 2000 at Campo Imperatore, Grand Sasso Laboratories, Italy.

One of the main results obtained by these two experiments is a picture of increasingly heavier composition above the 'knee' caused by a break in the spectrum of the light components. Conventional acceleration models predict a change of the composition towards heavier components. The discovery of the knee in the heavy components, represented by iron, would be a convincing verification of these theories. From the observed rigidity dependent breaks of the spectra of different lighter primaries observed between 10^{14} and 10^{16} eV, the iron 'knee' is expected around $E_0=10^{17}$ eV.



KASCADE experiment

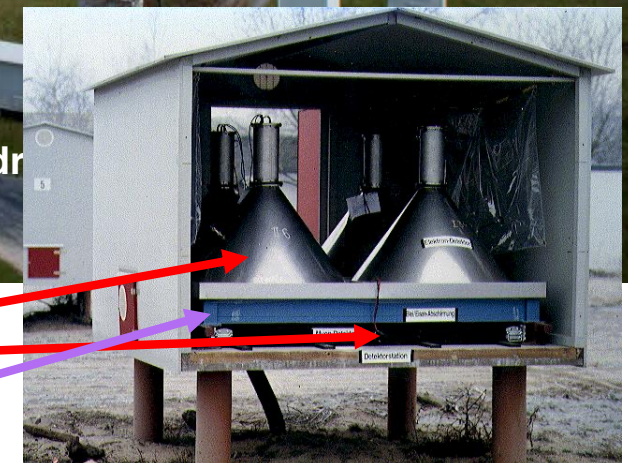
The field array (200m x 200m) consists of 252 detector stations arranged on a rectangular grid with a distance of 13 meters to each other. 16 (resp. 15) of the stations form a so-called cluster with an electronics container in the centre and which act as an independent shower experiment. In the middle of the array one can see the building with the KASCADE central detector

The original KASCADE Array is a Scintillator Array which measures the electrons, photons and muons of extensive air showers outside the core region in 252 detector stations on a rectangular grid of 13 m spacing, hence forming an array of 200 x 200 m².

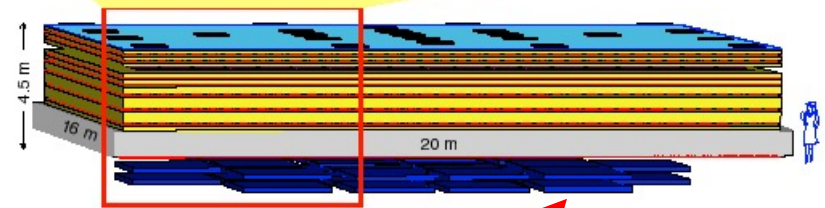
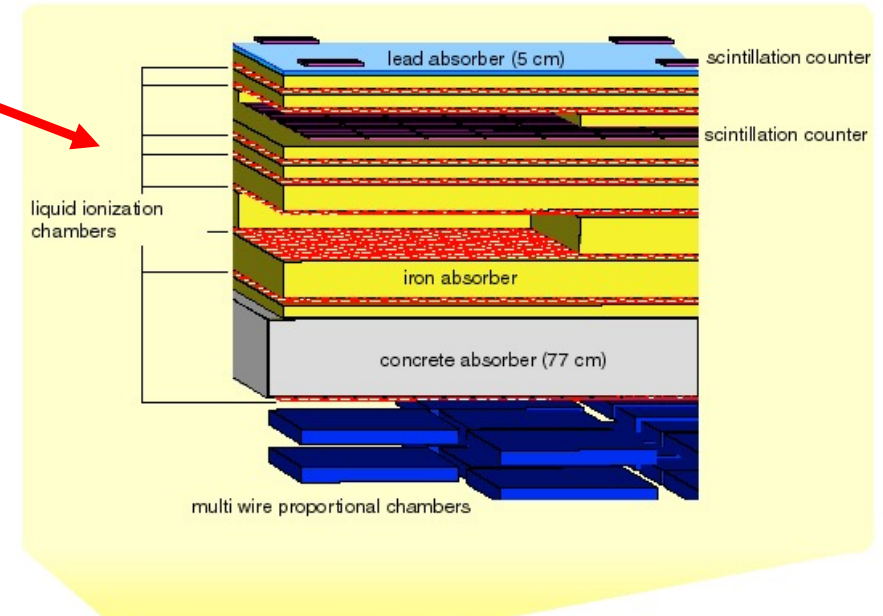
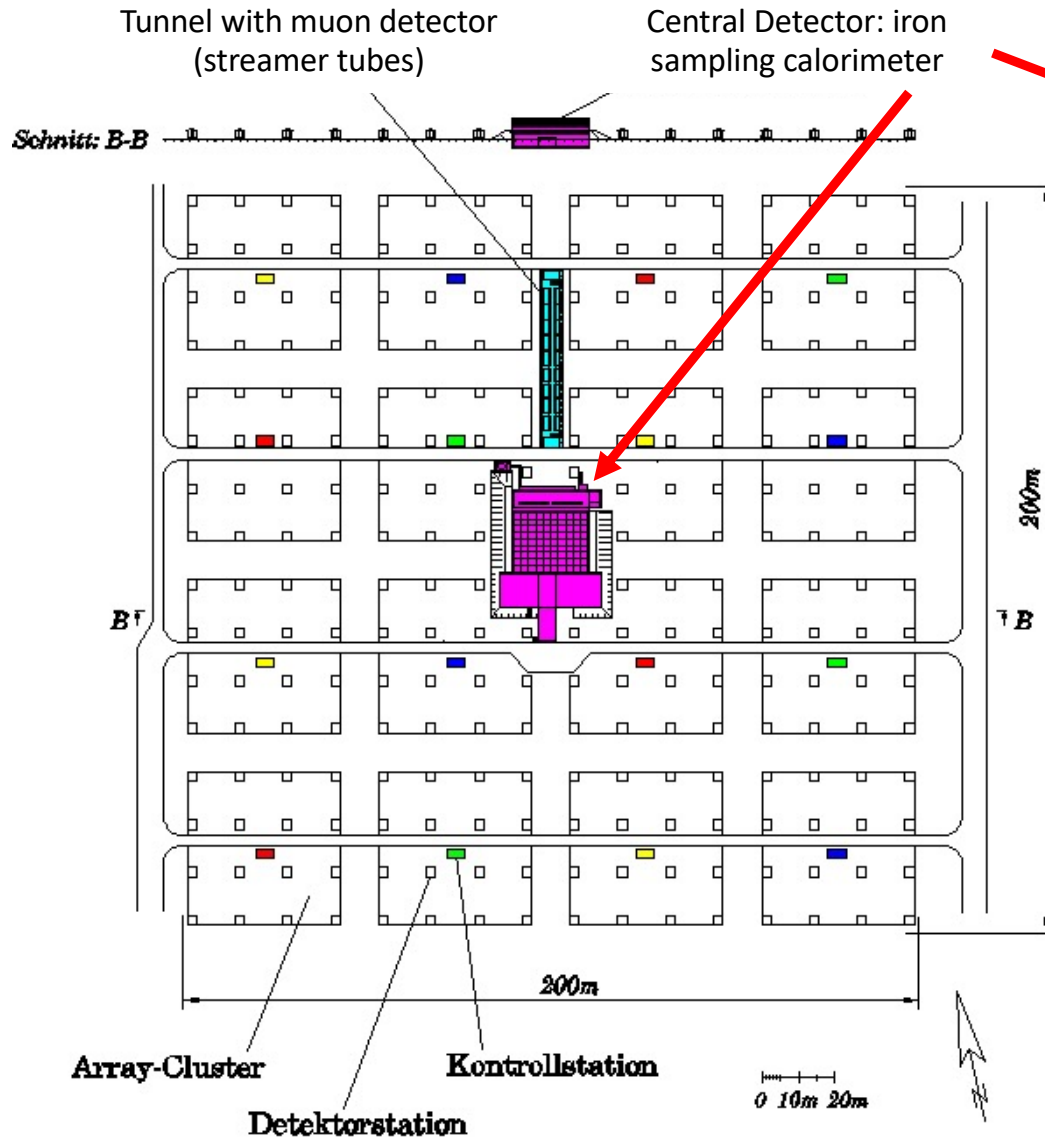
T. Antoni et al. NIM A513 (2003) 490



In each station there are up to four electron-gamma detectors and one muon-detector under a iron-lead-absorber of about 20 attenuation lengths.

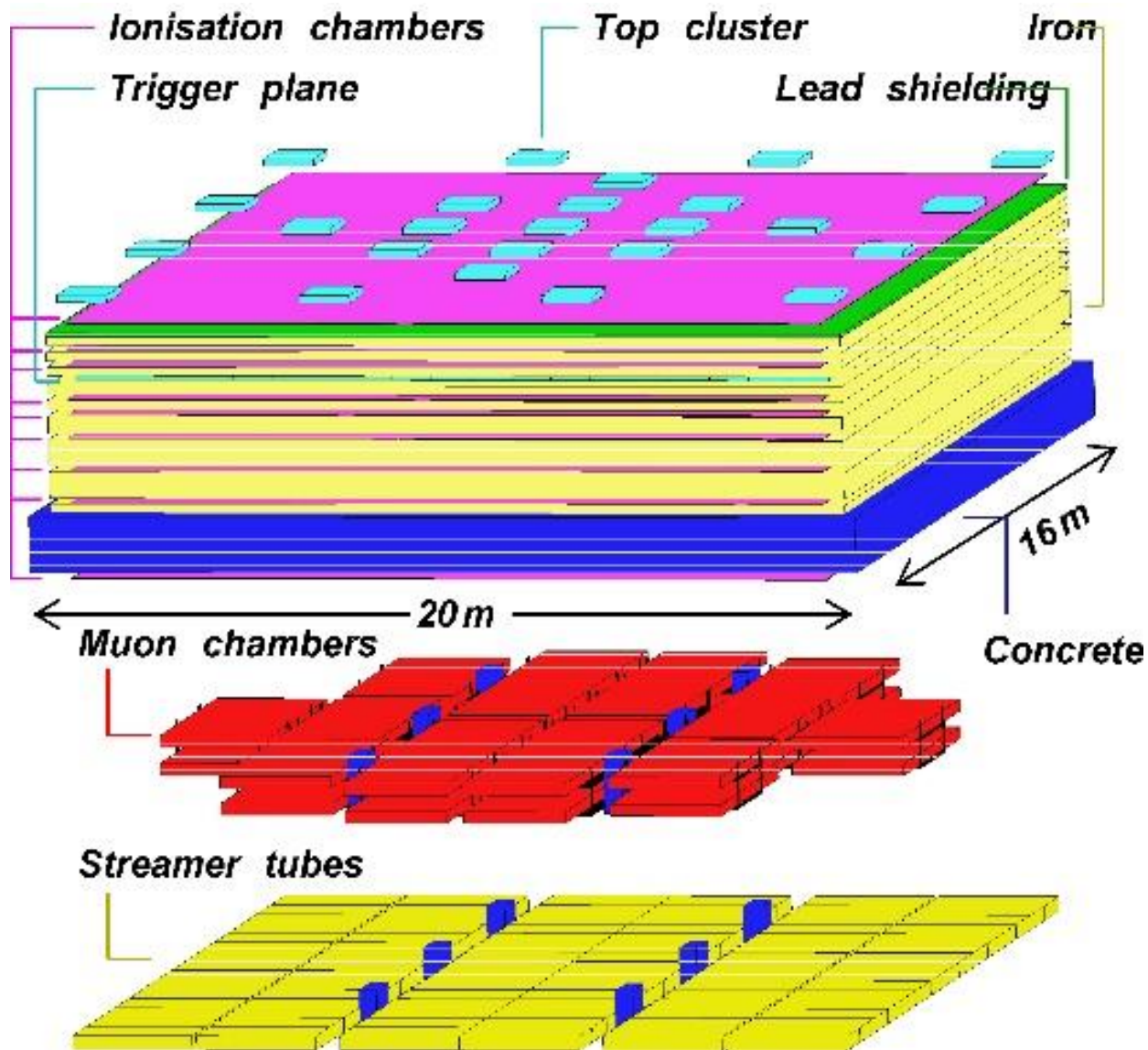


KASCADE: the central detector



Multiwire proportional chambers to detect muons below the iron-sampling calorimeter

KASCADE: the central detector



KASCADE-GRANDE experiment

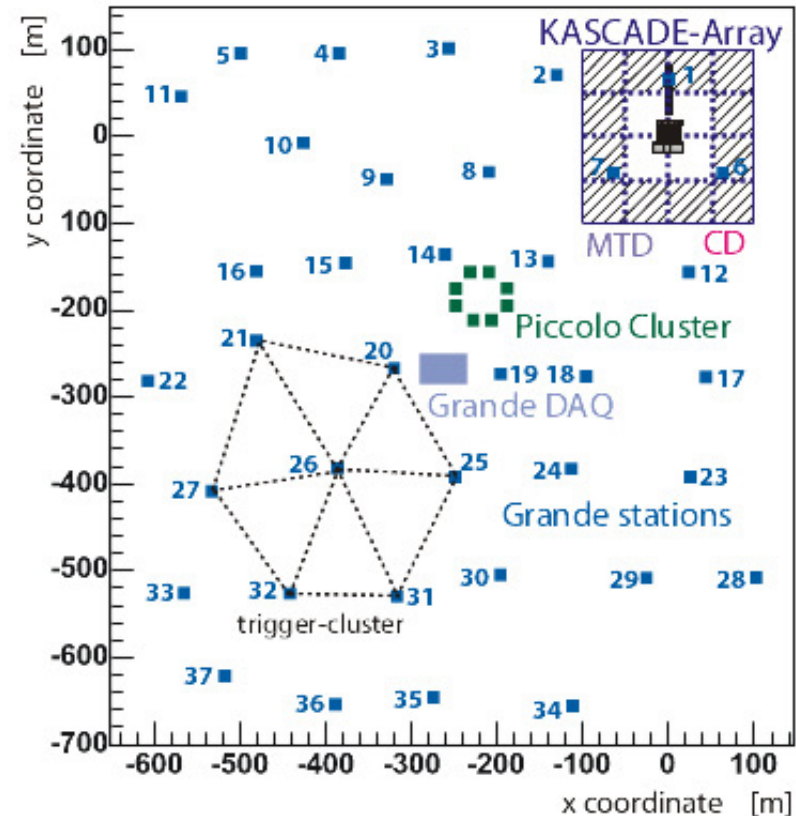


KASCADE-Grande is an extensive air shower experiment array to study the cosmic ray primary composition and the hadronic interactions in the energy range $E_0=10^{16}$ - 10^{18} eV.

KASCADE-Grande

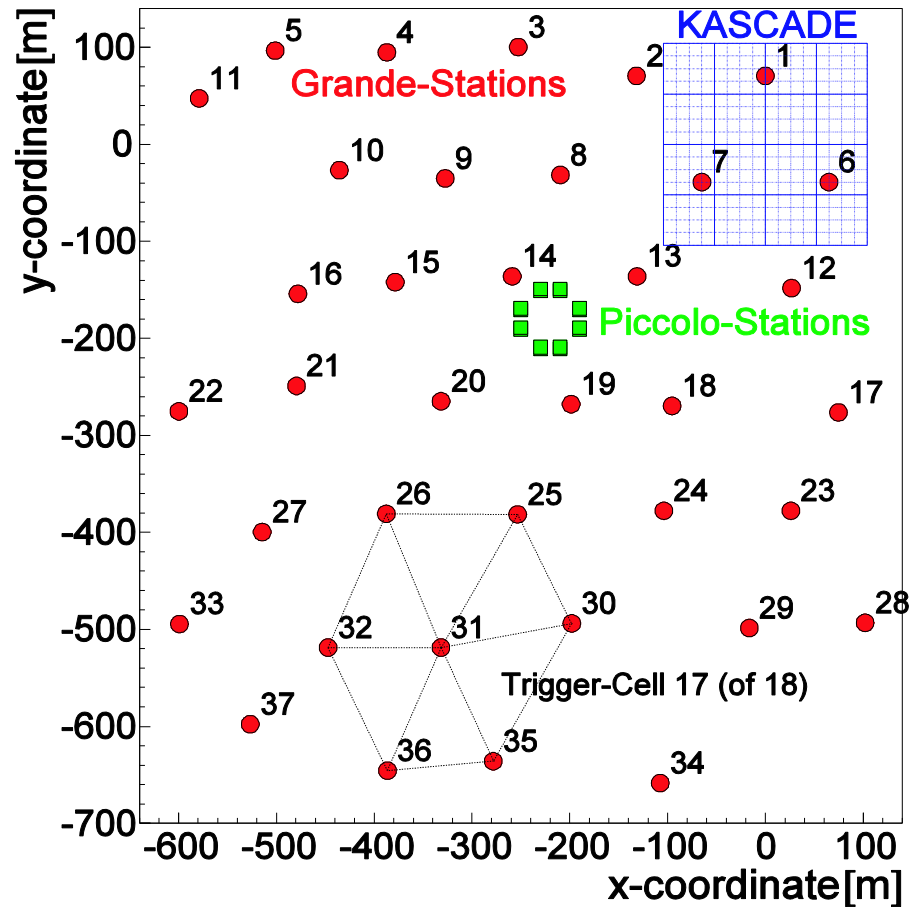
The **KASCADE-Grande Detector Array** has been realized by means of 37 stations at a mutual distance of about 130 m covering an area of 0.5 km² next to the KASCADE site in order to operate jointly with the KASCADE detector components.

KASCADE-Grande was realized to expand the energy range for cosmic ray studies from 10¹⁴-10¹⁷ eV primary energy range up to **10¹⁸ eV**. This is performed by extending the area covered by the KASCADE electromagnetic array from 200×200m² to **700×700m²** by means of 37 scintillator detector stations of 10 m² active area each. This new array is named Grande and provides measurements of the all-charged particle component of extensive air showers, while the original KASCADE array particularly provides information on the muon content. Additional dense compact detector set-ups being sensitive to energetic hadrons and muons are used for data consistency checks and calibration purposes.



The **KASCADE-Piccolo Trigger Array** consists of an array of 8 stations equipped with 10m² of plastic scintillator each and is placed towards the centre of the Grande array. The main aim of piccolo is to provide an external trigger to Grande and to KASCADE for coincidence events.

KASCADE-Grande detectors & observables



Grande array → cover an area of 0.5 km², detecting EAS with high resolution

Detector	Detected EAS component	Detection Technique	Detect or area (m ²)
Grande	Charged particles	Plastic Scintillators	37x10
KASCADE array e/γ	Electrons, γ	Liquid Scintillators	490
KASCADE array μ	Muons (E _μ th =230 MeV)	Plastic Scintillators	622
MTD	Muons (Tracking) (E _μ th =800 MeV)	Streamer Tubes	4x128

- Shower core and arrival direction

- Shower Size (N_{ch} number of charged particles)

- Grande array

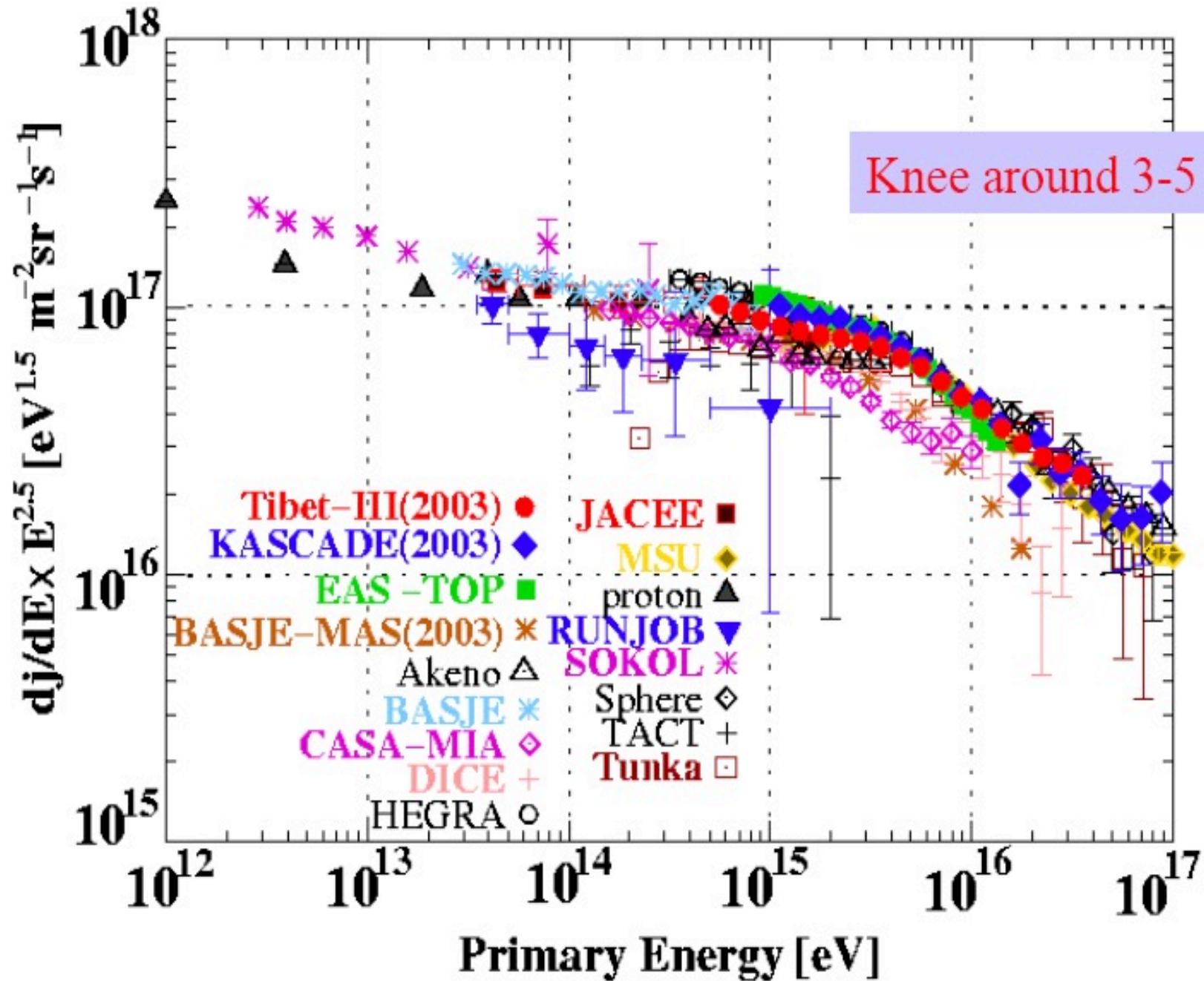
- μ Size (E_μ>230 MeV)

- KASCADE array μ detectors

- μ density & direction (E_μ>800 MeV)

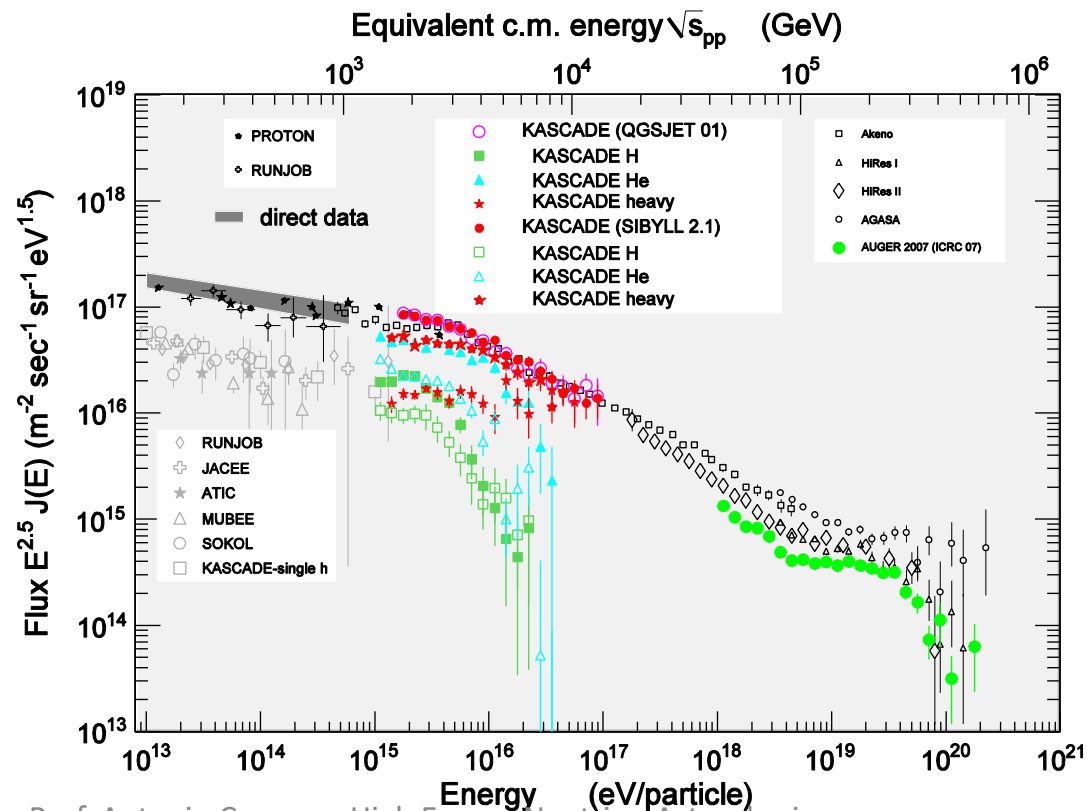
- Streamer Tubes

$Flux \times E^{2.5}$ for charged primary Cosmic Rays around the knee

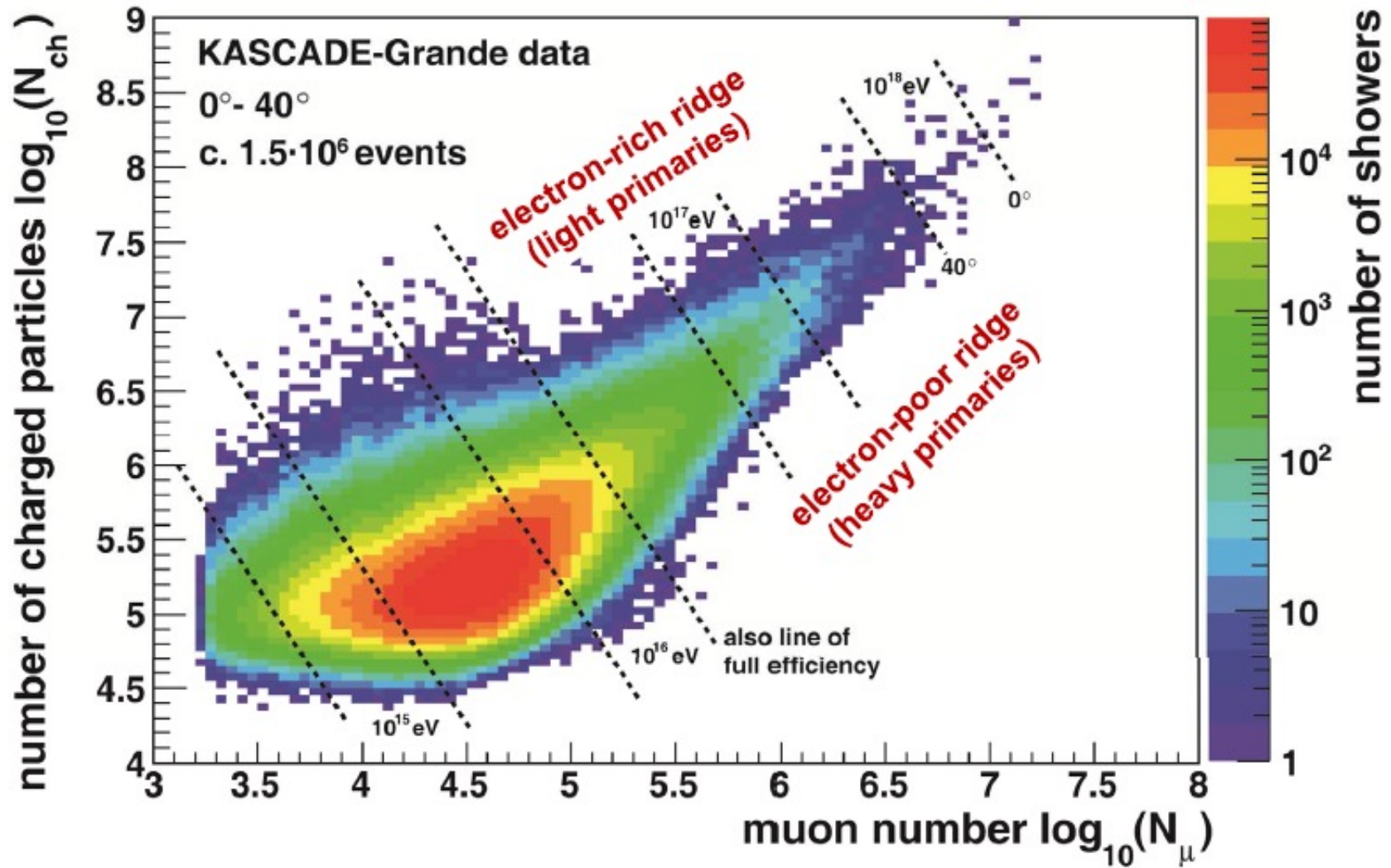


The "Knee" of primary Charged Cosmic Rays spectrum

- Knee is due to the light component of cosmic rays
- Change of slope of the heavy component observed at 8×10^{16} eV
- Knee interpretation either by acceleration limit in galactic sources or by propagation effects
- Not yet identified the transition to extragalactic primaries



Approach to Chemical Composition



All particle energy spectrum

- Combination of N_{ch} and N_{μ}
- Five different angular bins

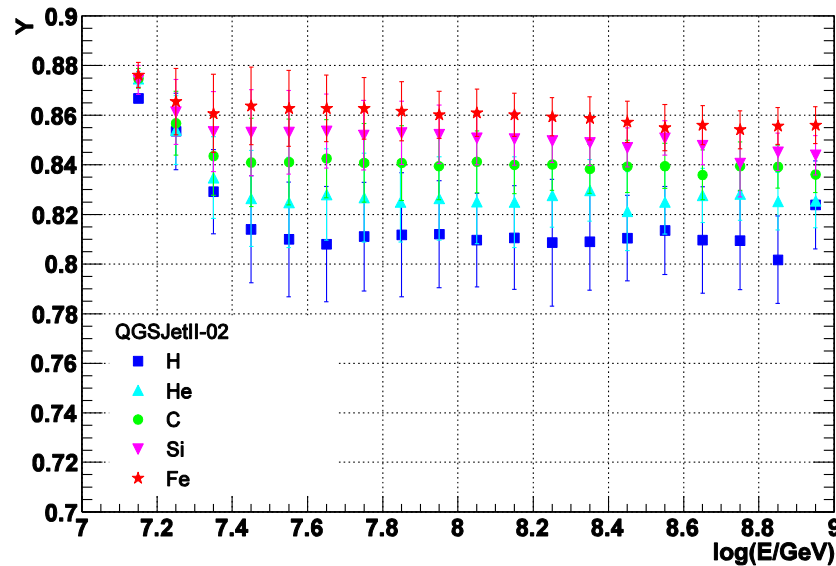
$$k = \frac{\log_{10}(N_{ch} / N_{\mu}) - \log_{10}(N_{ch} / N_{\mu})_H}{\log_{10}(N_{ch} / N_{\mu})_{Fe} - \log_{10}(N_{ch} / N_{\mu})_H}$$

- k parameter evaluates chemical composition, used as a weight in the expression correlating N_{ch} and E

$$\log_{10} E = [a_H + (a_{Fe} - a_H) \cdot k] \cdot \log_{10} N_{ch} + b_H + (b_{Fe} - b_H) \cdot k$$

- Based on QGSJet II-02

KASCADE and the N_{ch}/N_{μ} ratio



Y_{CIC} is constant with E
($E >$ full efficiency)

For a specific hadronic interaction model

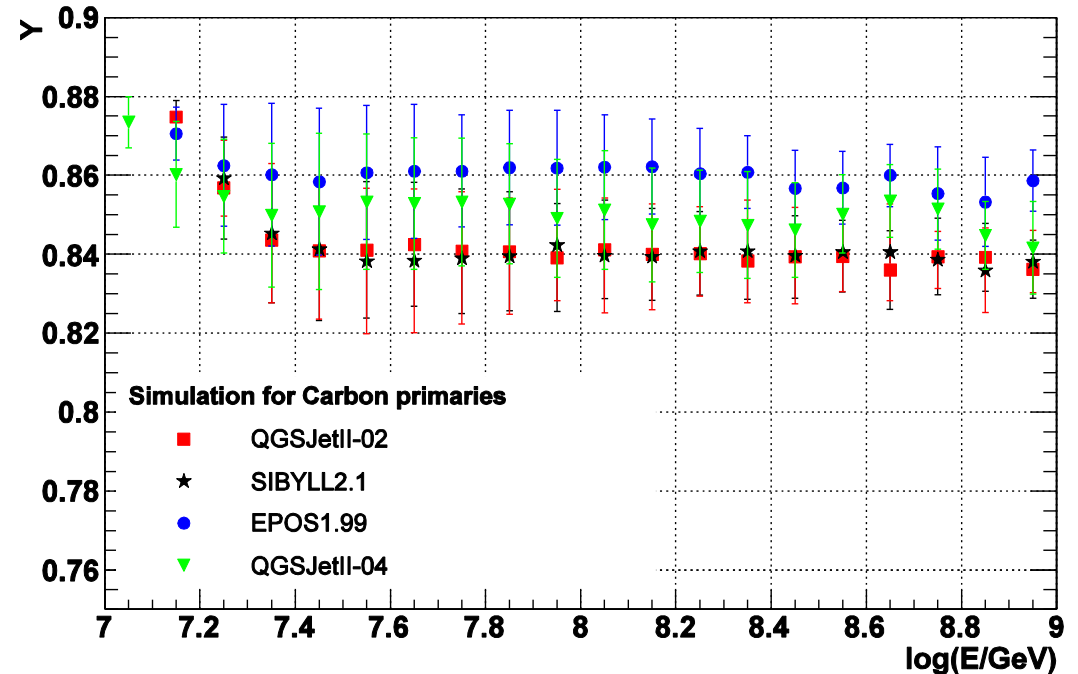
Y_{CIC} increases with primary mass

choice of $Y_{CIC} \rightarrow$ choice of a primary mass

For a particular primary element

Y_{CIC} increases when calculated by a model generating EAS with higher N_{μ}

\rightarrow for the same primary mass the choice of Y_{CIC} is shifted

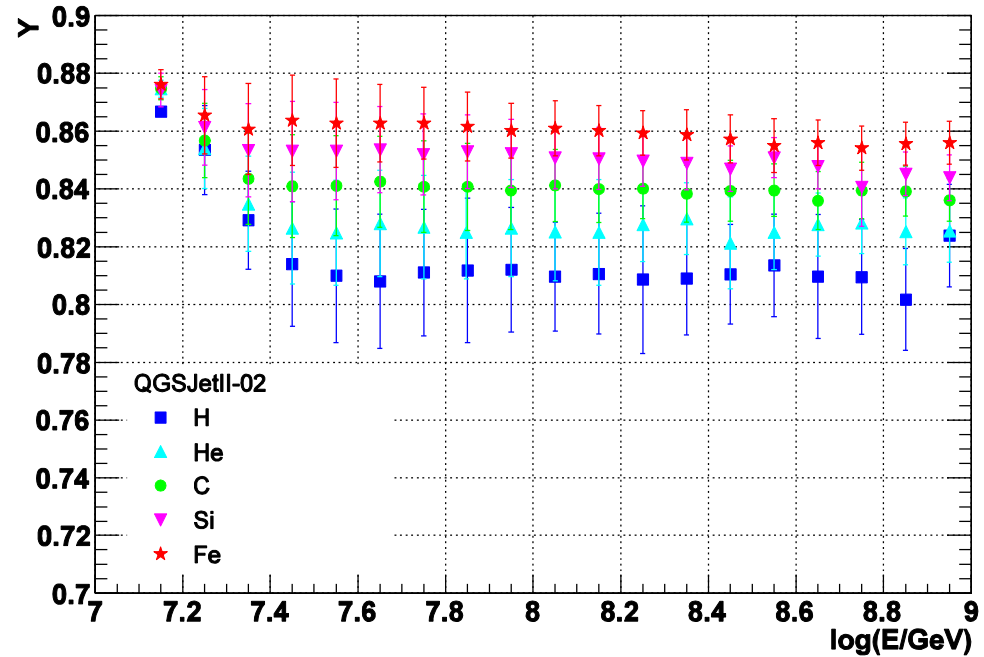
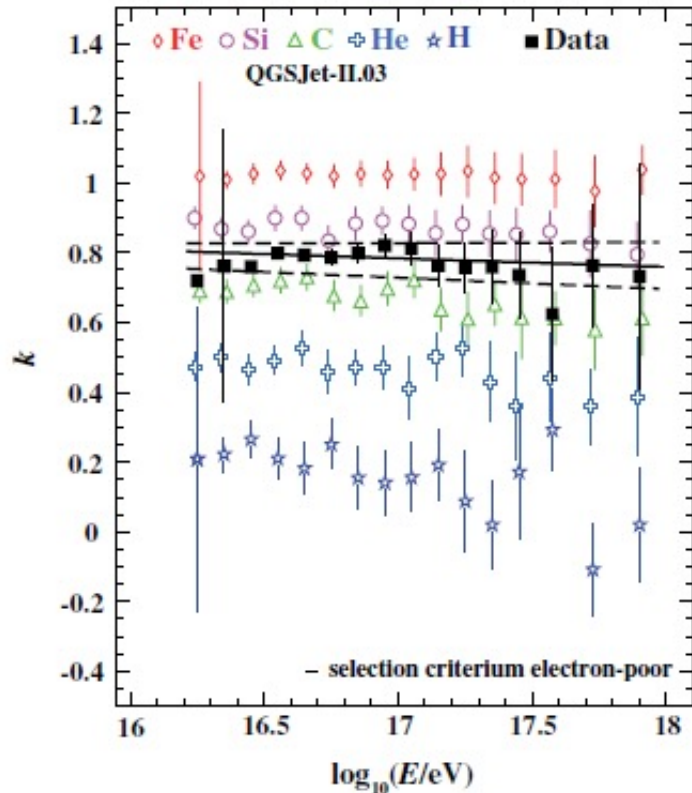


$$Y_{CIC} = \frac{\ln N_{\mu}(\mathcal{G}_{ref})}{\ln N_{ch}(\mathcal{G}_{ref})}$$

KASCADE

Event by event separation in two mass groups by N_{ch}/N_{μ} ratio

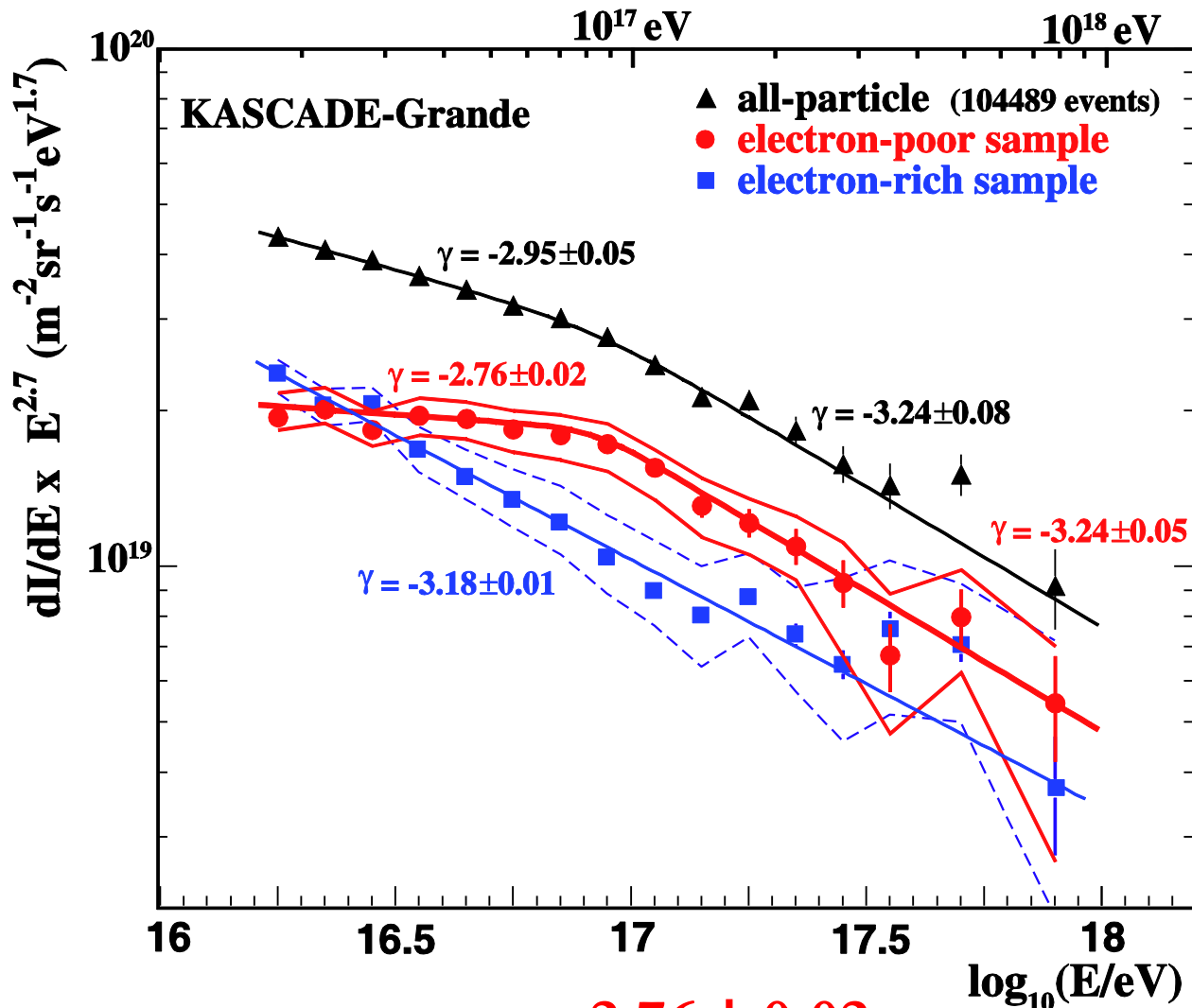
Two different ways of taking into account the EAS attenuation in atmosphere



$$k = \frac{\log_{10}(N_{ch}/N_{\mu}) - \log_{10}(N_{ch}/N_{\mu})_H}{\log_{10}(N_{ch}/N_{\mu})_{Fe} - \log_{10}(N_{ch}/N_{\mu})_H}$$

$$Y_{CIC} = \frac{\ln N_{\mu}(\mathcal{G}_{ref})}{\ln N_{ch}(\mathcal{G}_{ref})}$$

KASCADE Energy spectra



$$\gamma_1 = -2.76 \pm 0.02$$

$$\gamma_2 = -3.24 \pm 0.05$$

$$E_b = 10^{16.92 \pm 0.04}$$

- Energy spectra of the samples obtained by an event selection based on the k parameter

- Spectrum of the electron poor sample \rightarrow

$$k > (k_C + k_{Si})/2$$

\rightarrow steepening

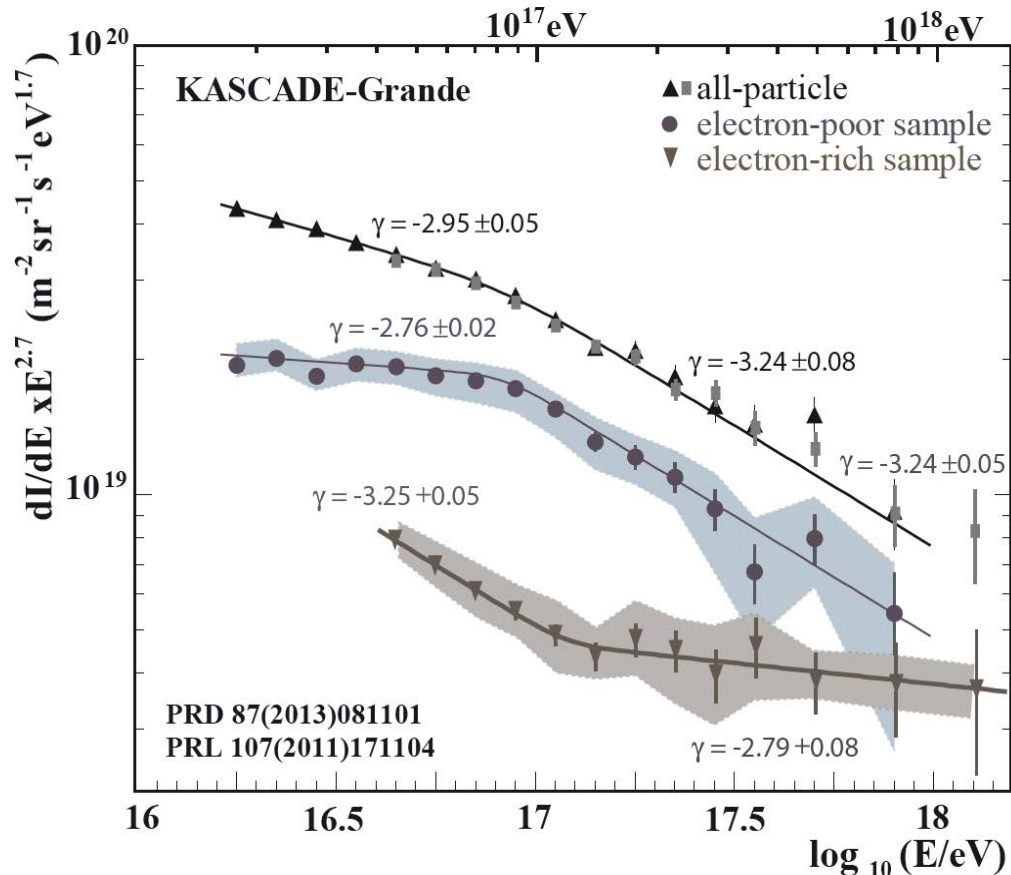
observed with increased significance $\rightarrow 3.5\sigma$

- Spectrum of electron rich events \rightarrow can be described by a single power law \rightarrow hints of a hardening above 10^{17} eV

Phys. Rev. Lett. 107 (2011) 171104

KASCADE summary

KASCADE-Grande energy spectra of individual mass groups



- steepening due to heavy primaries (3.5σ)

- hardening at $10^{17.08}$ eV (5.8σ) in light spectrum

- slope change from $\gamma = -3.25$ to $\gamma = -2.79!$

Phys.Rev.Lett. 107 (2011) 171104

Phys.Rev.D (R) 87 (2013) 081101

M.Bertaina (KASCADE-Grande) PoS(ICRC2015)???

J.C. Arteaga (KASCADE-Grande) PoS(ICRC2015)314

Development of new detection techniques: electromagnetic signals in radio wavelengths (1)



LOPES collaboration:

-) KASCADE-Grande
-) U Nijmegen, NL
-) MPIfR Bonn, D
-) Astron, NL
-) IPE, FZK, D

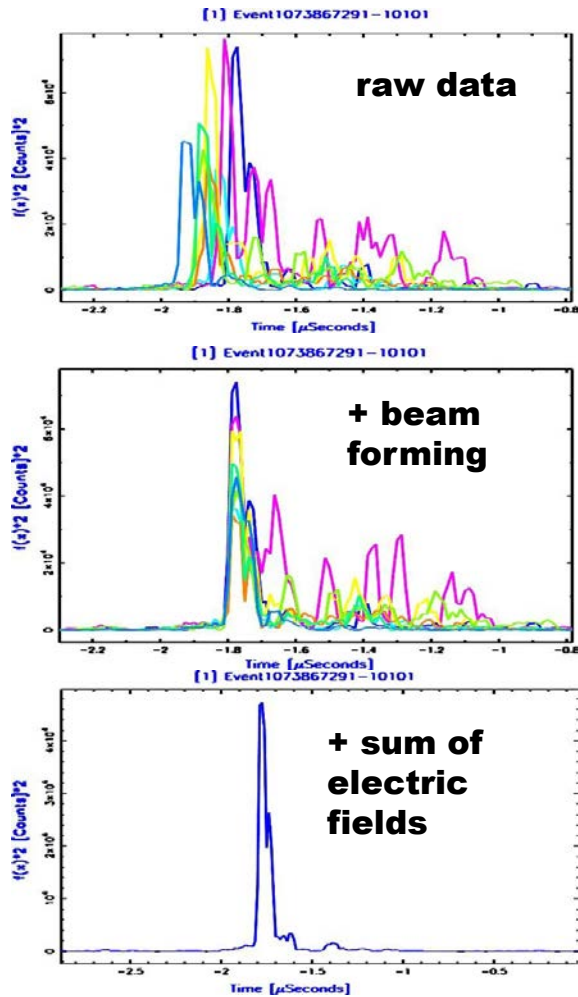
LOPES



→ Development of a
new detection
technique!

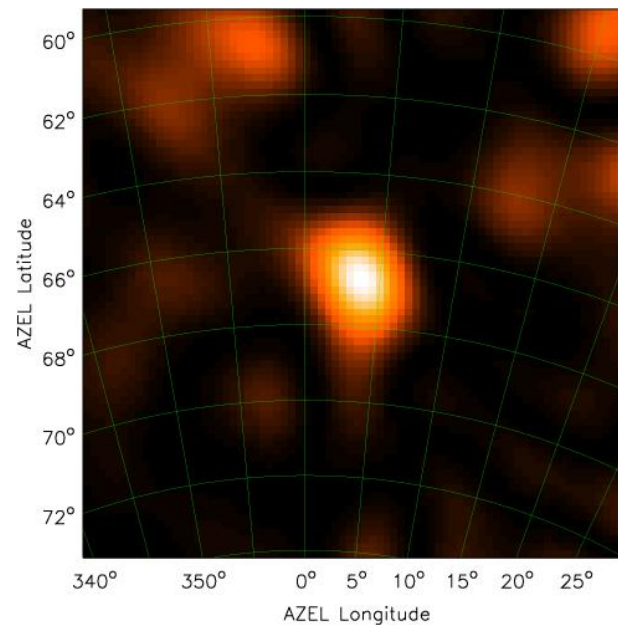
Development of new detection techniques: electromagnetic signals in radio wavelengths (2)

2. Radio data analysis

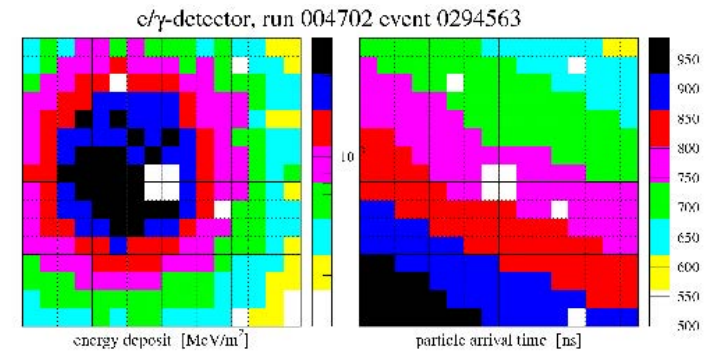


LOPES:
Proof of principle

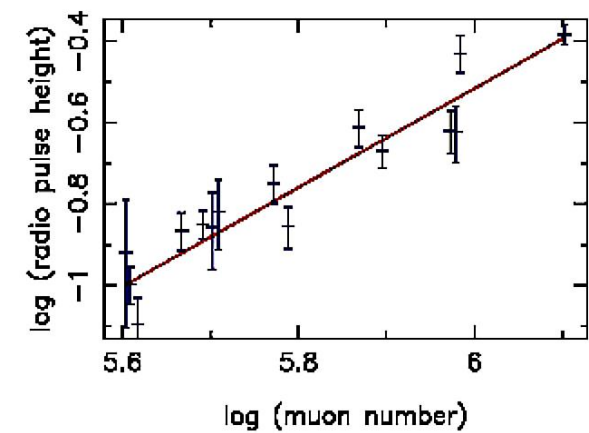
3. Skymapping



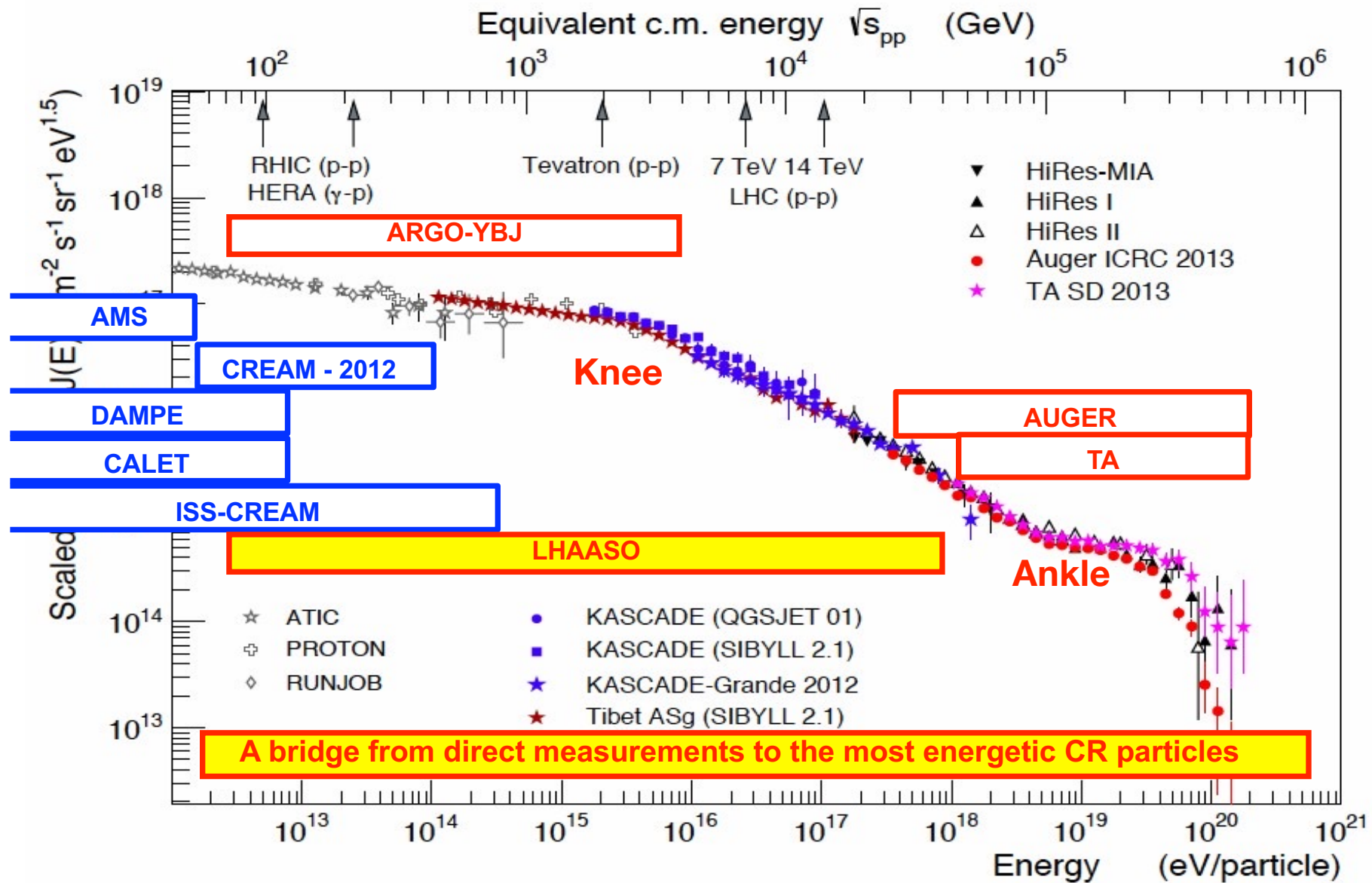
1. KASCADE measurement



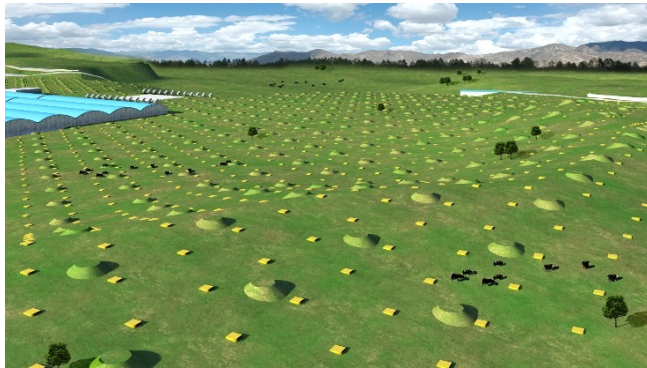
4. Many events meanwhile >500 events



An overview of present/future C.R. detectors

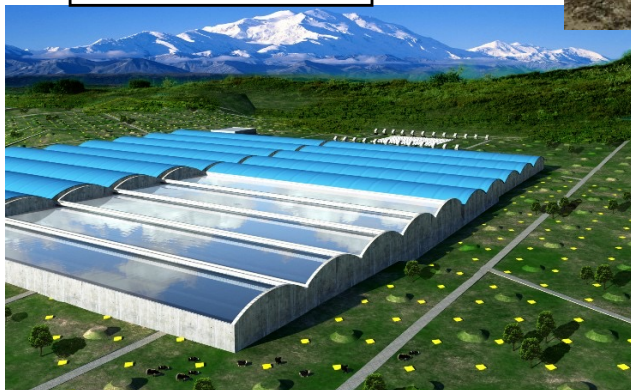
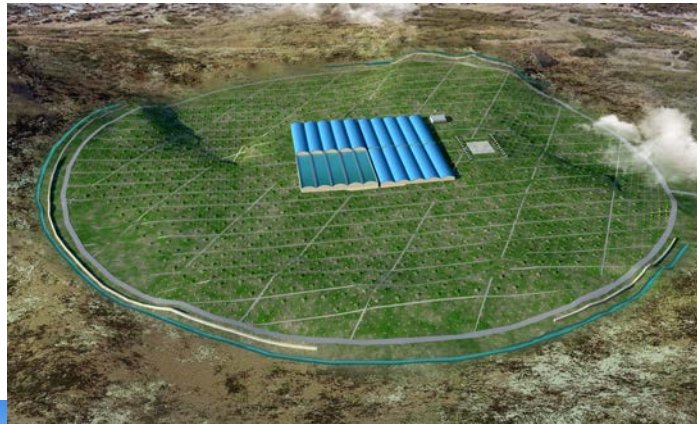


LHAASO: high altitude Atmospheric Showers detector in construction: main components

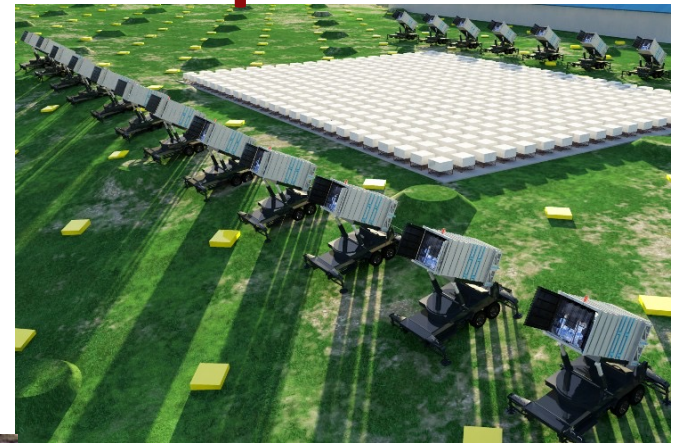


1 KM2A:
5635 EDs
1221 MDs

WCDA:
3600 cells
90,000 m²

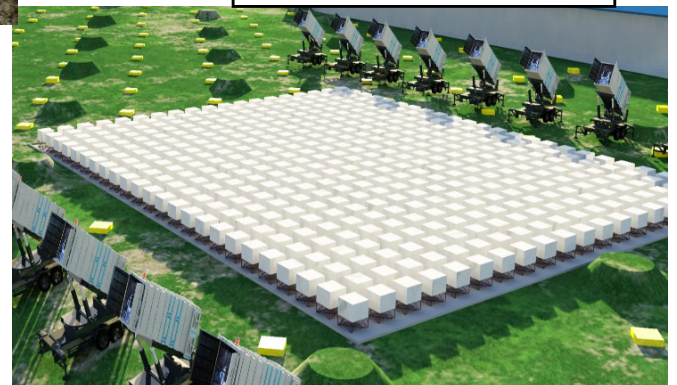


Coverage area: 1.3 km²

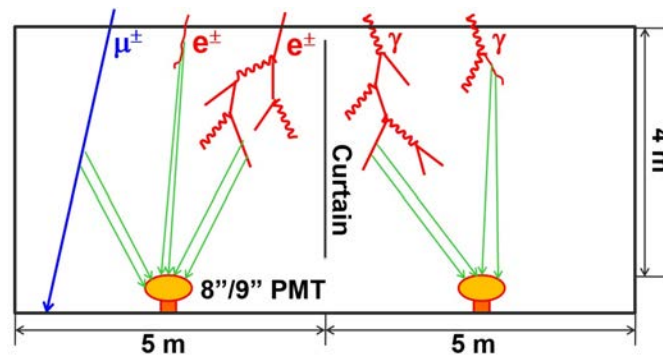
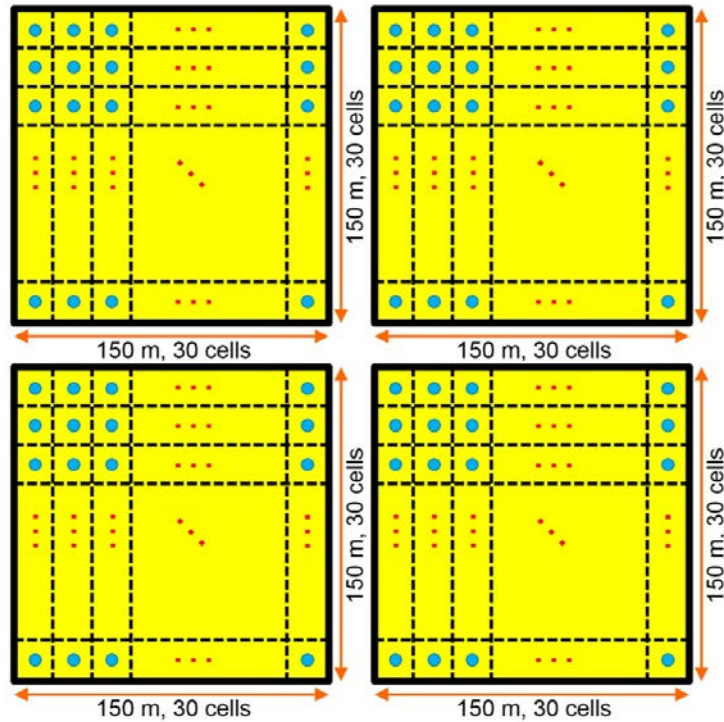


WFCTA:
24 telescopes
1024 pixels each

SCDA:
452 detectors

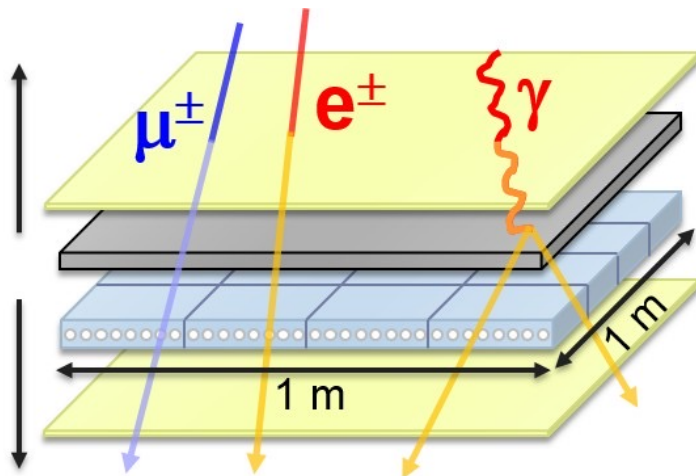


LHAASO: Water Cherenkov Detector Array



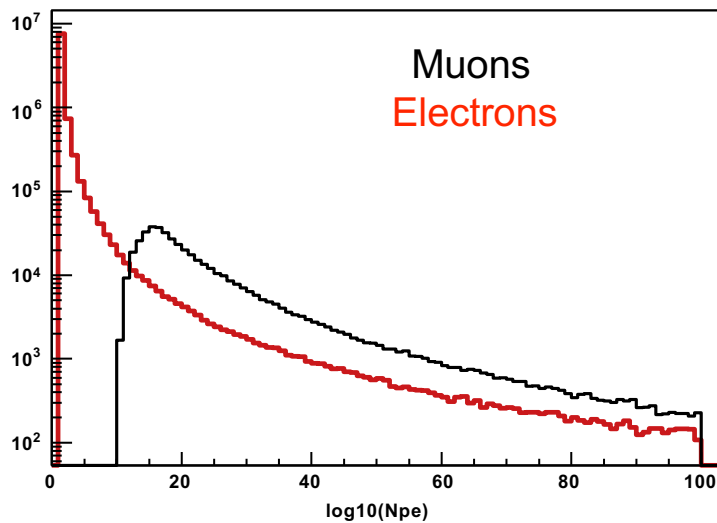
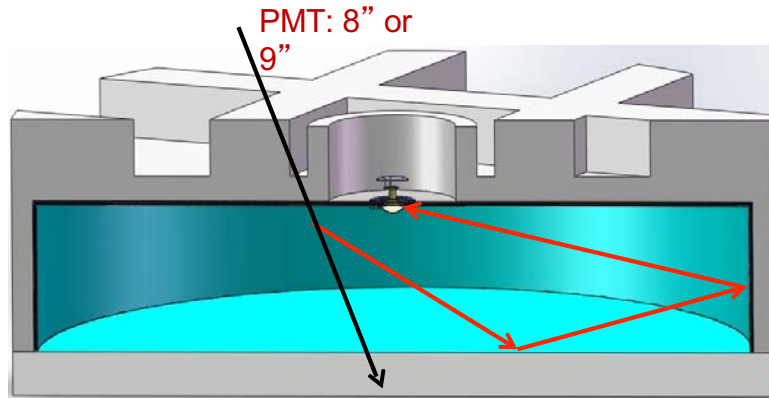
Item	Value
Cell area	25 m ²
Effective water depth	4 m
Water transparency	> 15 m (400 nm)
Precision of time measurement	0.5 ns
Dynamic range	1-4000 PEs
Time resolution	<2 ns
Charge resolution	40% @ 1 PE 5% @ 4000 PEs
Accuracy of charge calibration	<2%
Accuracy of time calibration	<0.2 ns
Total area	90,000 m ²
Total cells	3600

Lhaaso; Electromagnetic particle Detector



Item	Value
Effective area	1 m ²
Thickness of tiles	2 cm
Number of WLS fibers	8/tile × 16 tile
Detection efficiency (> 5 MeV)	>95%
Dynamic range	1-10,000 particles
Time resolution	<2 ns
Particle counting resolution	25% @ 1 particle 5% @ 10,000 particles
Aging	>10 years
Spacing	15 m
Total number of detectors	5635

LHAASO: Muon Detector



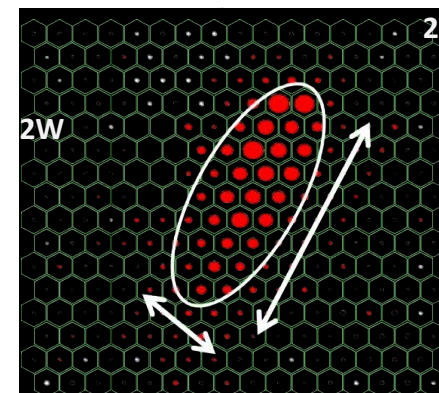
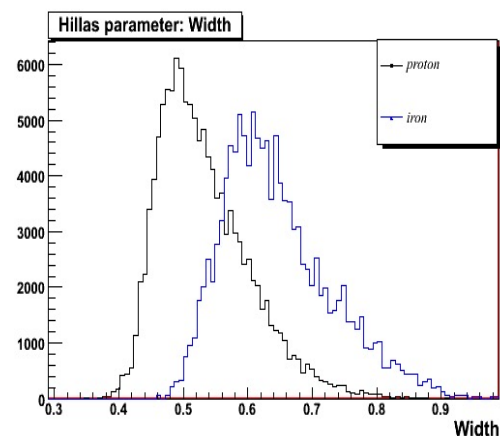
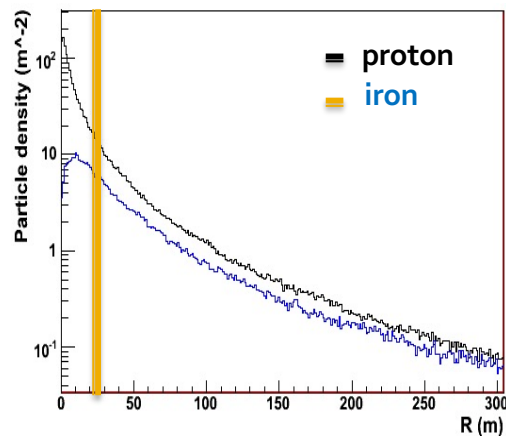
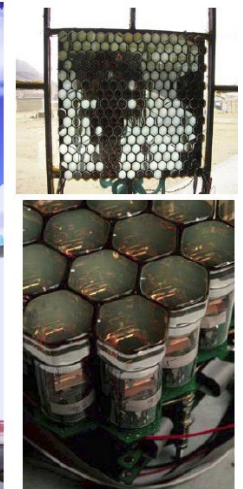
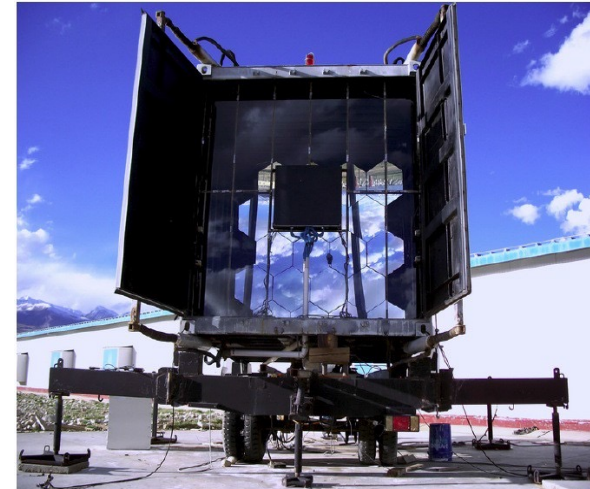
Photoelectron distribution at $R > 100\text{m}$ from the shower core

Item	Value
Area	36 m ²
Depth	1.2 m
Molasses overburden	2.5 m
Water transparency (att. len.)	> 30 m (400 nm)
Reflection coefficient	>95%
Time resolution	<10 ns
Particle counting resolution	25% @ 1 particle 5% @ 10,000 particles
Aging	>10 years
Spacing	30 m
Total number of detectors	1221

LHAASO: Wide field of view Cherenkov Telescope Array

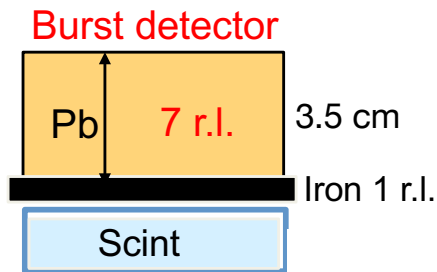
24 telescopes (Cherenkov/Fluorescence)

- 5 m² spherical mirror
- 16x16 PMT array
- FOV: 14°x 14°
- Elevation angle: 60°

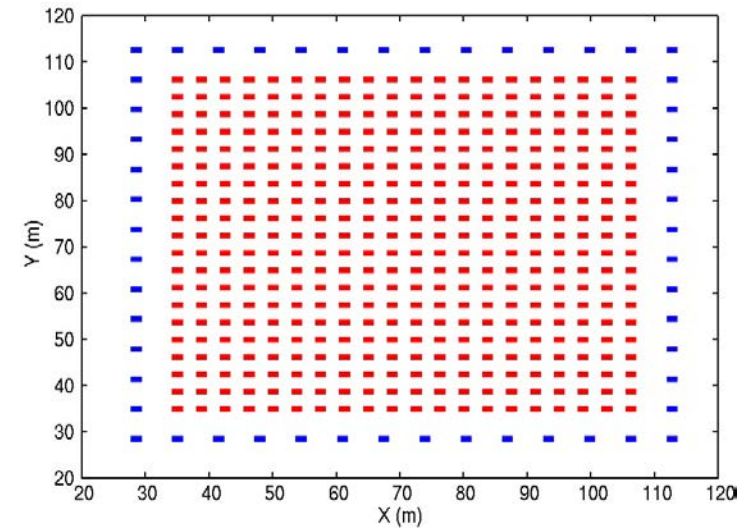


LHAASO: Shower Core Detector Array

425 close-packed **burst detectors**, located near the centre of the array, for the detection of high energy secondary particles in the shower core region.



The burst detectors observe the electron size (**burst size**) under the lead plate induced by high energy e.m. particle in the shower core region

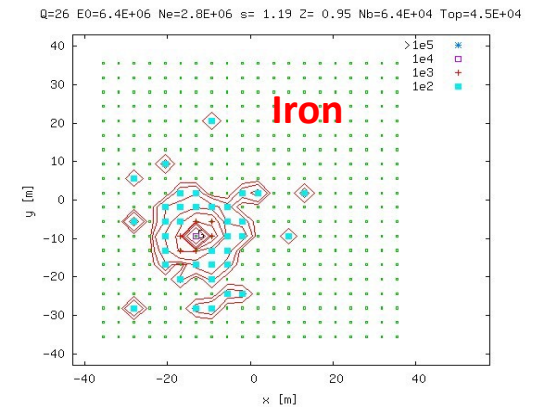
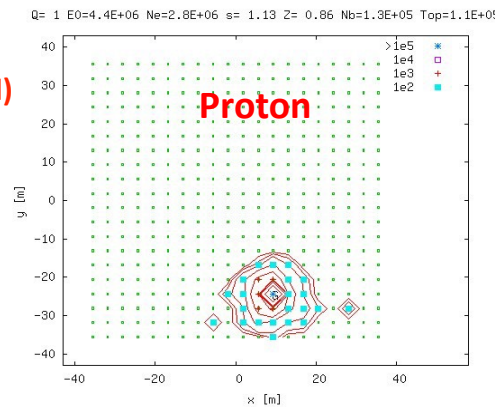


Each burst detector is constituted by 20 optically separated scintillator strips of 1.5 cm x 4 cm x 50 cm read out by two PMTs operated with different gains to achieve a wide dynamic range (1- 10⁶ MIPs).

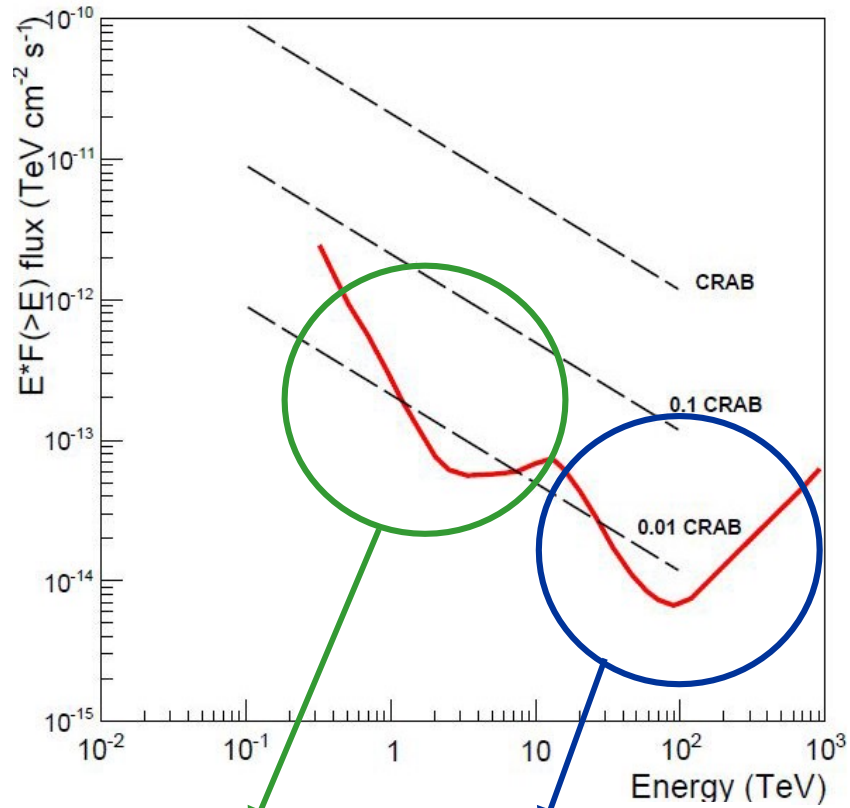
Number of SCD: 0.5m² x 452
 Cover Area: 5170m²
 Energy region: 30 TeV 10 PeV
 Core position resolution: 1.5 m @50 TeV



Lead plate (80 cm X 50 cm X 7 rl)
 Iron plate (1 m X 1 m X 1 rl)



LHAASO sensitivity for Crab-like sources

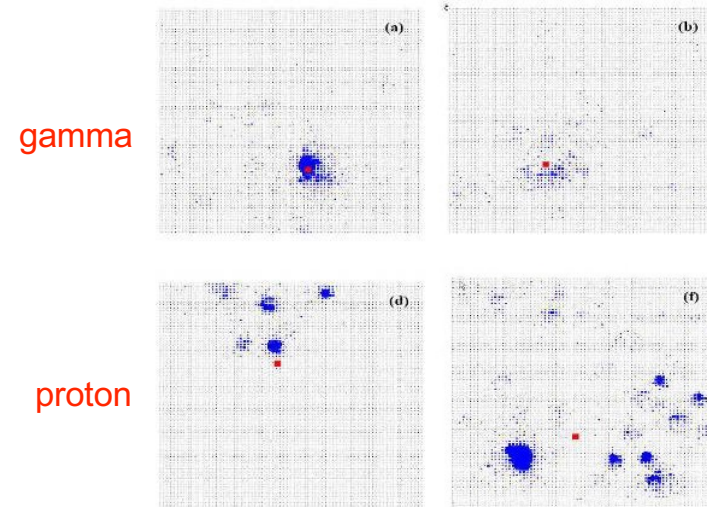


WCDA

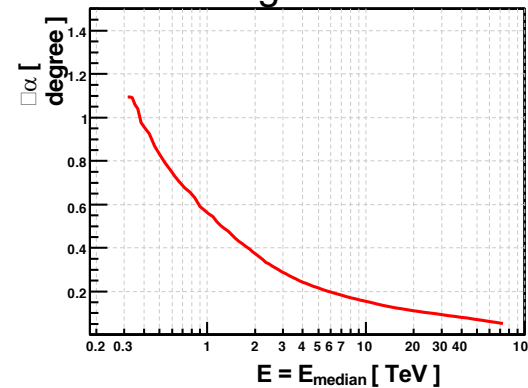


KM2A (EDs + MDs)

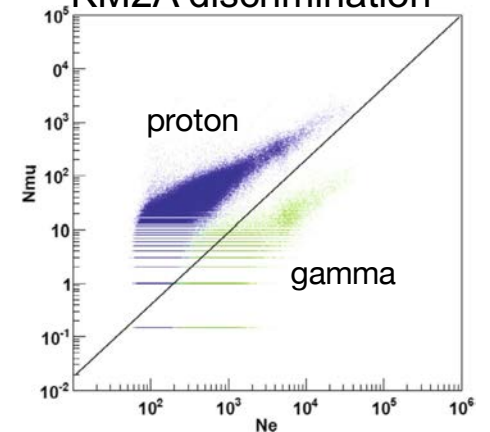
WCDA discrimination



WCDA angular resolution



KM2A discrimination



Charged primary Cosmic Rays for $E \gg \text{TeV}$

So far we have mainly discussed experiments measuring gamma fluxes:

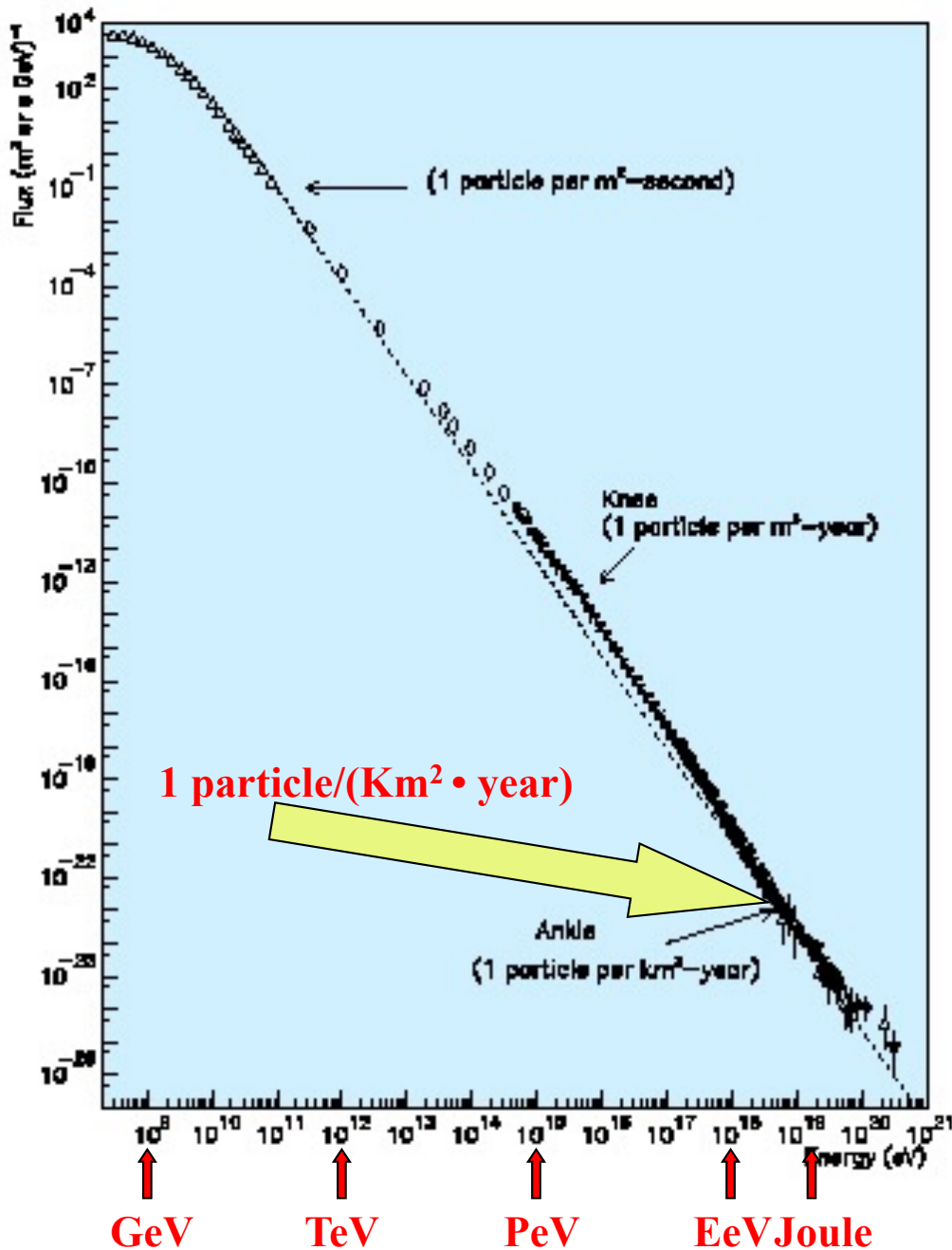
- very good tool for astronomy
- large background due to the much more intense charged component

High energy charged primary cosmic rays carry many information:

- what happens for $E \sim 10^{15}$ eV
- does the primary CR composition changes with energy ?? Can our detector distinguish a light CR (proton, He, ...) from an heavy one (Fe, ...) ?
- are these CR of galactic origin or there is an extragalactic component ?

What kind of experimental technique can answer to all these questions ?

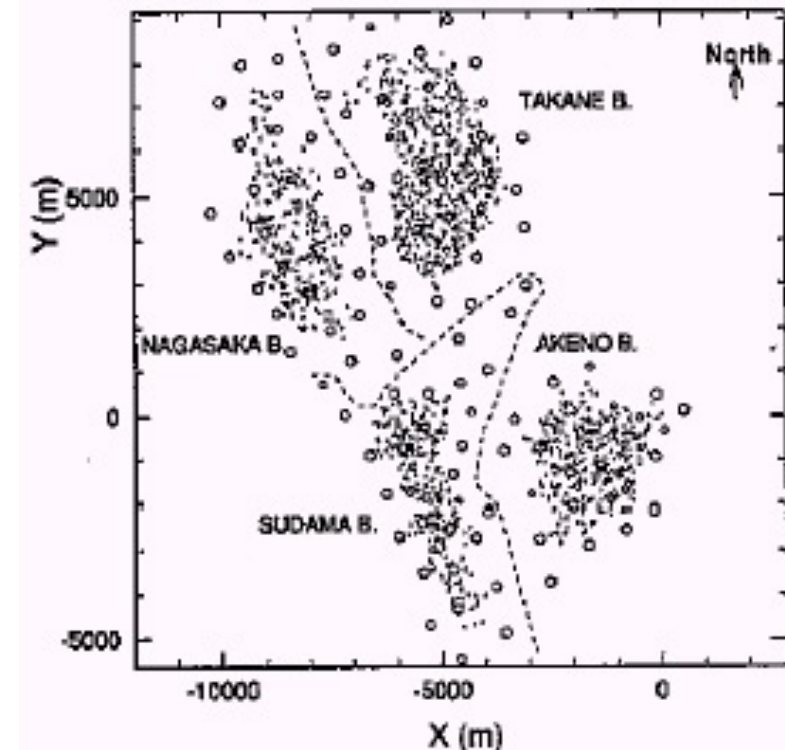
Detection of U.H.E. Cosmic Rays ($E \gg 100$ PeV)



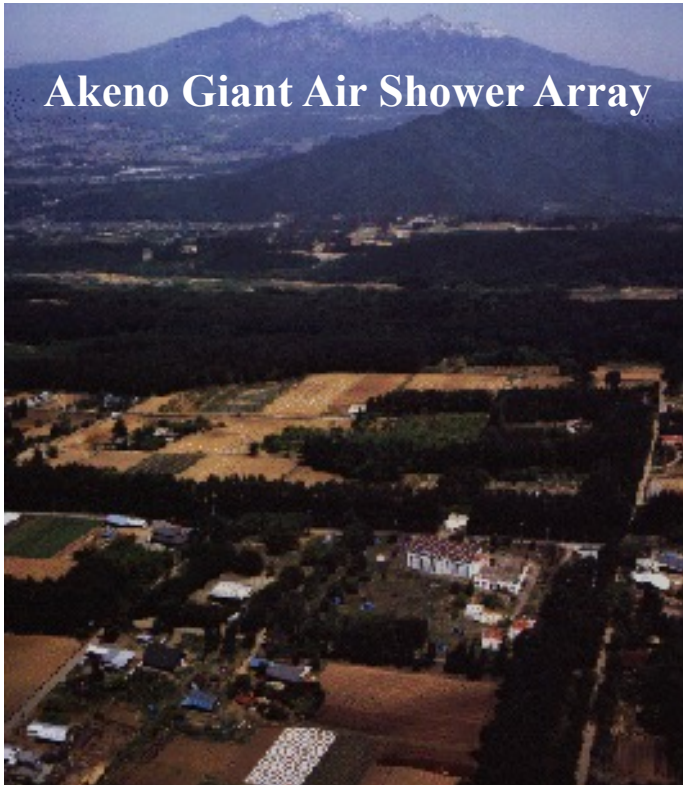
The study of cosmic rays with $E \gg 100$ PeV requires:

- \Rightarrow large equipment (sampling, fluorescence detection in the atmosphere, ...)
- \Rightarrow on the earth's surface or in space

Ad esempio **A**keno **G**iant **A**ir **S**hower **A**rray



AGASA: the first observations of CR with $E_{\text{shower}} > 10^{20}$ eV



Akeno Giant Air Shower Array

The apparatus, entered into operation in 1990 to observe C.R. with energy $> E_{\text{eV}} = 10^{18}$ eV) consists of 111 surface modules (plastic scintillators 2.2 m² spaced about 1km to cover a total area of ~ 100 km²) and 27 buried modules (proportional counters inter-spaced with PB or Fe absorbers or concrete) used as muon detectors.

It is divided into 4 sectors: Akeno, Sudama, Takane, Nagasaka. The AKENO sector (operates since 1984) consists of a region "densely populated" of scintillators and a region with more "dispersed" counters.

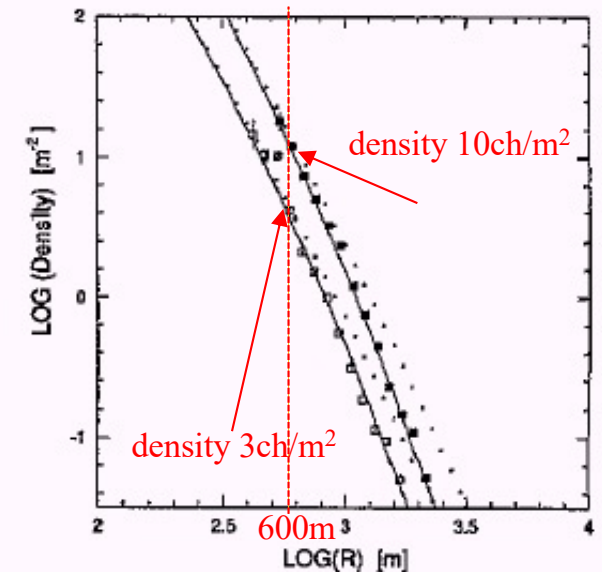
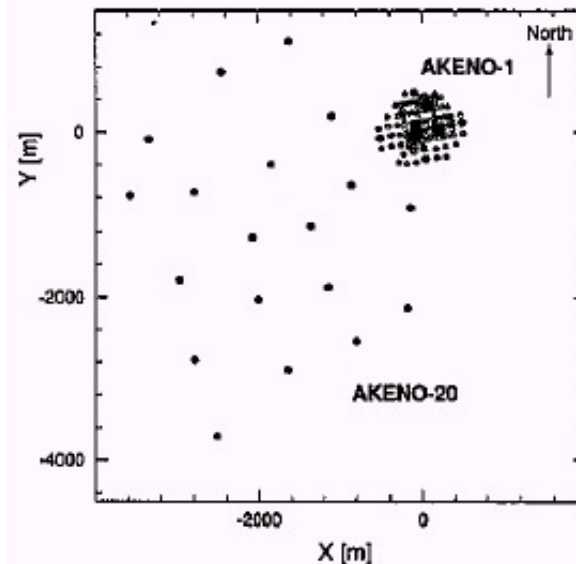
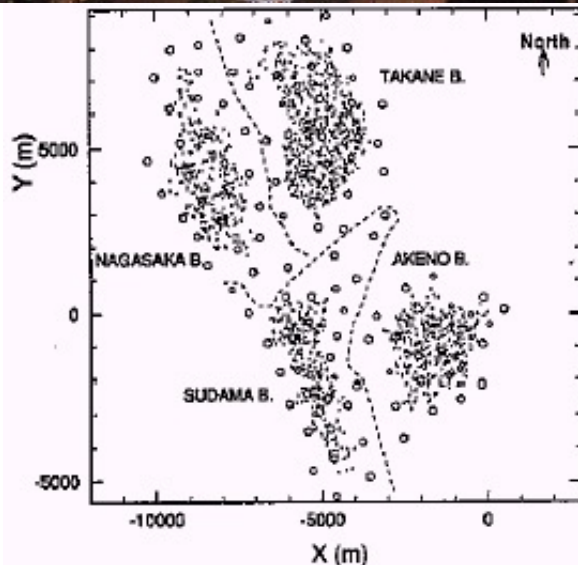
Shower parameters: energy reconstructed through the "particle density" 600m away from the "core" of the shower. The measurement of this density requires knowledge of the lateral distribution of the swarm:

AKENO-20 -> centre of the shower

AKENO -1 -> measures the density

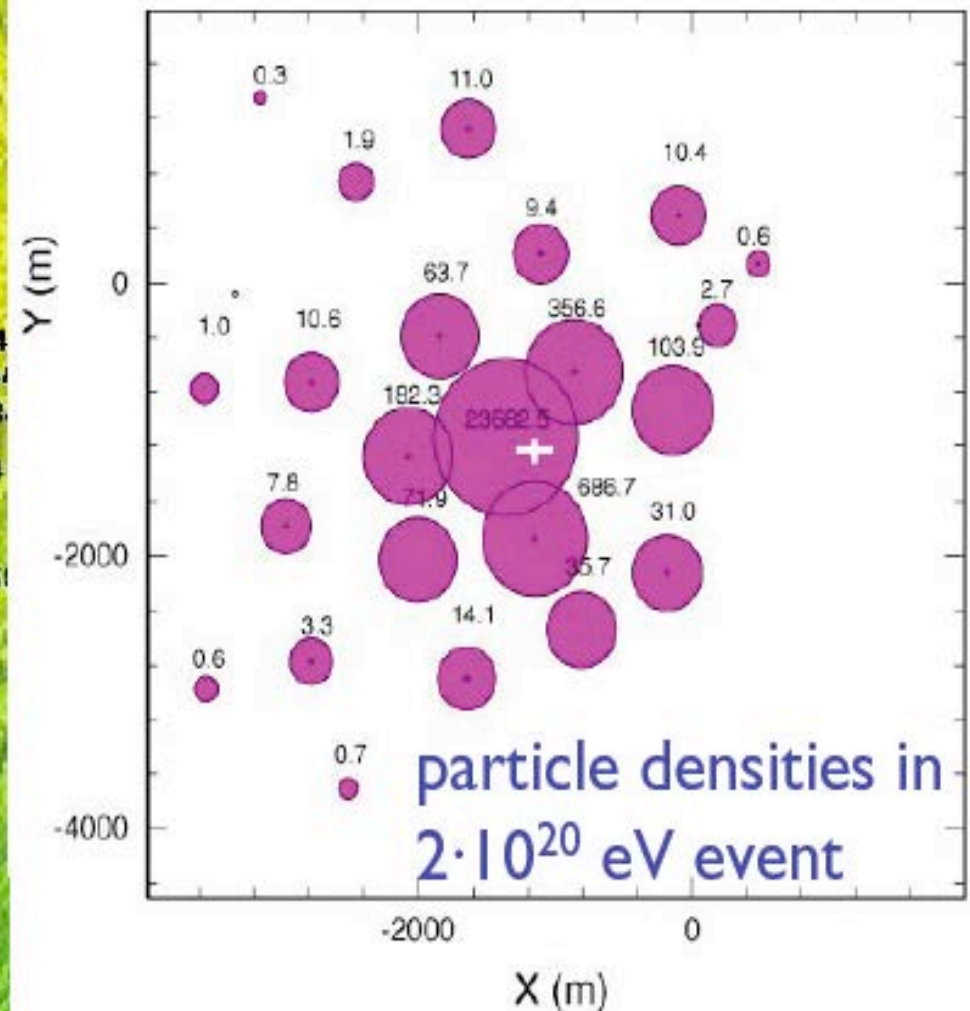
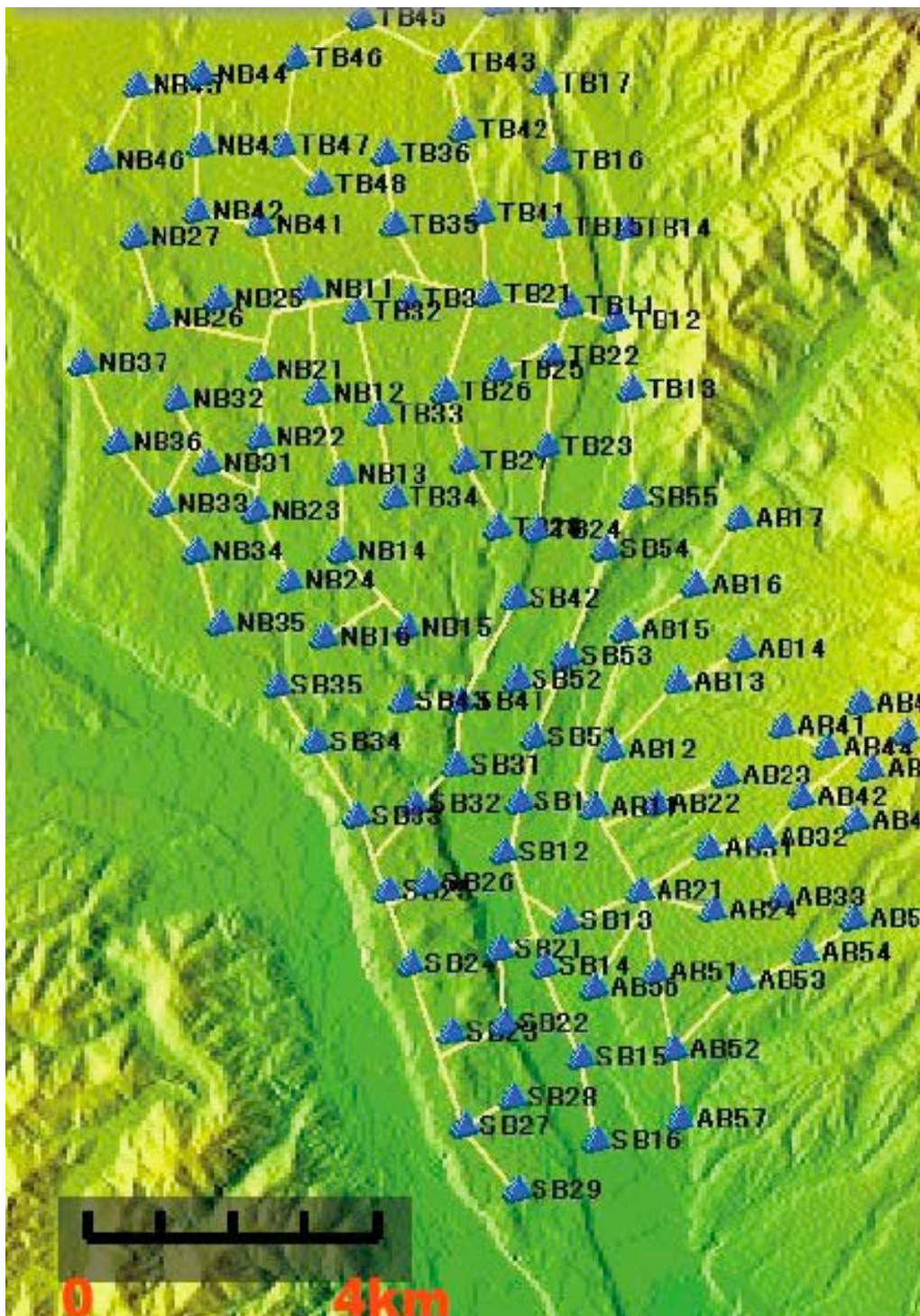
$$\rho(R) = C \left(\frac{R}{R_M} \right)^{-1.2} \left(1 + \frac{R}{R_M} \right)^{-(\eta-1.2)}$$

Density as a function of the distance R_M =Moliere radius = 91.6m in Akeno



AKENO

"Sampled" surface $\sim 100 \text{ km}^2$
111 scintillation counters with area 2.2 m^2
Active until January 2004



The AGASA Telescope Array (Japan)

Akeno Giant Air Shower Array (AGASA) group has published its results on the discovery of 8 air-shower events with the primary energies beyond 10^{20} eV out of 9 years observation.

Space becomes opaque to particles with energies in excess of several times 10^{19} eV because of the 2.7K cosmic microwave background.

Greisen and Zatsepin and Kuzmin independently pointed out that CMB radiation would make space opaque to cosmic rays of very high energy (GZK mechanism). This limitation implies that the sources for these extremely high energy particles need to be less than about 50Mpc from the Earth. Particles with energies in this range are expected to be deflected very little by magnetic fields within or beyond the galaxy. Yet none of these high energy cosmic rays points back to a possible known source.

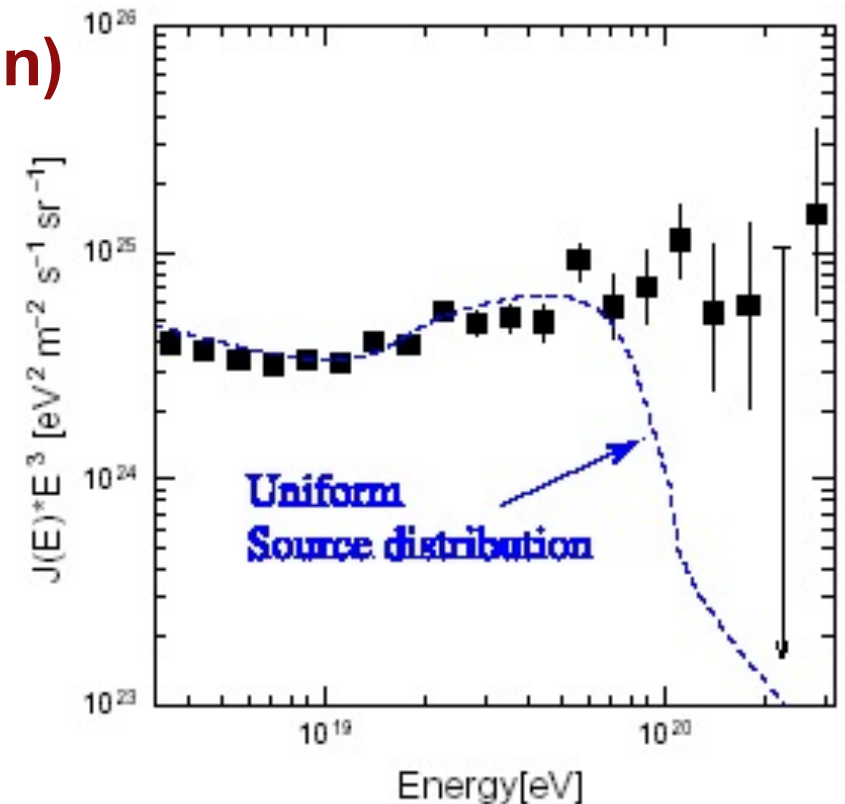


Fig. 3. The energy spectrum of cosmic rays with events up to 60° . The arrows are Poisson upper limits of 90% C.L. The dashed curve is the expected energy spectrum for sources uniformly distributed in the universe taking account of the energy resolution of the AGASA experiment.

The energy spectrum observed by AGASA using events with zenith angles up to 60° is shown in Fig.3, multiplied by E^3 in order to emphasize the detailed structure of the steeply falling spectrum. Error bars represent the Poisson upper and lower limits at 68% and arrows are 90% confidence level (C.L.) upper limits. There is no cutoff around GZK energy ($\sim 4 \times 10^{19}$ eV) and the spectrum extends up to a few times 10^{20} eV. The updated spectrum is consistent with that by Takeda *et al.* (1998).

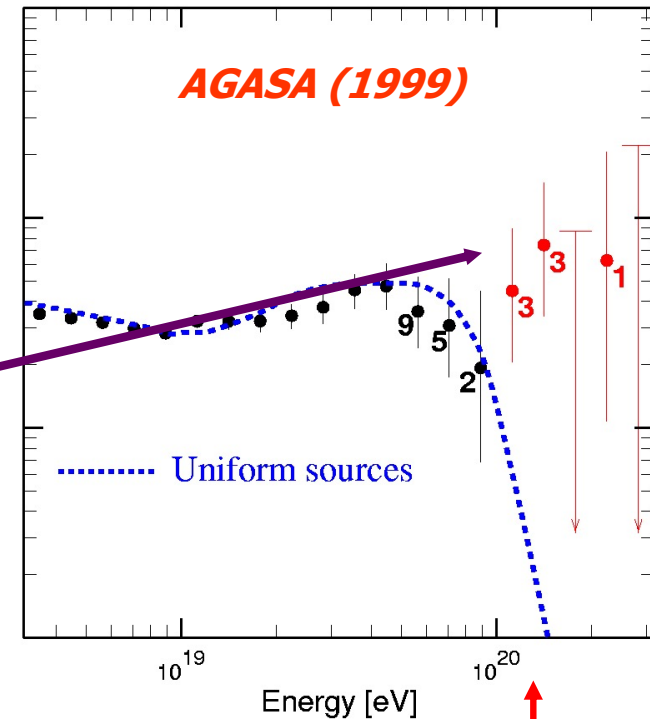
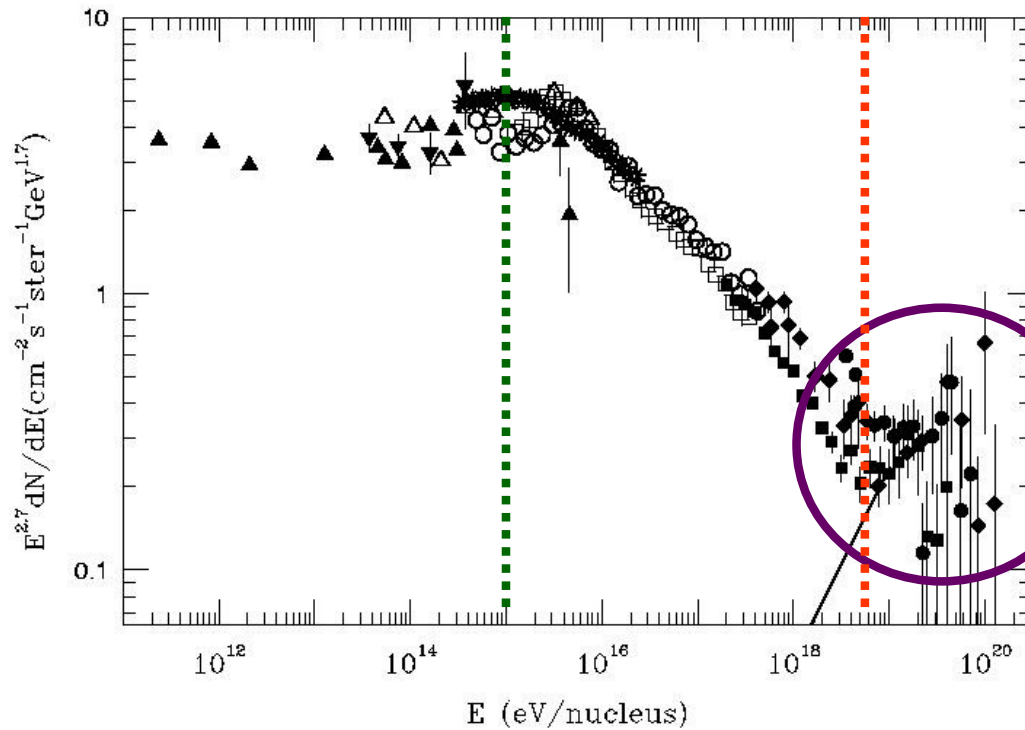
... finally: observed U.H.E. C.R. but their origin cannot be explained

galactic origin

galactic component decreases

Extra galactic ?

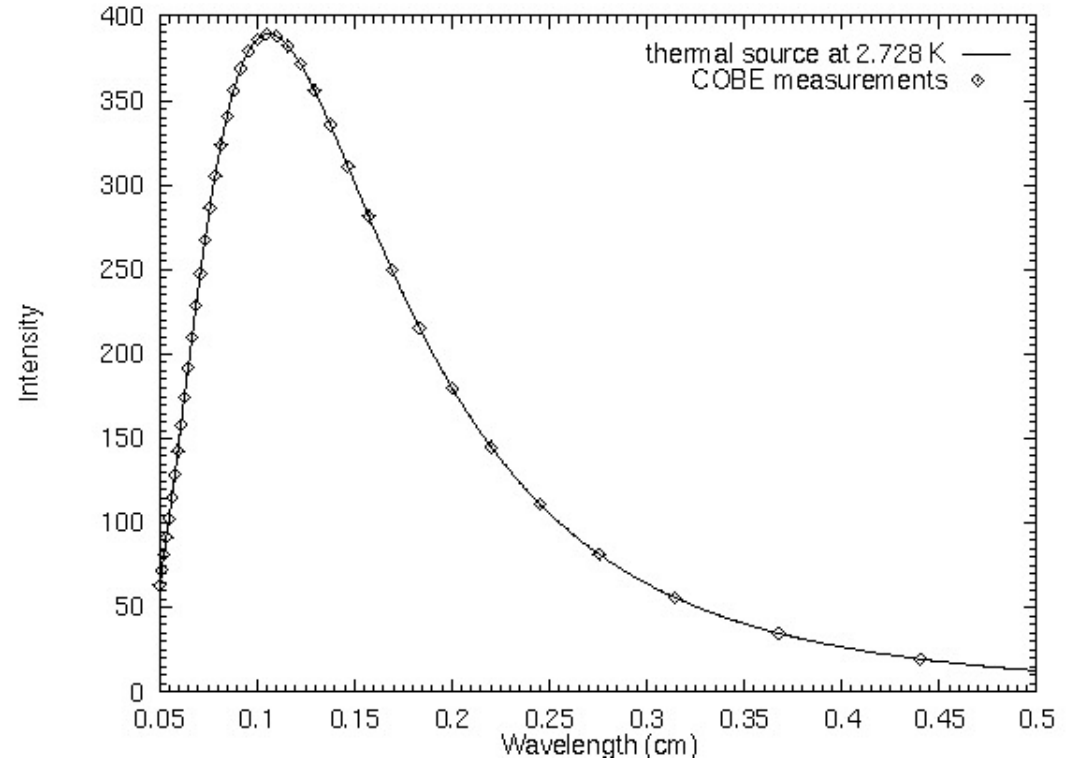
10^{20} eV \approx 17 Joules



Cut-off expected if GZK effect is active

General Properties of the CMBR

- * The radiation has very low temperature: $T \sim 2.7$ Kelvins.
- * The spectrum of the radiation is well-described by a blackbody spectrum.
- * The radiation is isotropic, i.e., it is very close to the same temperature all across the sky: temperature differences of $< 0.004\%$ on angular scales of 7 degrees (excluding a well-known 0.12% variation known as the dipole anisotropy).
- * The temperature over the sky, although very smooth does exhibit structure.



Per $T = 2.725$ K (present day CBR temperature)

$$\mathbf{kT = (8.617 \cdot 10^{-5} \text{ eV/K}) \cdot 2.725 \text{ K} = 2.35 \cdot 10^{-4} \text{ eV}}$$

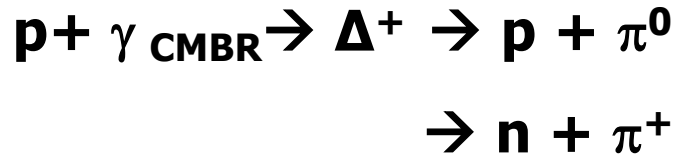
$$\mathbf{\text{But: } E_{\text{peak}} = 2.70 \cdot k \cdot 2.725 = 6.34 \cdot 10^{-4} \text{ eV}}$$

$$\mathbf{E_{\text{mean}} = 2.82 \cdot k \cdot 2.725 = 6.62 \cdot 10^{-4} \text{ eV}}$$

let's use for these photons an energy in the high energy

$$\mathbf{\text{tail } E_{\gamma} = 1.4 \cdot 10^{-3} \text{ eV}}$$

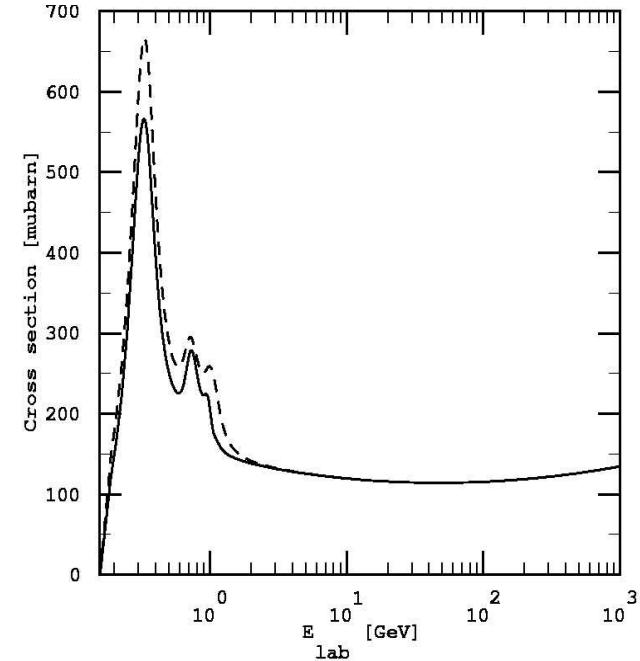
Nucleons propagation and interactions in the Universe:



Per $T = 2.725 \text{ K}$ (present day CMBR temperature)

$\langle E_{\text{CMBR}} \rangle \approx 6.62 \cdot 10^{-4} \text{ eV}$, but we will not use $\langle E_{\text{CMBR}} \rangle$

let's use for these photons an energy in the high energy tail $E_\gamma = 1.4 \cdot 10^{-3} \text{ eV}$



$$s_{out} = (m_p + m_\pi)^2$$

$$s_{in} = (E_p + E_{\text{CMBR}})^2 - (\vec{p}_p + \vec{q}_{\text{CMBR}})^2 = E_p^2 + E_{\text{CMBR}}^2 + 2E_p E_{\text{CMBR}} - p_p^2 - q_{\text{CMBR}}^2 - 2|\vec{p}_p| \cdot |\vec{q}_{\text{CMBR}}| \cos(\theta)$$

$$s_{in} = E_p^2 - p_p^2 + 2E_p E_{\text{CMBR}} - 2|\vec{p}_p| \cdot |\vec{q}_{\text{CMBR}}| \cos(\theta) \approx m_p^2 + 2E_p E_{\text{CMBR}} (1 - \cos(\theta))$$

la condizione di produzione della risonanza Δ^+ richiede $s_{in} \geq (m_p + m_\pi)^2$

$$m_p^2 + 2E_p E_{\text{CMBR}} (1 - \cos(\theta)) \geq m_p^2 + m_\pi^2 + 2m_p m_\pi \quad \text{per } \theta = \pi \Rightarrow 1 - \cos(\theta) = 2$$

$$E_p \geq \frac{2m_p m_\pi + m_\pi^2}{4E_{\text{CMBR}}} = \frac{2 \cdot 938 \cdot 10^6 \cdot 140 \cdot 10^6 + (140 \cdot 10^6)^2}{4 \cdot 1.4 \cdot 10^{-3}} \approx 5.0 \cdot 10^{19} \text{ eV} = 50 \text{ EeV} \sim 8J$$

... a possible explanation for the “GZK cutoff”

$N\pi$ production

Proton attenuation length

$$L = \left(\sigma_{N\gamma} \rho_{CMBR} \right)^{-1}$$
$$\approx \left(130 \mu b \cdot 410 \text{ cm}^{-3} \right)^{-1} \approx 6 \text{ Mpc}$$

al picco della risonanza

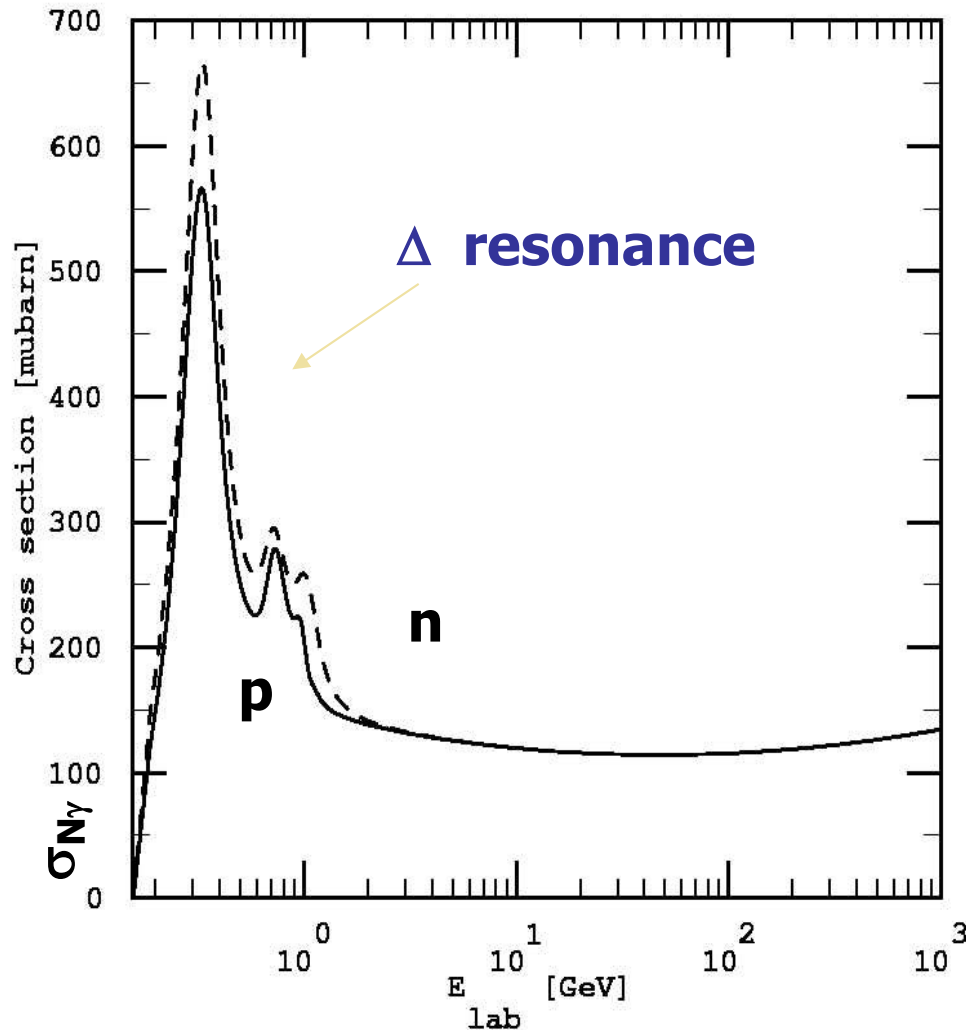
$$\approx \left(550 \mu b \cdot 410 \text{ cm}^{-3} \right)^{-1} \approx 1,4 \text{ Mpc}$$

Remember:

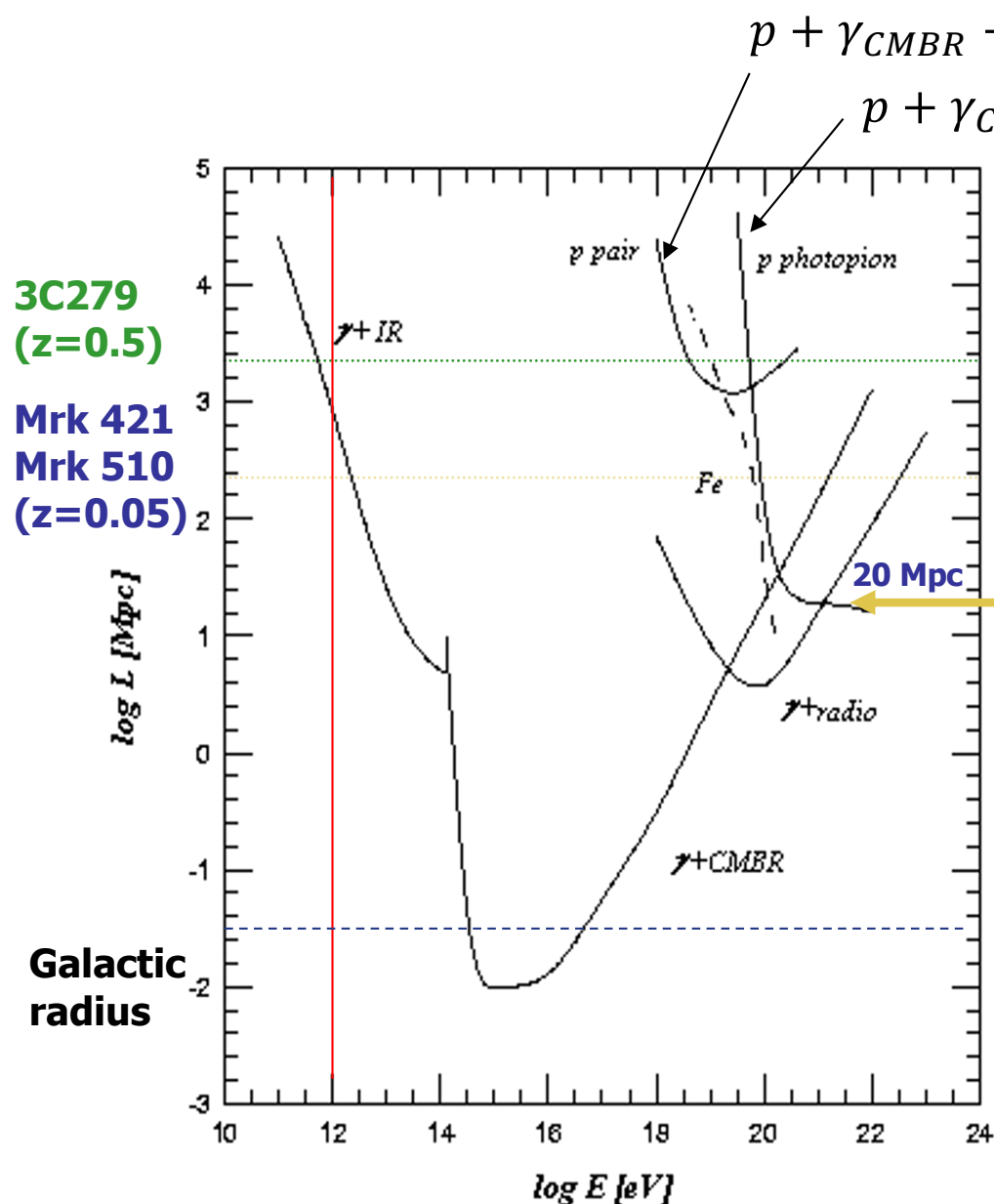
-the density of CMBR photons is

$$\rho_{CMBR} \sim \text{photon/cm}^3 = 410/\text{cm}^3$$

$$1 \text{ pc} \sim 3.086 \cdot 10^{18} \text{ cm}$$



The “GZK cutoff” effect: a limited propagation for p and γ



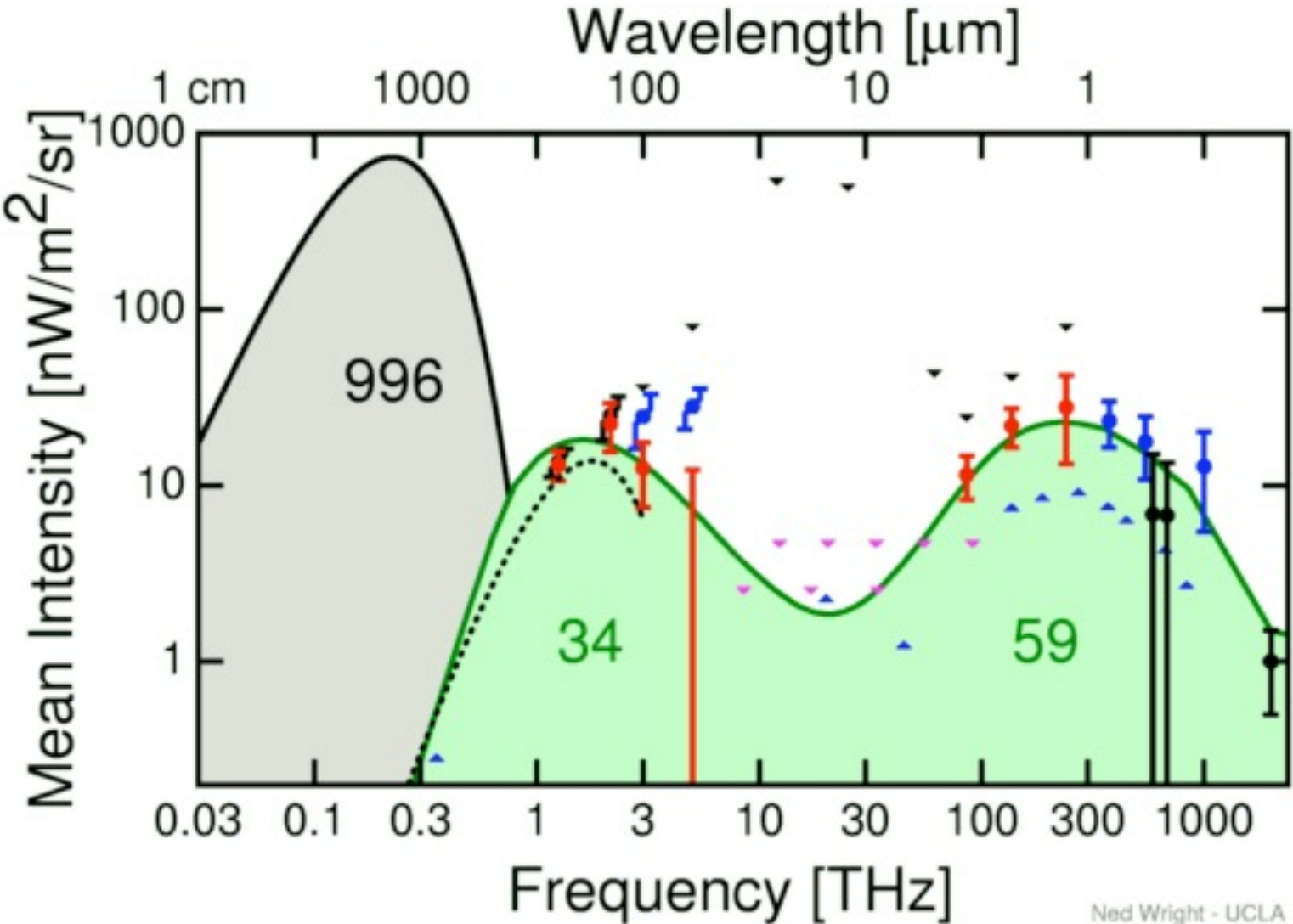
γ observed from extragalactic sources only up to TeV energies

UHE protons and gammas are strongly attenuated in the Universe

AGASA and Fly's Eye 10^{20} eV events analysis has not conducted to source identification.

Only UHE neutrinos could be detected from far Universe

Interactions with the cosmic infrared radiation must also be considered



↑
 $\sim 4 \cdot 10^{-3} \text{ eV}$

↑
 $\sim 4 \text{ eV}$

Photons have a limited path too...

Interacting both with the CMBR and the "Infrared" (IR) radiations

photons: pair production $\gamma_{HighEnergy} \gamma_{CMBR} \Rightarrow e^+ e^-$

$$E_{\gamma} \geq \frac{m_e^2}{E_{CMBR}} \approx \frac{10^{12} eV^2}{1.4 \cdot 10^{-3}} \approx 0.7 \cdot 10^{15} eV$$

"regeneration" via Inverse Compton Scattering but at lower energy
(EGRET observations) $\sigma \propto 1/E_{\gamma}$

heavy nuclei:

loose ~ 4 nucleons/Mpc

Greisen Zatsepin Kuzmin effect

Particles lose energy interacting with background radiation/particles

- **protons**



- **photons**

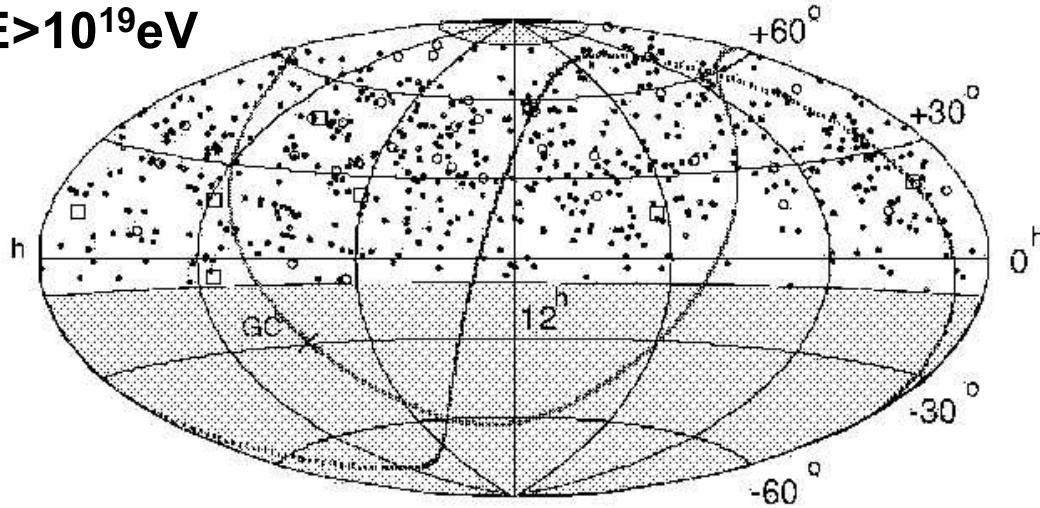


- **neutrinos**



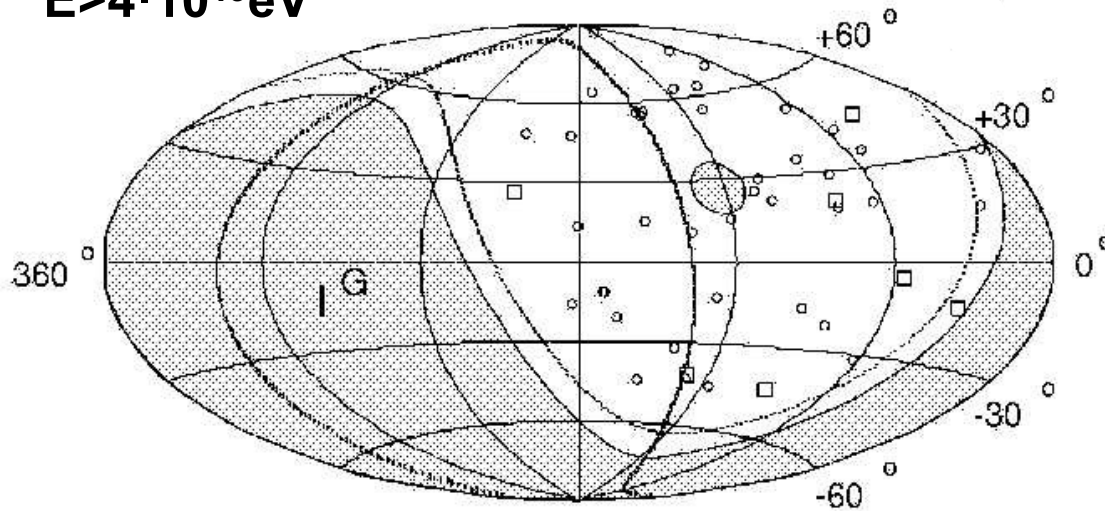
AGASA about the origin of Ultra High Energy C.R.s

$E > 10^{19} \text{ eV}$



Galactic coordinates
AGASA data are consistent with isotropic distribution of sources

$E > 4 \cdot 10^{19} \text{ eV}$

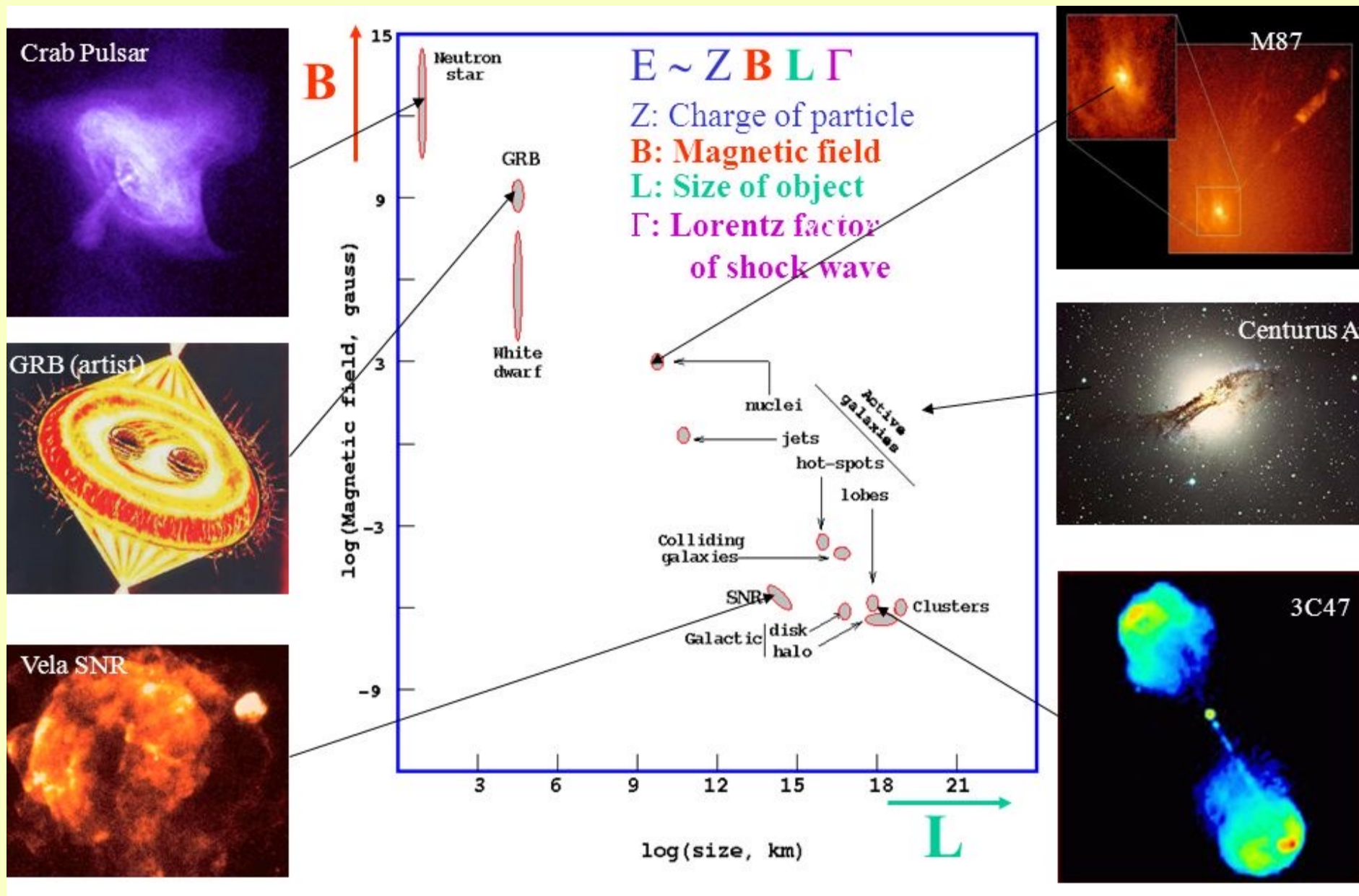


Equatorial coordinates

Possible acceleration mechanisms

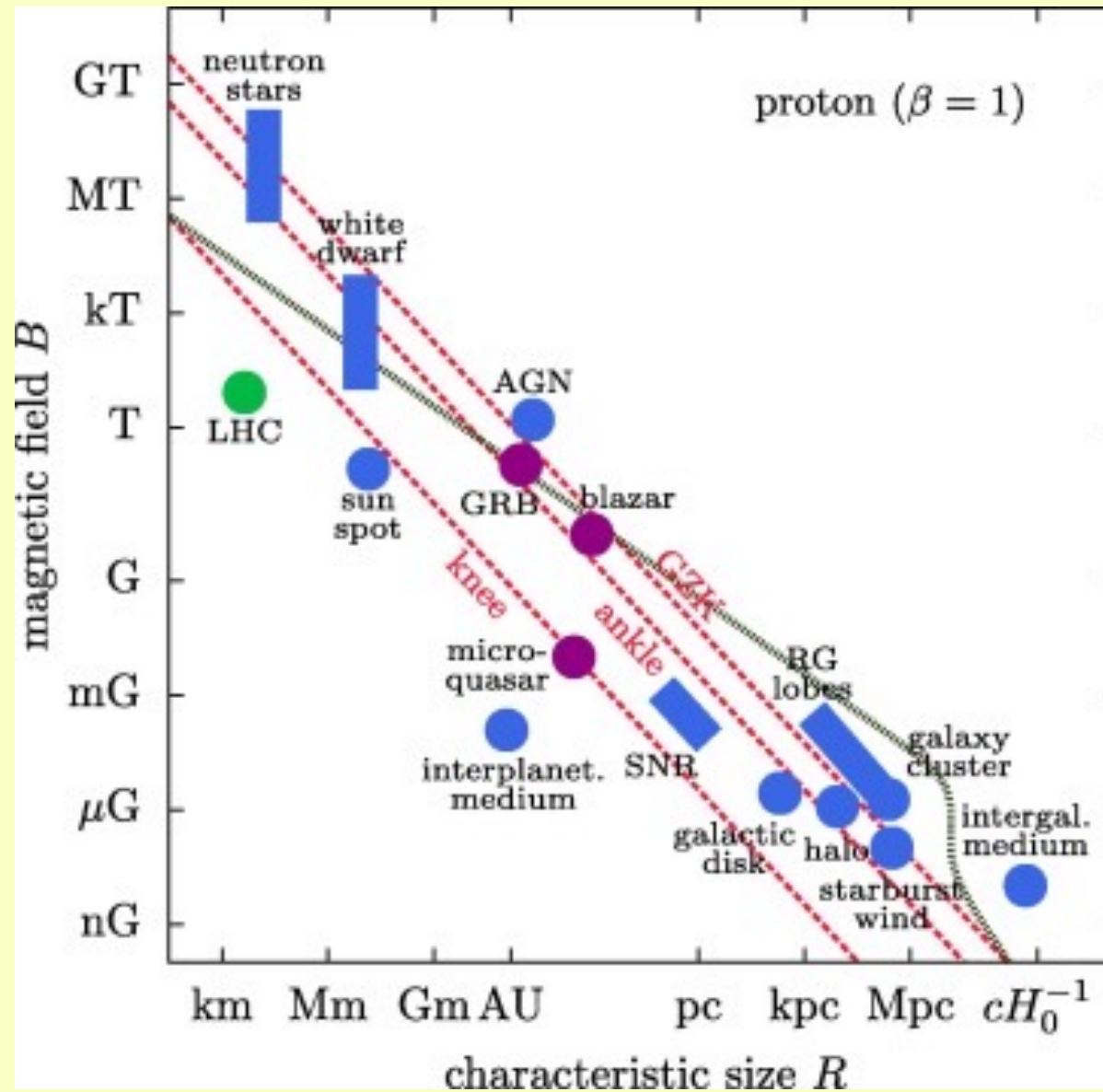
- Fermi acceleration mechanisms, of the second type ($\Delta E/E \propto \beta$) or of the first type ($\Delta E/E \propto \beta^2$)
- Rotating magnetic field of neutron stars, $B \sim 10^8 \text{T}$, rotation period $T \sim 10 \text{ ms}$. $E_{\text{max}} \sim Bc \sim 10^{20} \text{ eV}$;
- Short shocks in high magnetic fields B ; $E_{\text{max}} \sim 10^{16} \text{ eV}$
- Long-lasting shock in weak B fields, galactic winds ; $E_{\text{max}} \sim 3 \cdot 10^{17} \text{ eV}$
- Supernova explosion in the wind of a predecessor object: favored solution to explain events with energy above the knee
- To justify events with $E \leq 10^{20} \text{ eV}$:
 - ✓ accretion in galaxy-sized objects (AGN and/or radio-galaxies)
 - ✓ processes of re-acceleration
 - ✓ decay of massive objects of cosmological origin (Top-Down theories)

Cosmic Accelerators and Hillas Plot (1)



Our Galaxy $L \sim 15 \text{ kpc} \sim 4.5 \cdot 10^{17} \text{ km}$, $B \sim 3 \cdot 10^{-6} \text{ G}$

Cosmic Accelerators and Hillas Plot (2)



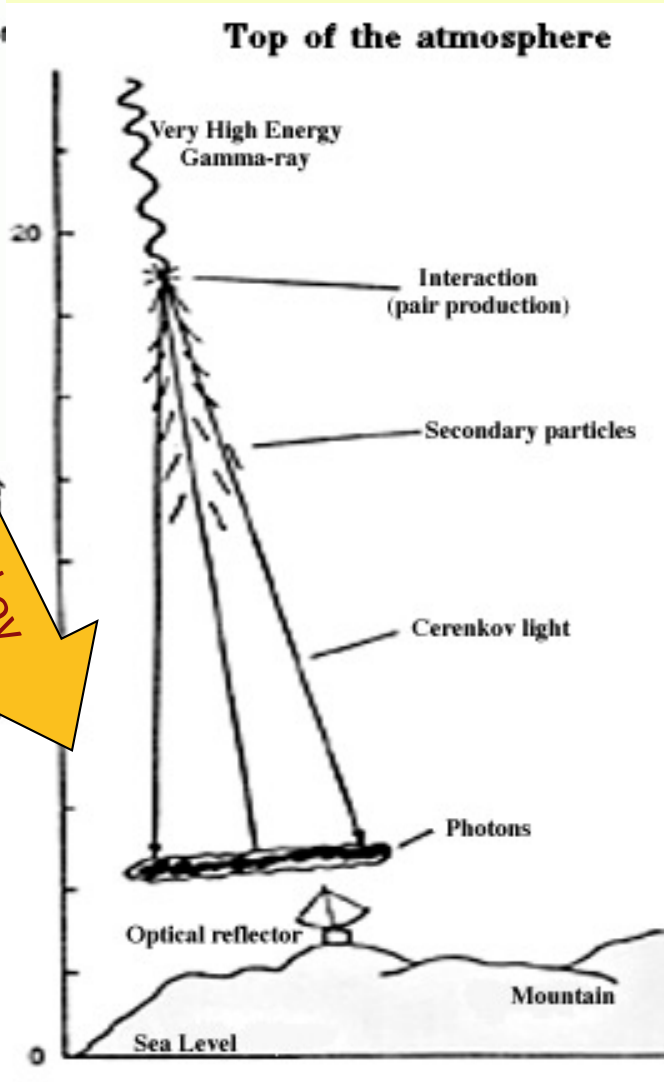
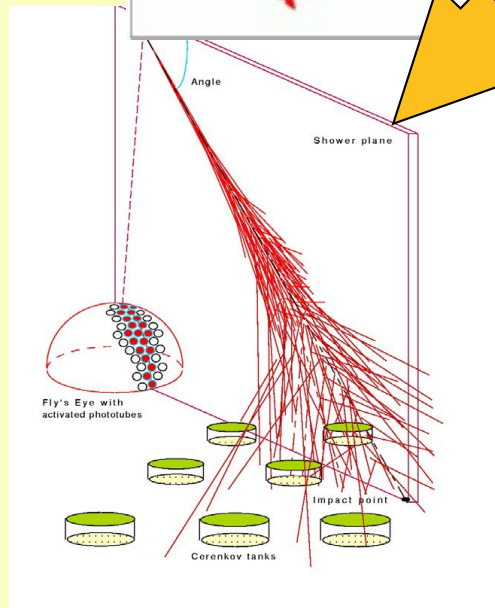
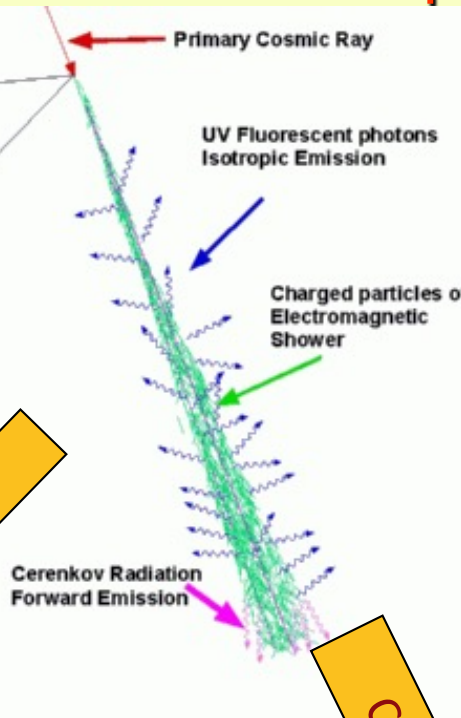
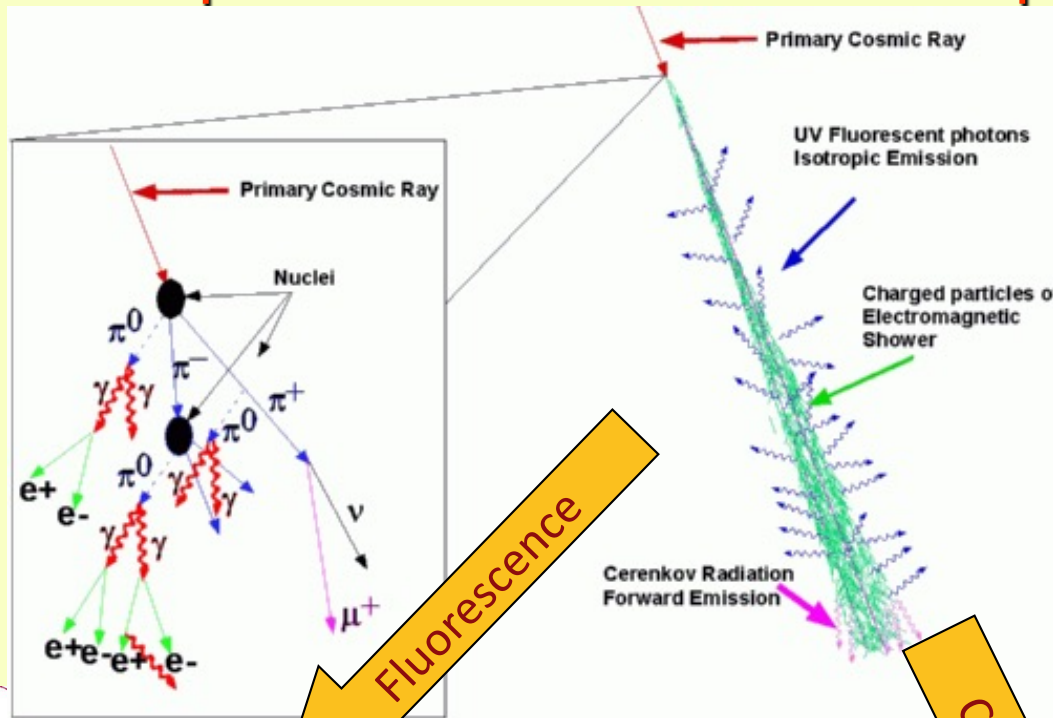
Our Galaxy $L \sim 15$ kpc $\sim 4.5 \cdot 10^{17}$ km, $B \sim 3 \cdot 10^{-6}$ G

The accelerating "shockwaves" EXIST !!!

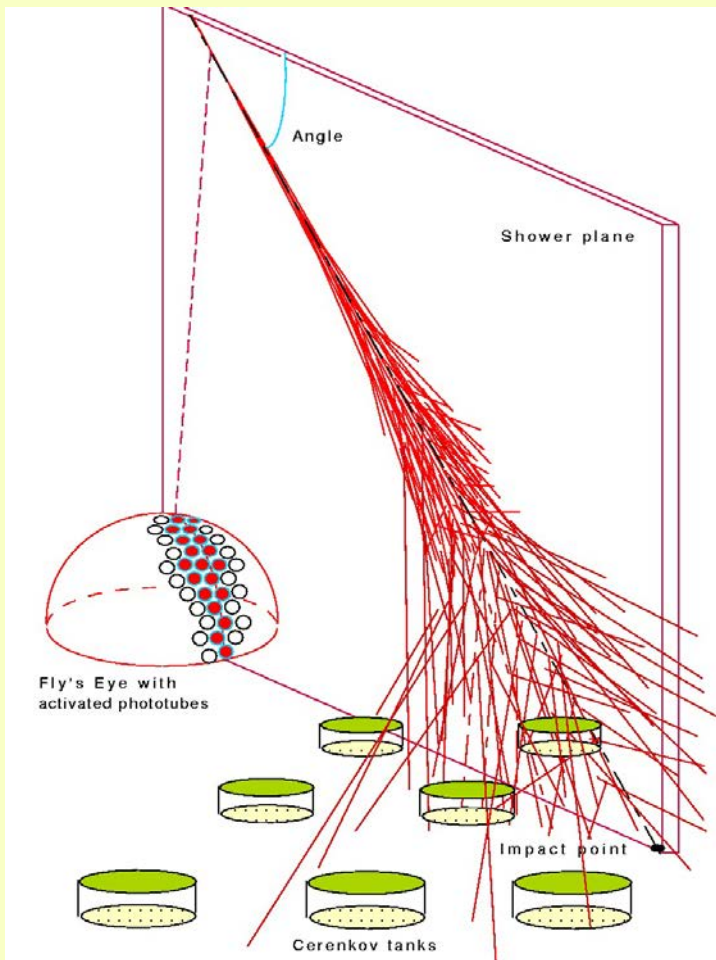


The Hubble Space Telescope imaged this view in February 1995. The arcing, graceful structure is actually a bow shock about half a light-year across, created from the wind from the star L.L. Orionis colliding with the Orion Nebula flow.

Extending the C.R. search energy range: fluorescence photons added to Cherenkov photon detection.



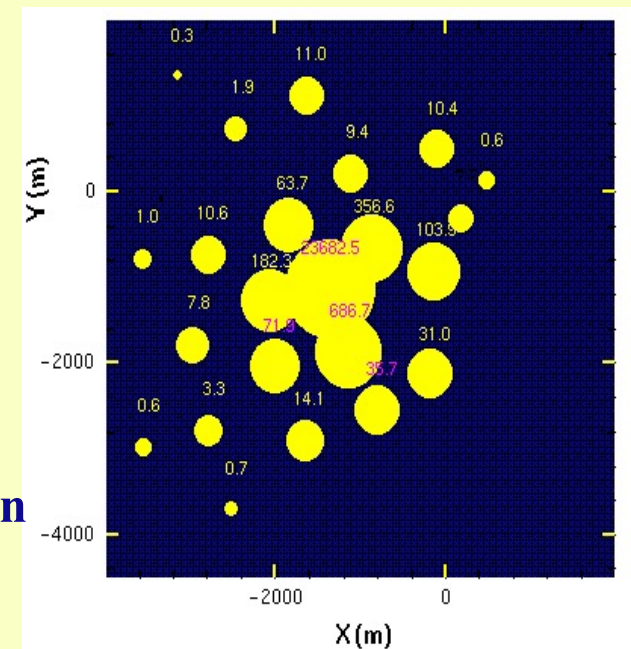
Detection of Cosmic Rays with energy EeV: "hybrid" experiments on the ground



- Experiments sensitive to the "fluorescence" of the N_2 induced by the swarms in the atmosphere (Fly's Eye): they observe **the longitudinal development of the shower**
- X_0, X_{max} ("chemical" nature of the primary)
- The experiments with ground detectors (AGASA) sample the lateral development of the showers **and in this way they can obtain E_0**

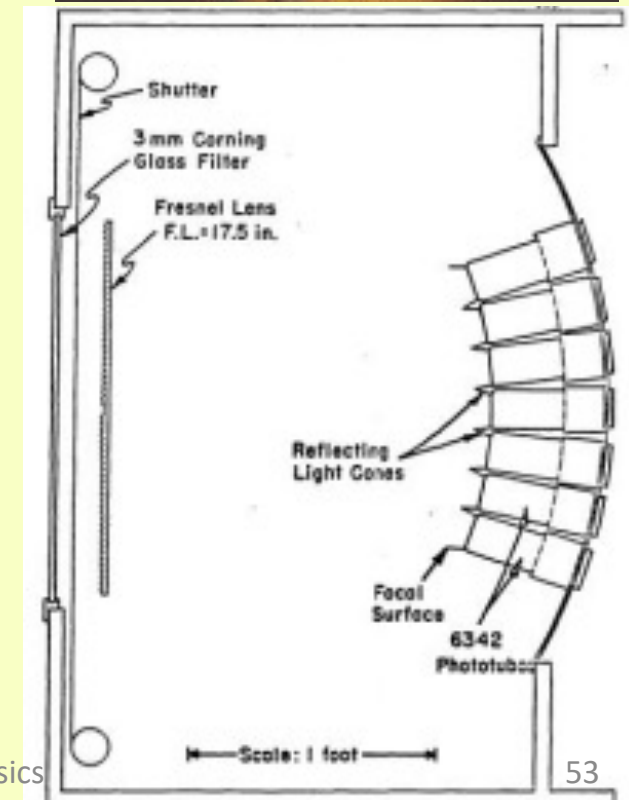
Cosmic Rays induce "extensive air showers" (EAS) in the atmosphere. Most of the C.R. initial energy goes into energy lost, dE/dx , from the shower particles in the atmosphere. Of this energy the fraction $\sim 5 \cdot 10^{-5}$ is visible as fluorescence light in air in the wavelength range 300nm-420nm:

~ 4.8 photons/m/electron



Apparati Fly's Eye, la storia

The first attempts to observe extensive air showers by the fluorescent (more correctly luminescent) emissions were made by a group led by Kenneth Greisen at Cornell University in the middle 1960's. Greisen was the first graduate student of Bruno Rossi. Rossi and Greisen both worked on the Manhattan Project in Los Alamos during World War II. Greisen was in fact an eyewitness at the Trinity test and filed an official report of his observations. In 1967, Greisen's group constructed a full-scale fluorescence experiment. The Cornell detector images the night-sky using **500 photo-multiplier tubes (PMT)**. **Each PMT** corresponds to a **pixel covering a solid angle of 0.01 steradian (~6 degrees by 6 degrees)**. The 500 PMT's are divided into 10 modules. Each module is equipped with a **0.1 m² Fresnel lens**. The Fresnel lens is shown on the left, and the PMT's are arranged at the focal surface (roughly spherical). An optical filter is placed before the lens at the entrance aperture to reduce night-sky background and eliminate contamination from filament lamps visible near the horizon. **The Cornell detector was triggered by requiring a coincidence between any two adjoining pixels. The signals are piped to a bank of 3" cathode ray tube displays, and recorded on 70 mm film.** This detector operated for several years but was not sensitive enough to detect UHE cosmic rays reliably. In particular, the 0.1m² lenses are too small to collect sufficient light, and the atmosphere in Up-state New York is too contaminated with water vapour and aerosols.



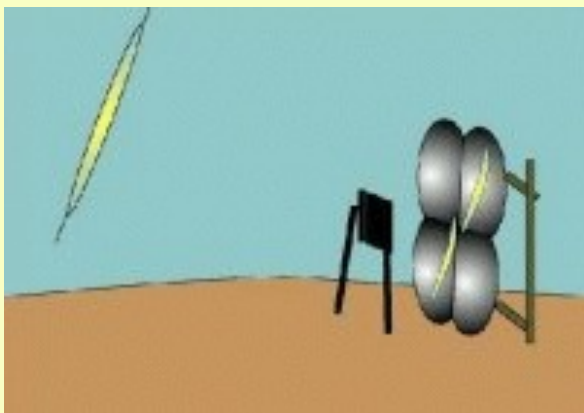
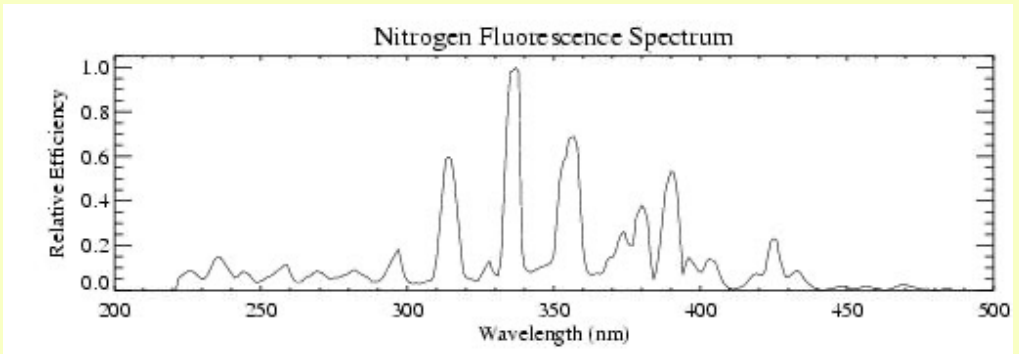
“fly’s eyes” signals - fluorescence in air

The term "fluorescence" refers to the process by which atoms absorb photons of one wavelength and emits photons at a longer wavelength. The passage of charged particles in an extensive air shower through the atmosphere results in the ionization and excitation of the gas molecules (mostly nitrogen). Some of this excitation energy is emitted in the form of visible and UV radiation.

Rigorously speaking, this is a "luminescence" process analogous to the emission by mercury in a fluorescent light. The name "Air Fluorescence" has been adopted by the astrophysics community to describe the scintillation light from extensive air showers. This misuse of the term is in due to the apparent similarity to the workings of a

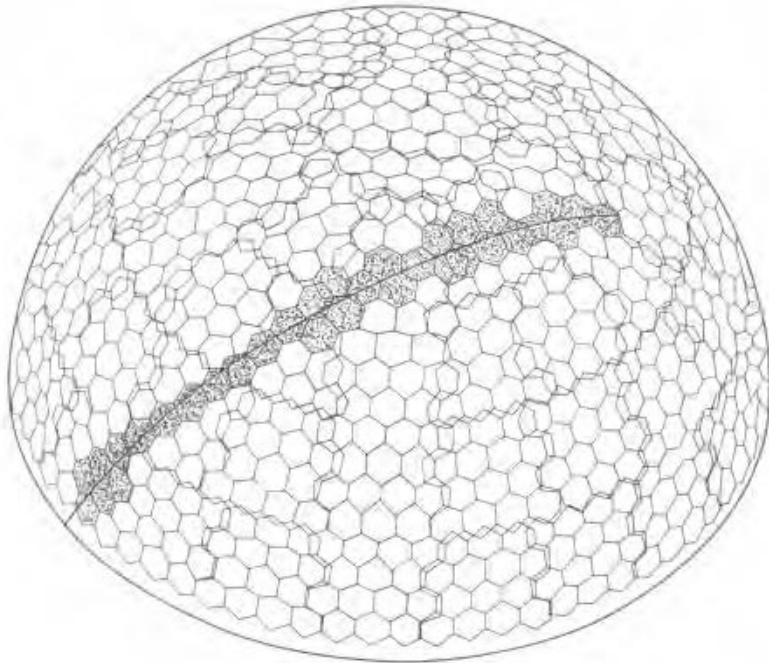
fluorescent light. On the positive side, this usage makes it easy to distinguish between a fluorescence detector from a scintillation detector (the latter is the name commonly used for desktop particle detection devices made from inorganic salts or organic plastics).

Schematic of a fluorescence air shower detector. The scintillation light is collected using a lens or a mirror and imaged on to a camera located at the focal plane.



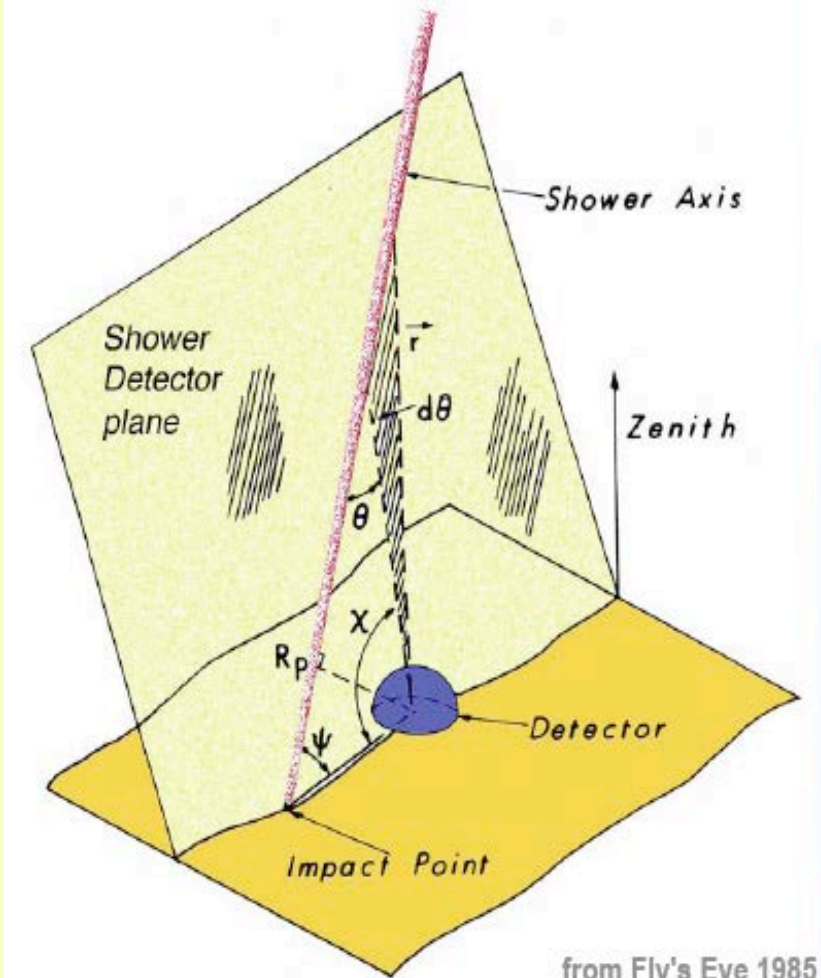
The camera pixelizes the image and records the time of arrival of light along with the amount of light collected at each pixel element. This technique can be made to work on clear, moonless nights, using very fast camera elements to record light flashes of a few microseconds in duration. The shower trajectory can be reconstructed by timing the atmospheric scintillation light radiated by the shower as it passes overhead.

Fly's Eye Detector Parameters

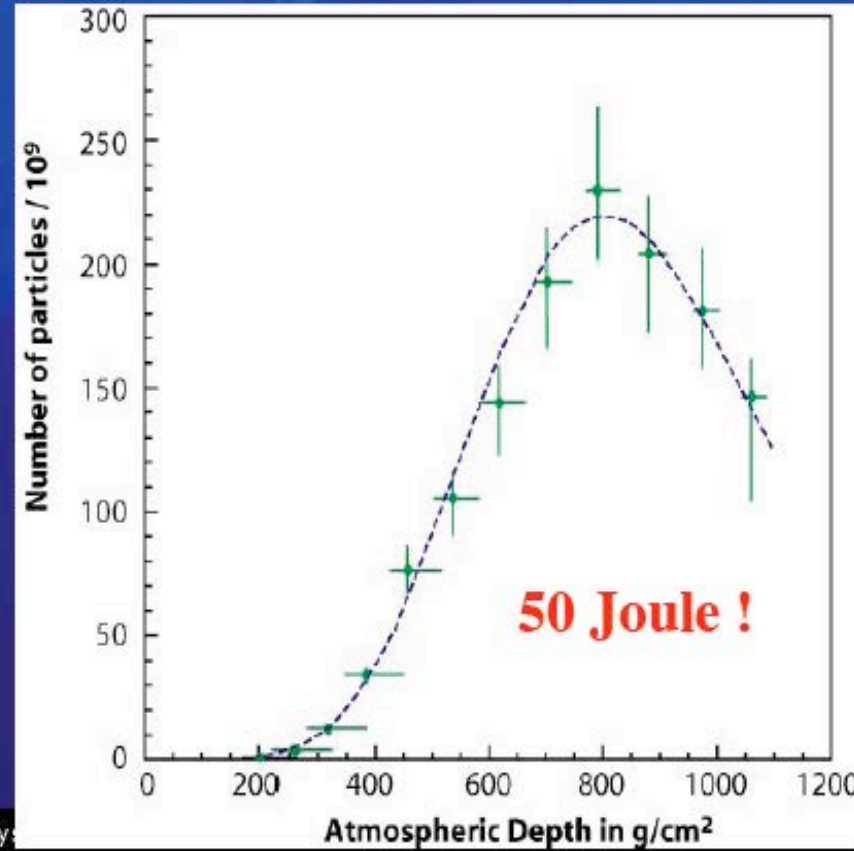
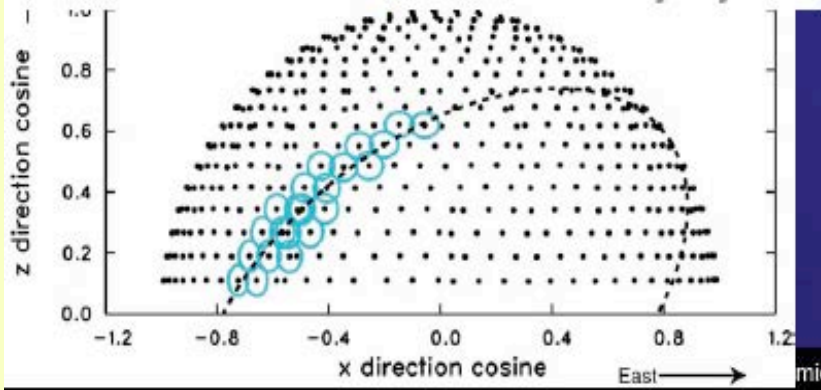


Number of mirrors	67
Diameter of mirrors	1.575 m
Focal Length	1.500 m
Number of PMT (and Winston cones)	880
Mirror Obscuration by PMT cluster	13%
Mirror-cone efficiency product	~ 0.7
PMT type	EMI 9861
B	
Peak PMT quantum efficiency at 360 nm	0.21
Angular Aperture per PMT	91.5 mr
Solid Angle per PMT	6.57 msr
Number of electronic channels	2640
Charge dynamic range	10^5 linear

The most energetic event seen by Fly's Eye

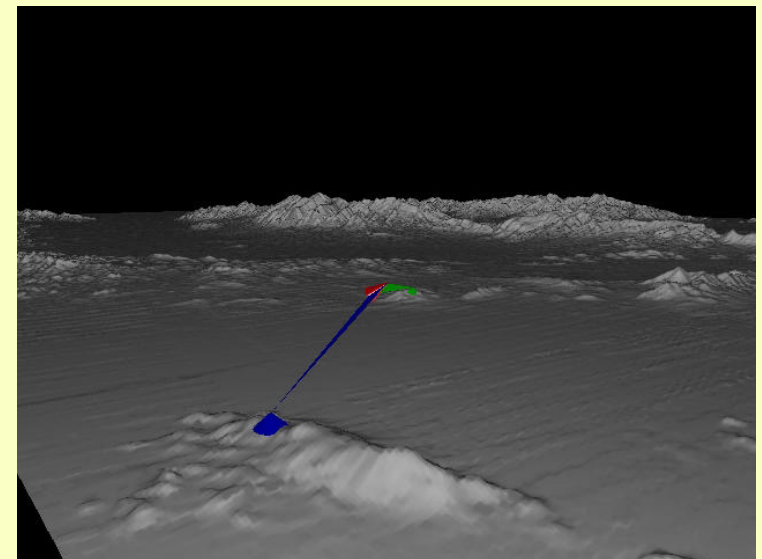
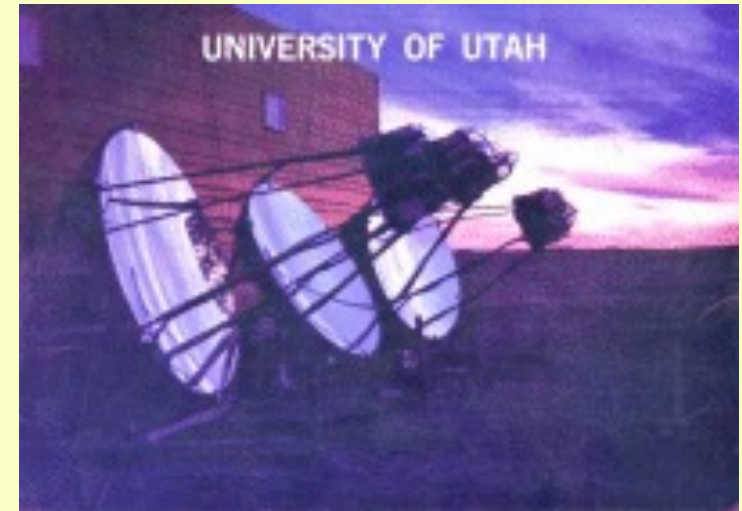


$3.2^{+0.4}_{-0.5} \times 10^{20}$ eV
(Astrophys. J. 1995)



From the first “Fly’s Eye” to HiRes

In 1976, Physicists from University of Utah were the first to detect fluorescence light from cosmic ray air showers. **Three prototype modules** were used in a test at Volcano Ranch near Albuquerque, New Mexico. **Each prototype module contained a 1.8 m diameter mirror for light collection, with 14 PMT's at the focal plane. Each PMT covers a solid angle about 0.008 steradians (~5 degrees by 5 degrees) in the sky. The large mirrors provided a 20-fold increase in the light collection area over that of the lenses used in them Cornell detector.** The clear desert air also provided much improved visibility over the Cornell experiment. The HiRes experiment is a new and significantly upgraded version of the original Fly's Eye experiment. **Cosmic rays make extensive air showers in the atmosphere. Most of the initial energy becomes charged particle energy loss, dE/dx , in the atmosphere. Of that about 5×10^{-5} appears as air fluorescence light which is mainly in the wavelength interval 300nm to 420nm. Thus the air fluorescence signal provides a calorimetric measurement directly proportional to the initial cosmic ray energy.** HiRes uses the resulting air fluorescence to measure the properties of the initial cosmic rays. **Showers are observed by 2 fluorescence eyes, in stereo,** to obtain a precision measurement.

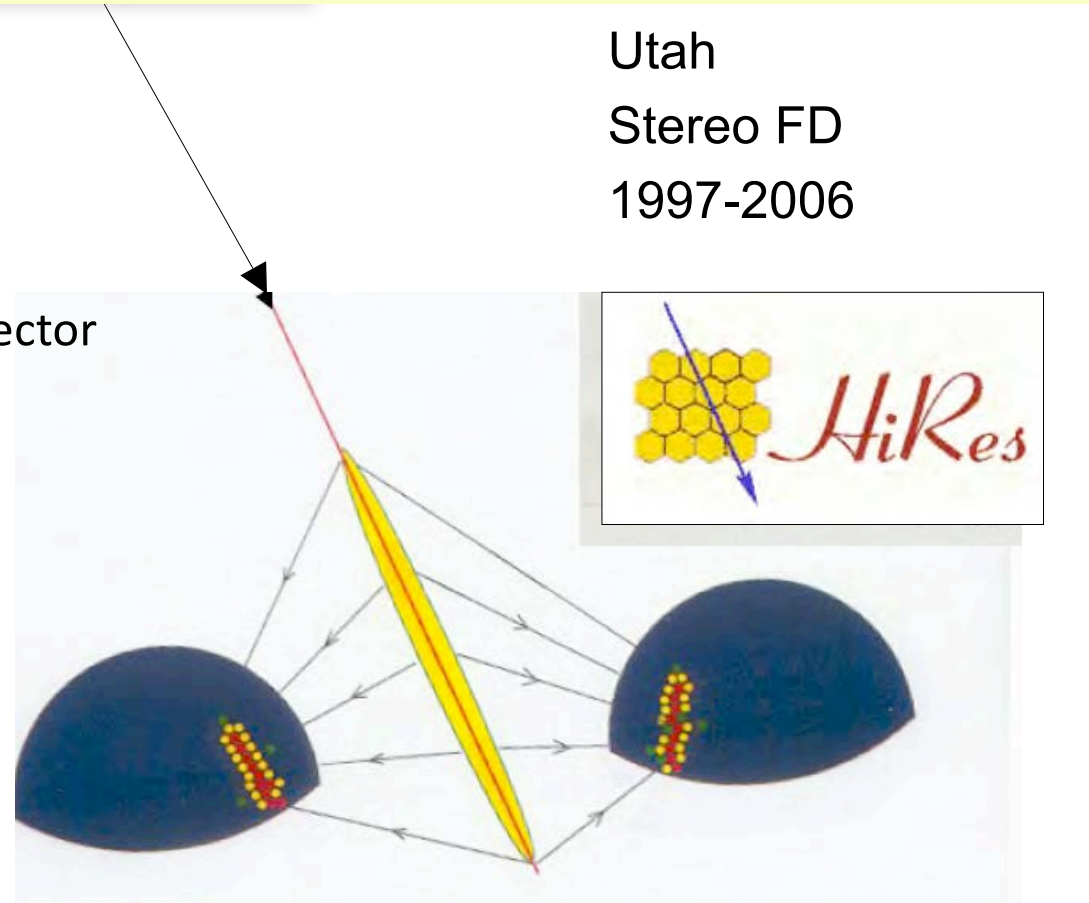


The fluorescence detectors require cloudless moonless nights with little aerosol light scattering. The optimal conditions are found in desert locations and have about a 10% duty factor.

HiRes Experiment "stereo"

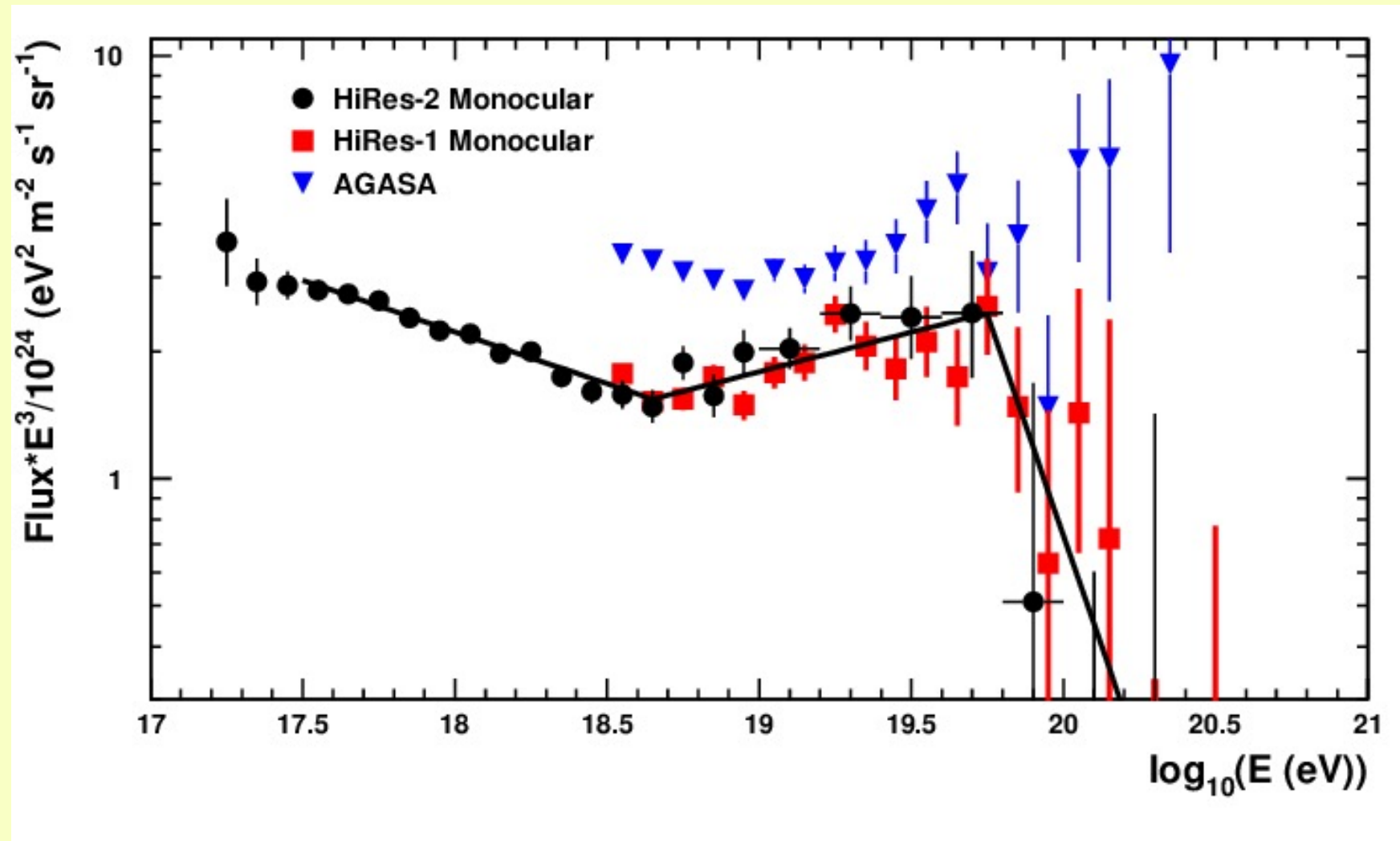
The stereo detection:

- allows the knowledge shower axis-detector
- improves the energy reconstruction
- improves the angular reconstruction

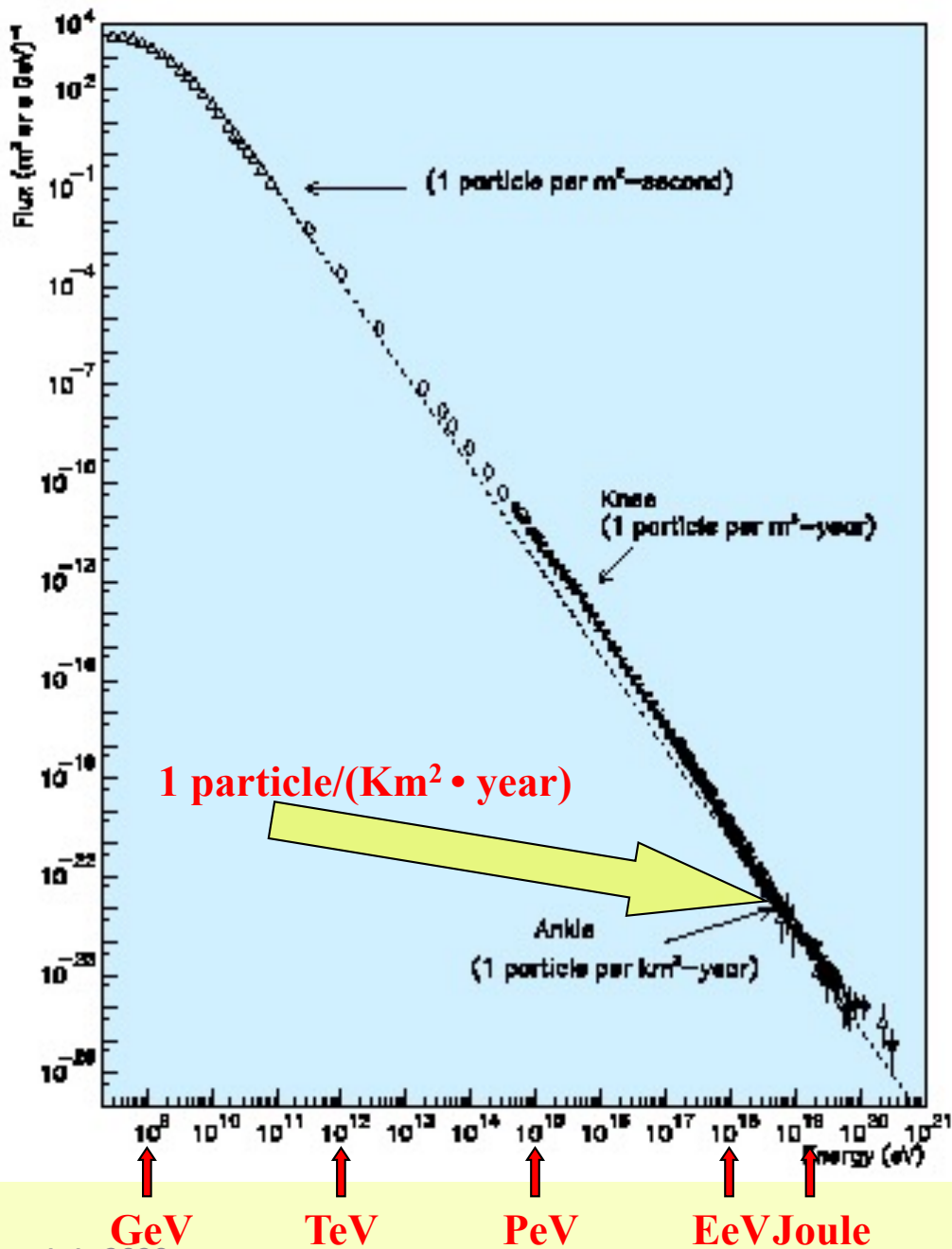


- Fluorescence UV photons imaged with a pixel detector
- Track the longitudinal profile

HiRes Energy spectrum



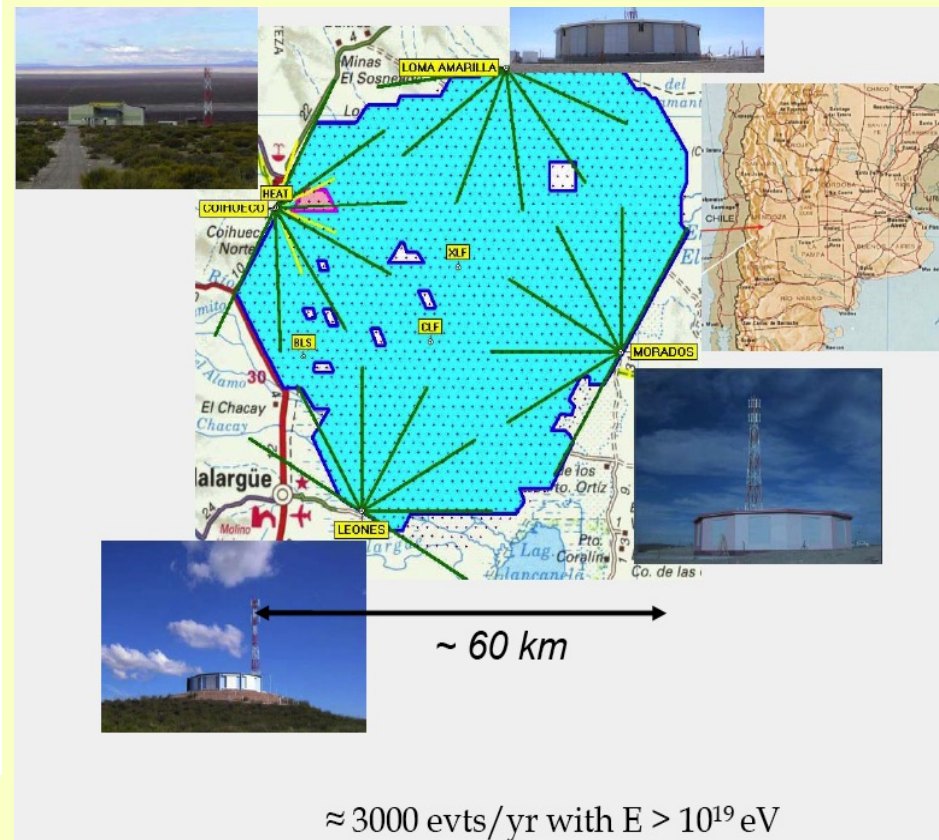
Detection of U.H.E. Cosmic Rays ($E \gg 100$ PeV)



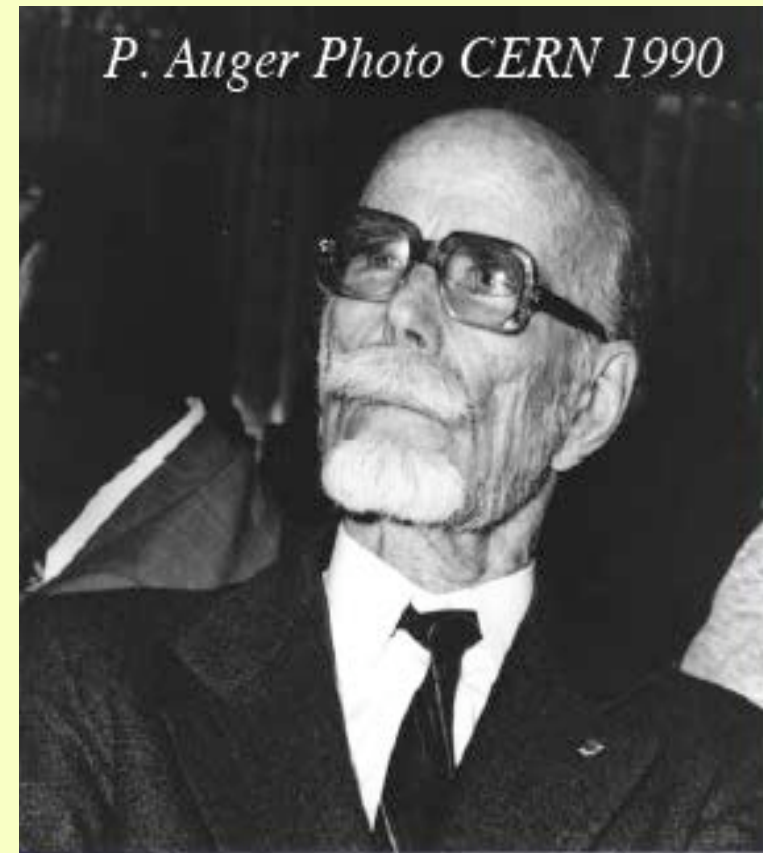
The study of cosmic rays with $E \gg 100$ PeV requires:

- \Rightarrow large equipment (sampling, fluorescence detection in the atmosphere, ...)
- \Rightarrow on the earth's surface or in space

An example the Pierre Auger Observatory



1938: Pierre Auger and P. Ehrenfest at the Jungfrauoch detecting C.R. showers



The Pierre Auger Observatory/experiment

Initial idea: two gigantic apparatuses of 3000 km² (North and South America) with **1600 water Cherenkov counters and 4 fluorescence detectors** to measure the energy, the arrival direction of the primary particles and their mass composition in the energy range $> 10^{19}$ eV. **Totale sensible surface ~ 3000 km².**

Expected fluxes:

$E > 10^{19}$ eV \rightarrow 1 R.C./(km²·year) \rightarrow collected ~ 3000 events/year

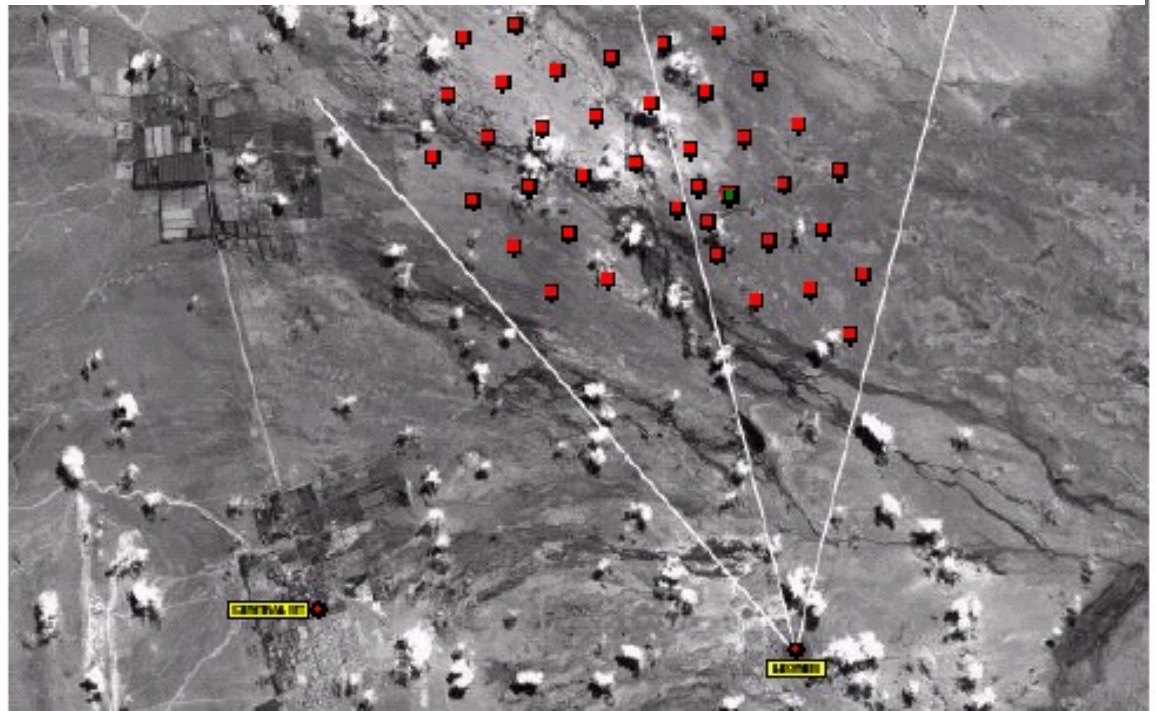
$E > 10^{20}$ eV \rightarrow 1 R.C./(km²·century) \rightarrow collected ~ 30 events/year

$\sim 15\%$ of such events will also be observable with fluorescence detectors

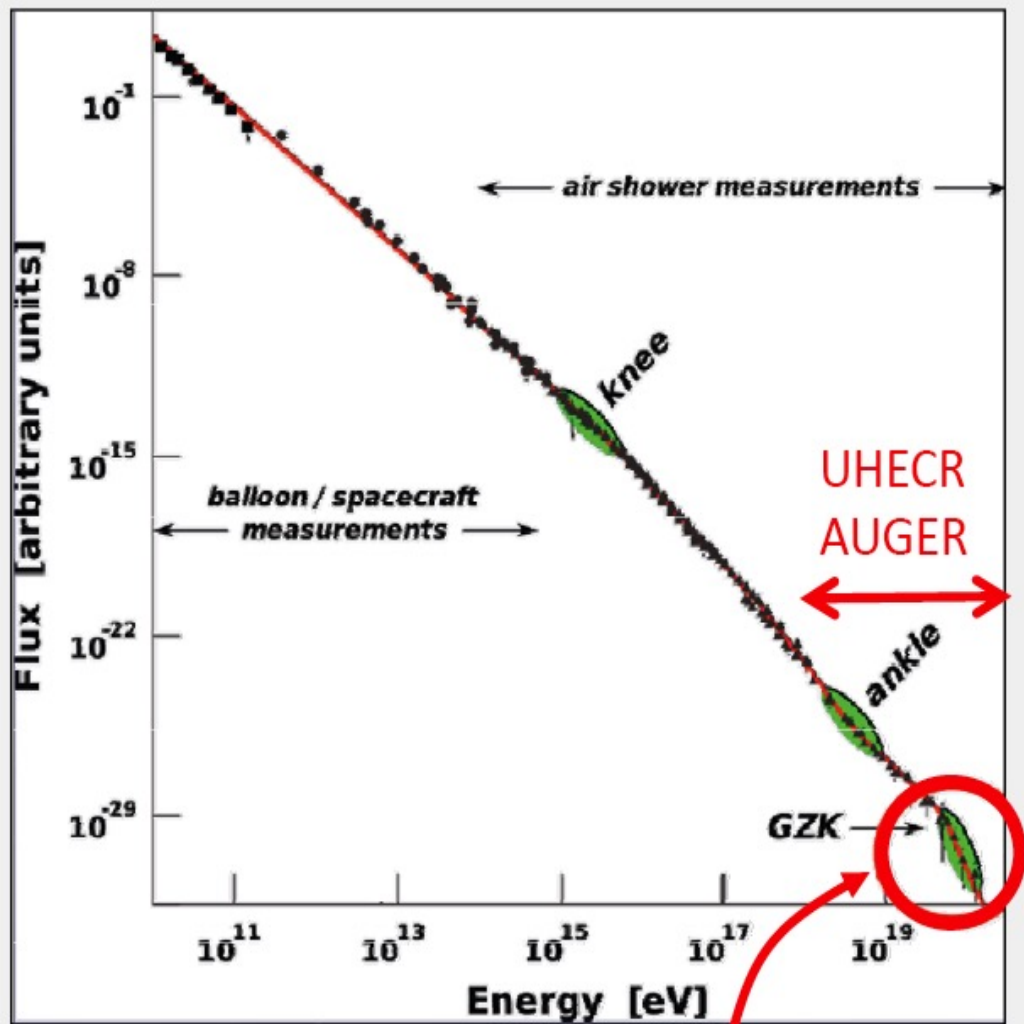
Cherenkov detectors are made with "tanks" containing 12 tons of water and photobubes. The modules use solar energy and transmit the information to the central computer "by radio" for data acquisition.



Satellite view of the South apparatus (Argentina). You can see the positions of the surface detectors (red squares, the distance between two detectors close ~ 1.5 km) The lines represent the "visual field", about 30° , of the first two fluorescence detectors.



Pierre Auger Observatory (PAO): scientific goals



< 1 particle/km²/century

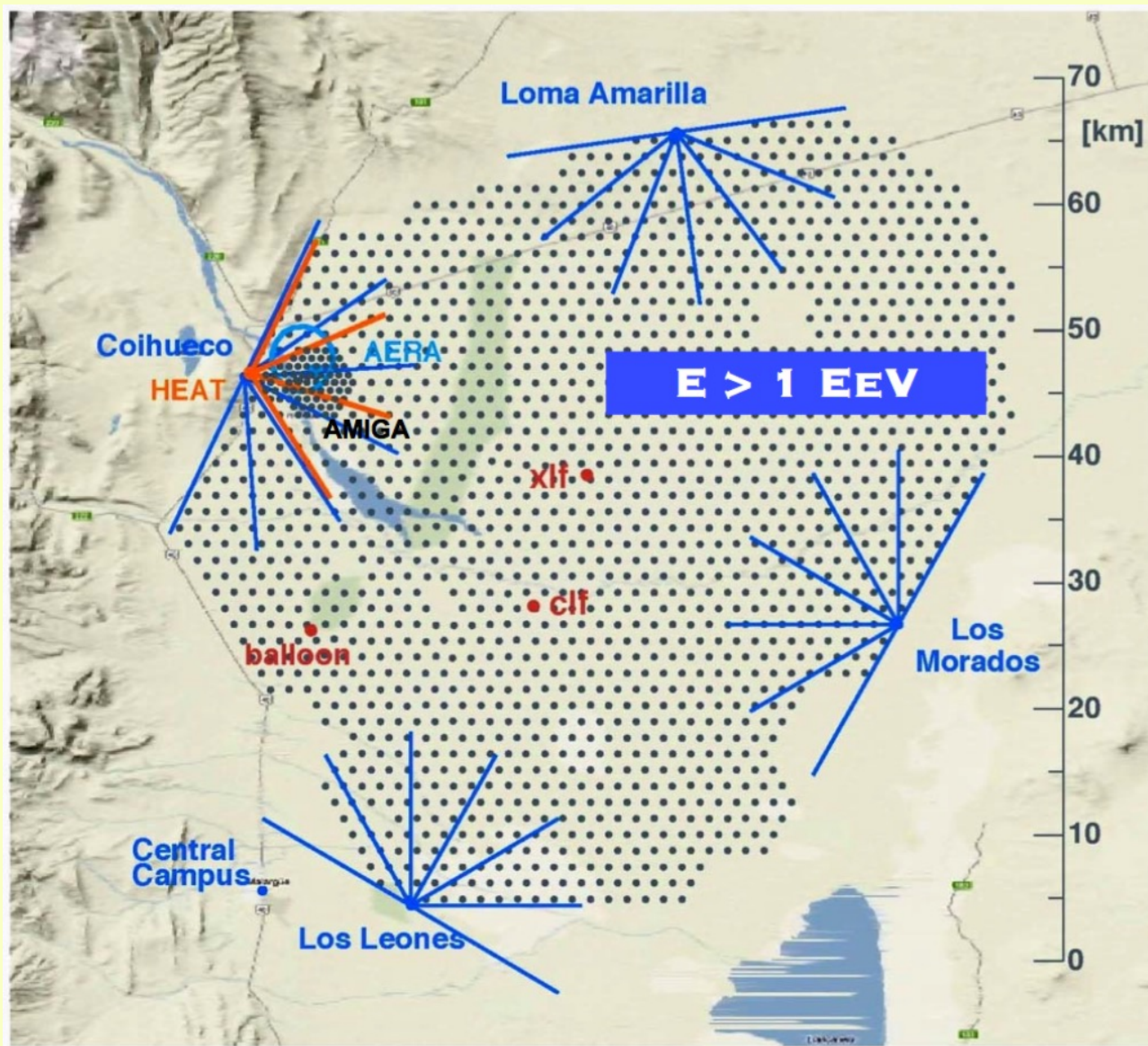
NEW ASTROPHYSICS

- ✓ Measured spectrum extends to $E > 10^{20}$ eV
- ✓ Where and how are cosmic rays accelerated to these energies
- ✓ No known astrophysical sources seem able to produce such enormous energies
- ✓ Chemical composition unknown

NEW PARTICLE PHYSICS

- ✓ The high energy end of the spectrum probes physics at energies out of reach of any man made accelerator

AUGER: the initial project



SURFACE DETECTOR ARRAY
1600 WATER-CHERENKOV STATIONS
1500 M SPACING
3000 KM²

SD-1500 m

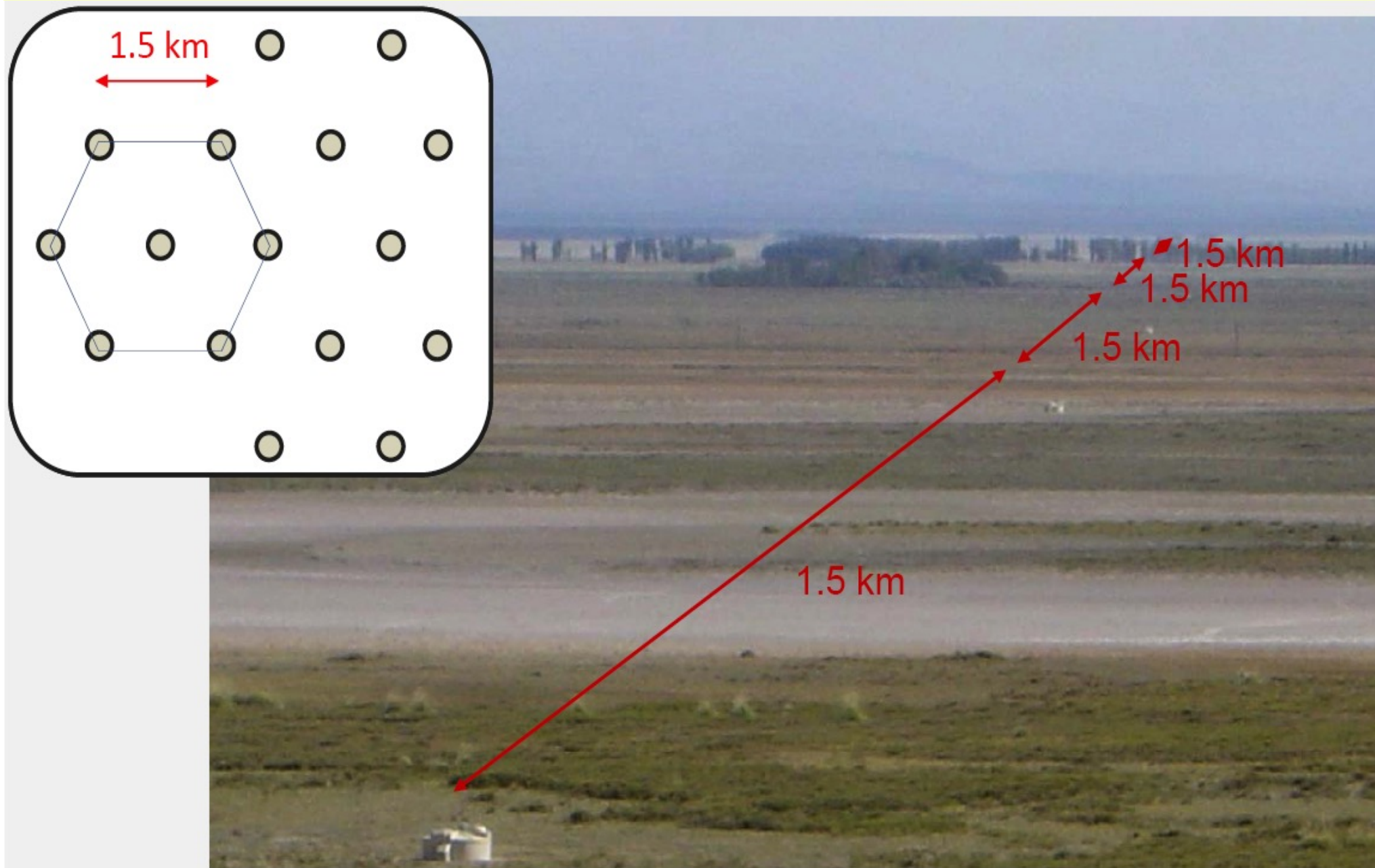
4 FLUORESCENCE DETECTORS
24 TELESCOPES
FOV 1-30°

FD

ATMOSPHERIC MONITORING
LASERS AND LIDARS

The complex block contains three photographs. The top photo shows a detector station on a hill with a solar panel. The middle photo shows a tall fluorescence detector tower. The bottom photo shows an atmospheric monitoring station with solar panels and a satellite dish.

"Pierre Auger Observatory": the Surface Detector (SD)



Scintillators or Cherenkov detectors ??

Advantages of scintillators:

- much light \Rightarrow may use cheaper PMTs
- less sensitive to abundant photons close to shower core

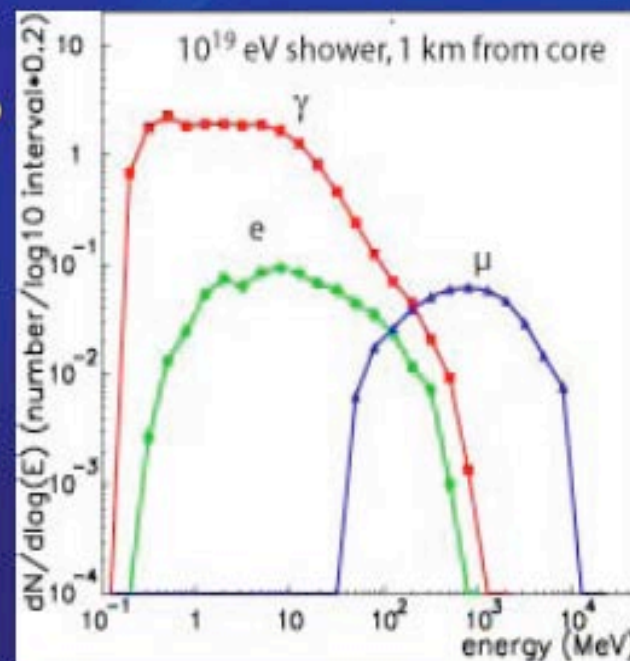
Advantages of water:

- large volumes easy and cheap to realize
- large cross-section to horizontal showers

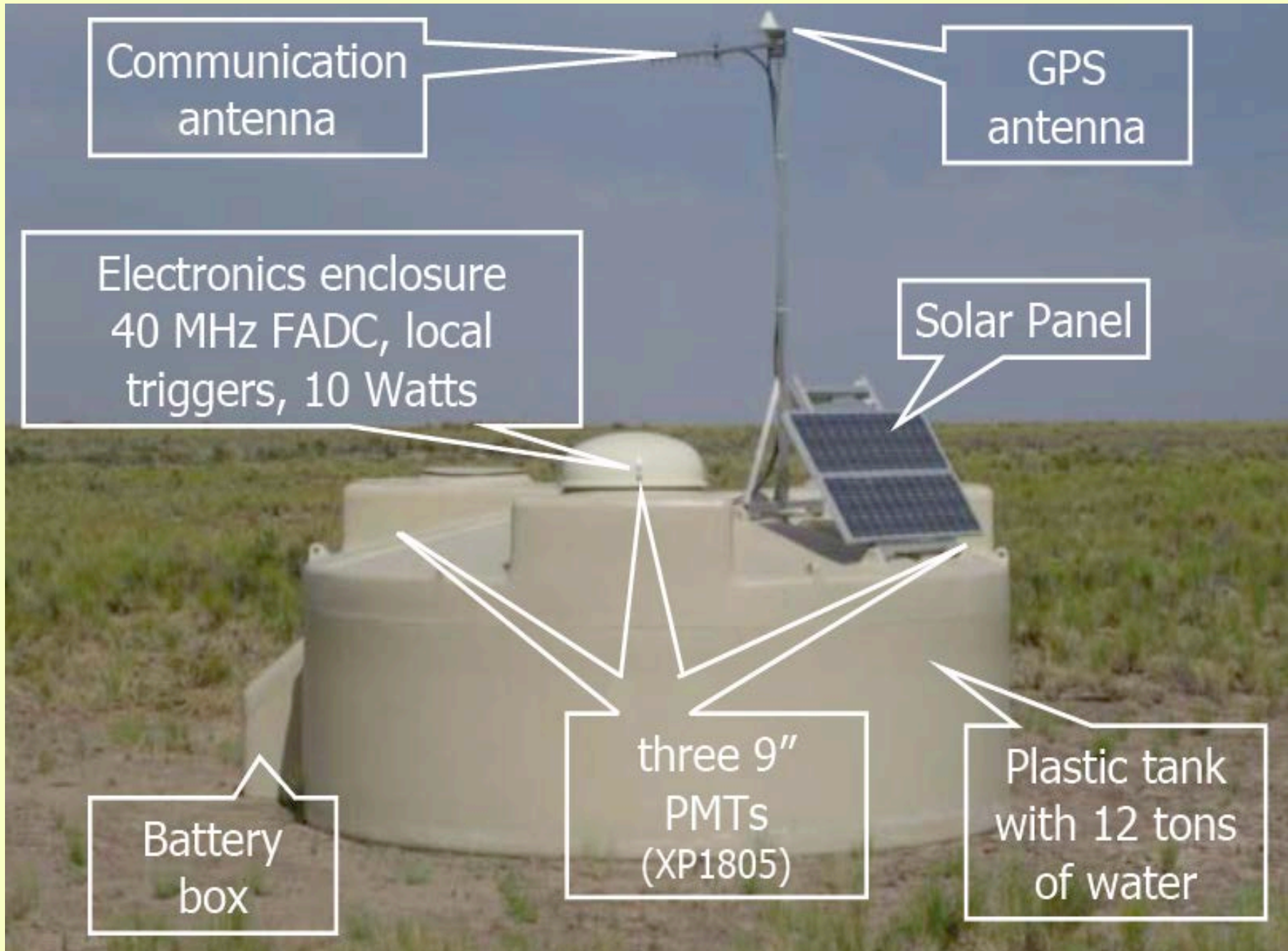
water tank

How to choose depth of water ?

- muon signal \propto water depth
- low energy electrons absorbed mostly within upper 30-40 cm
 \rightarrow can be optimized for ' μ -counting'

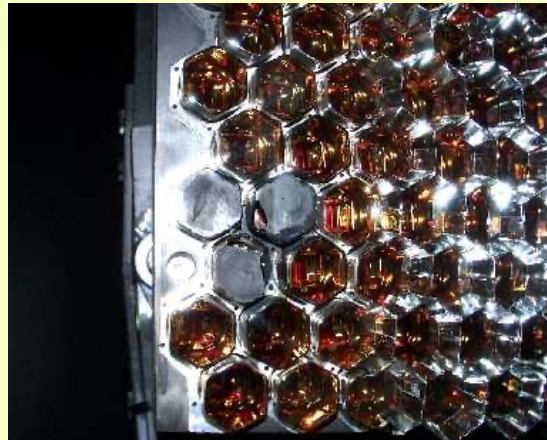
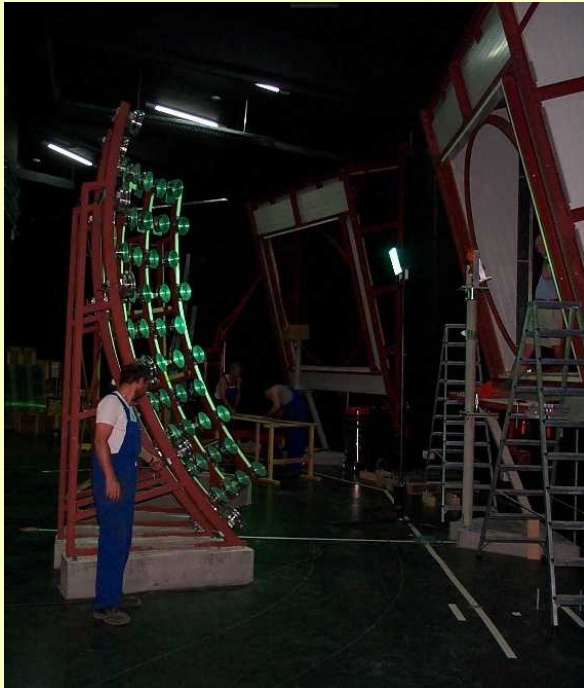


Basic module of the "Pierre Auger Observatory": the "Cherenkov" detector

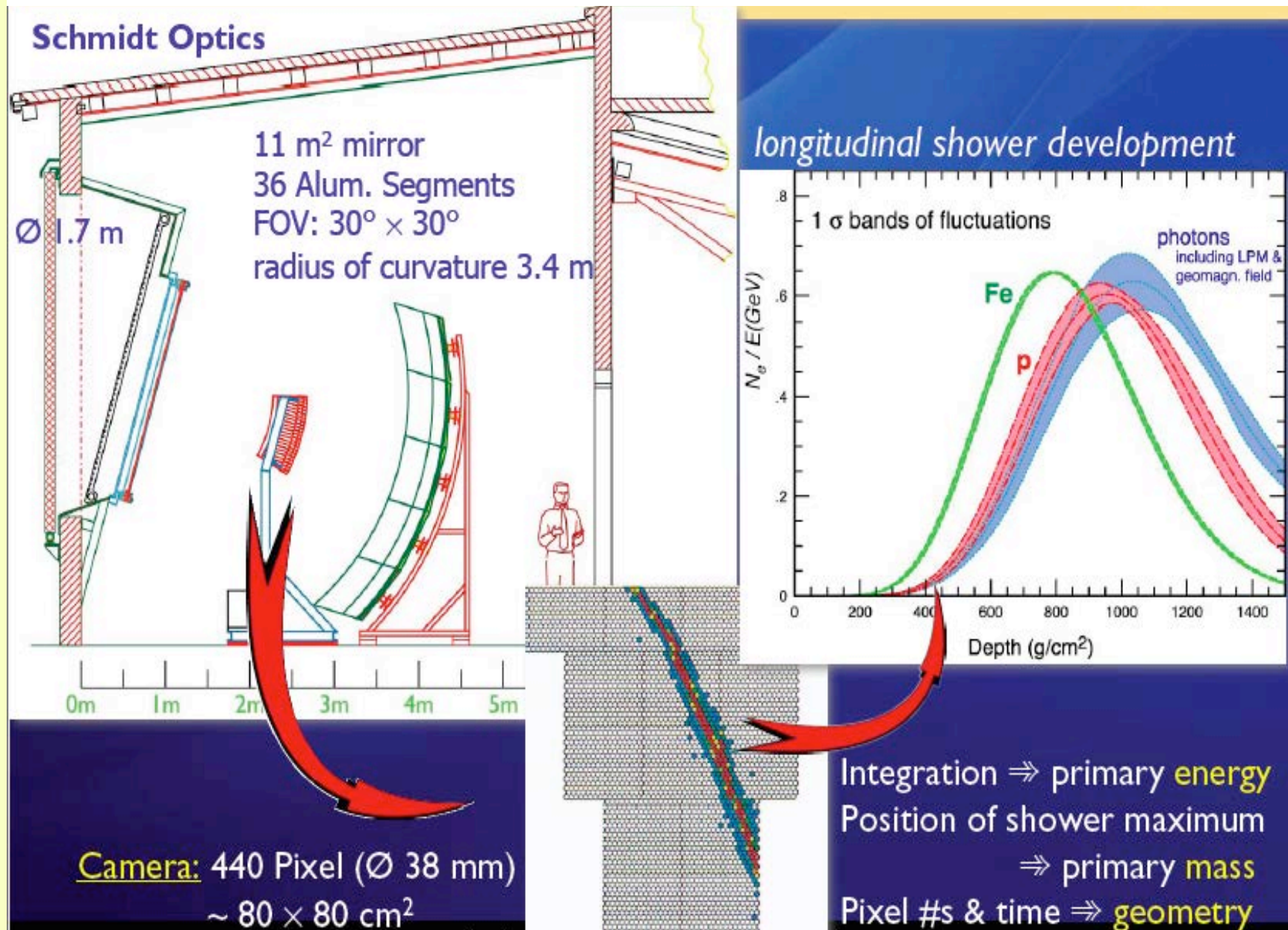


Other modules of the "Pierre Auger Observatory": the fluorescence detectors

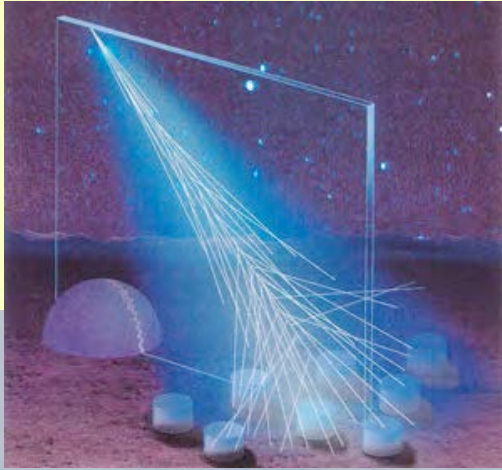
Made **4 fluorescence detectors**. They observe the atmosphere above the detector: 3 positioned on the perimeter and the fourth inside the occupied detector area. **The field of view of each of the three external detectors is 180° in azimuth and $\sim 30^\circ$ in elevation. The central detector has a view, in azimuth, of 360° .** The light is collected by 30 mirrors with 3m diameters and focused on photomultipliers (in total 13,000 PMTs, the sky will be observed with pixels of 1.5° .) Showers with energy $\sim 10^{19}$ eV can be seen at ~ 30 km away.



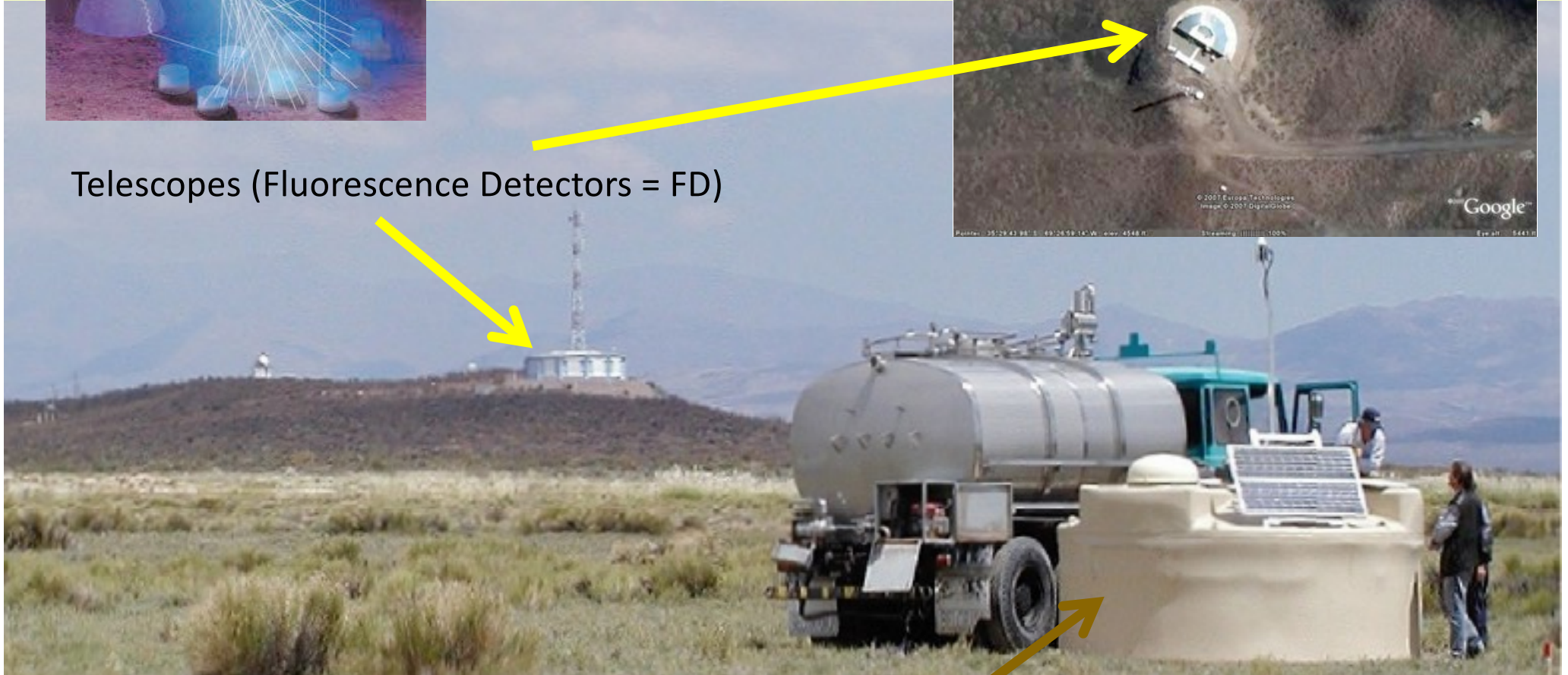
Observing Fluorescence light



The Auger hybrid detector

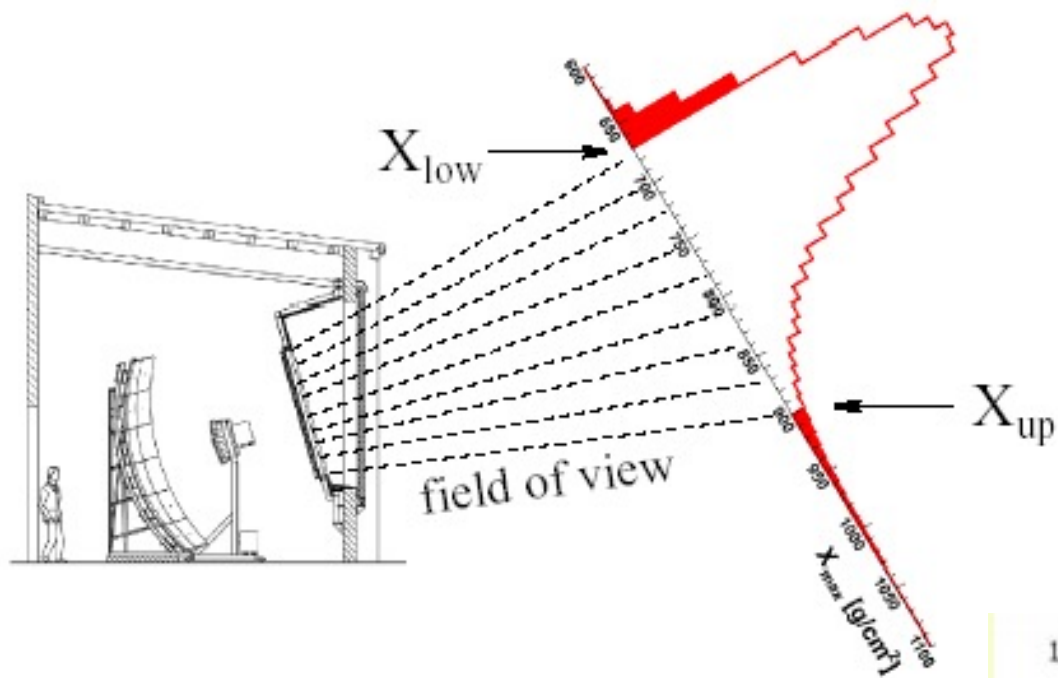


Telescopes (Fluorescence Detectors = FD)

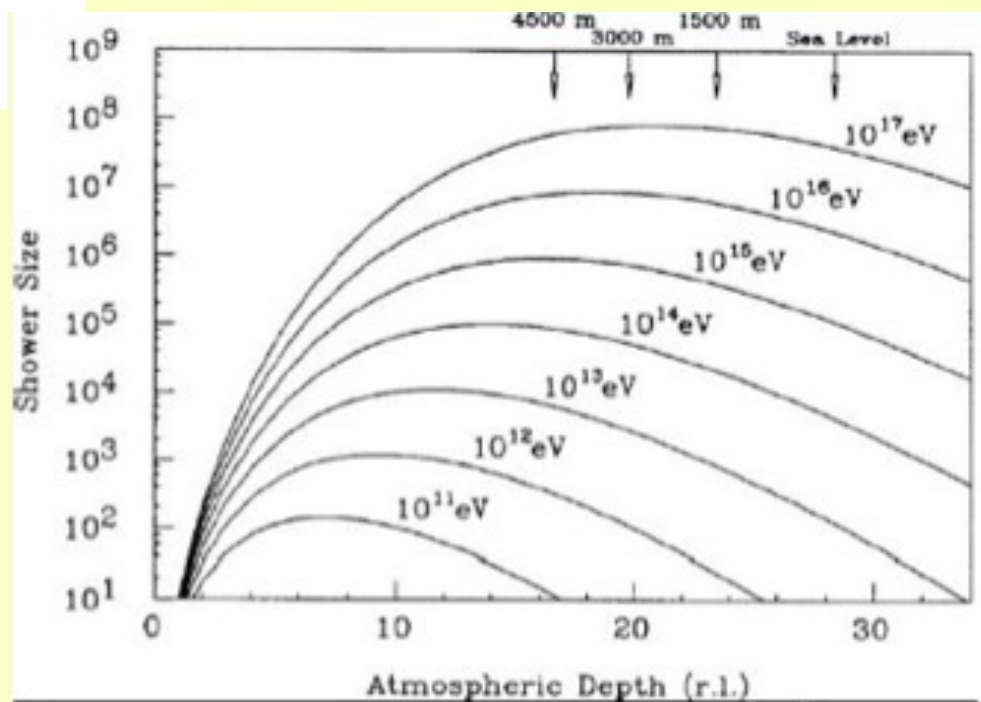


Tank (Surface Detector)

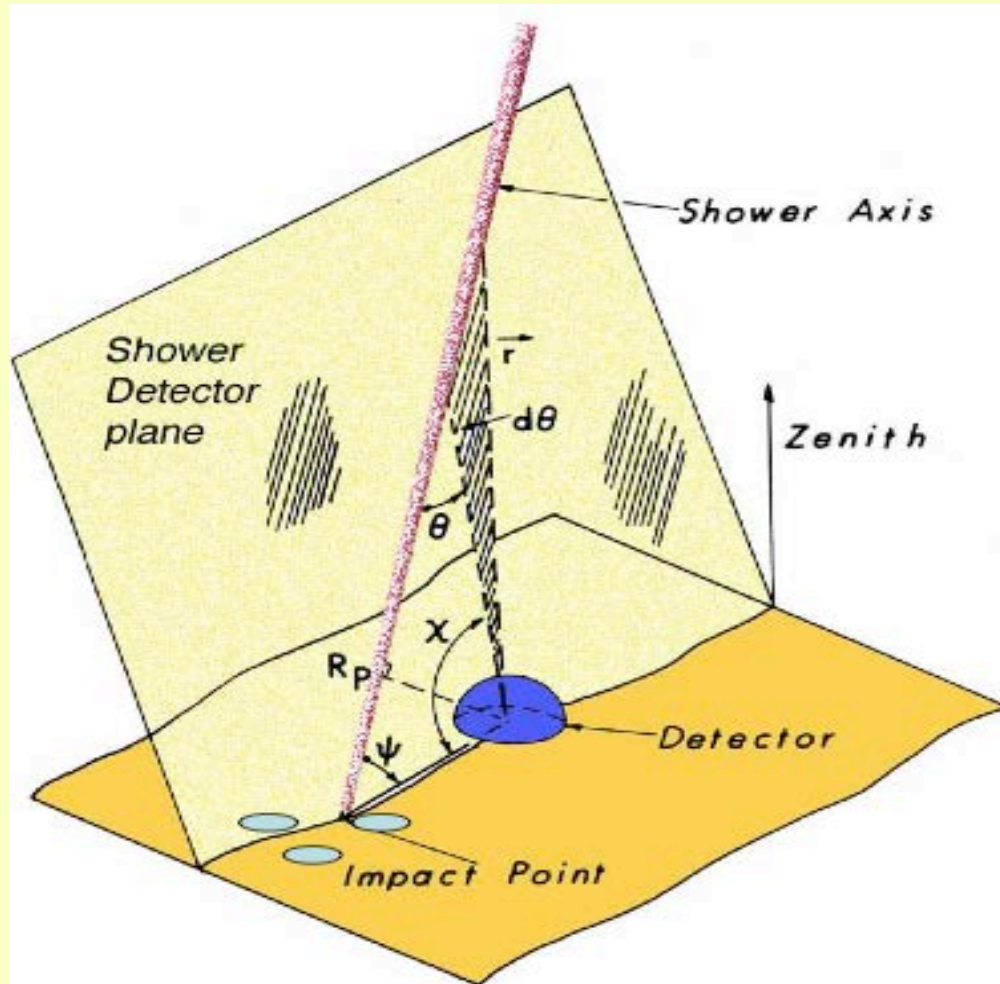
The fluorescence detectors



Fluorescence telescopes cover a field of view ranging from about 5 km to 1 km above sea level. Sufficient to cover most of the longitudinal development of the showers of these energies.



The "hybrid detector": SD + FD (1)



The essence of the hybrid approach

Precise **shower geometry** from degeneracy given by SD timing

Essential step towards high quality energy and X_{\max} resolution

Times at angles, χ , are key to finding R_p

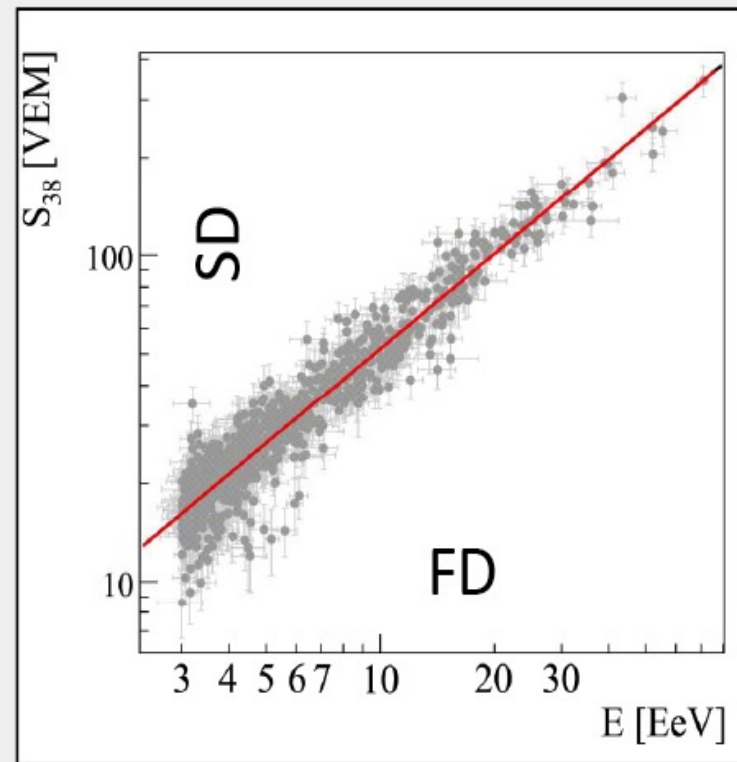
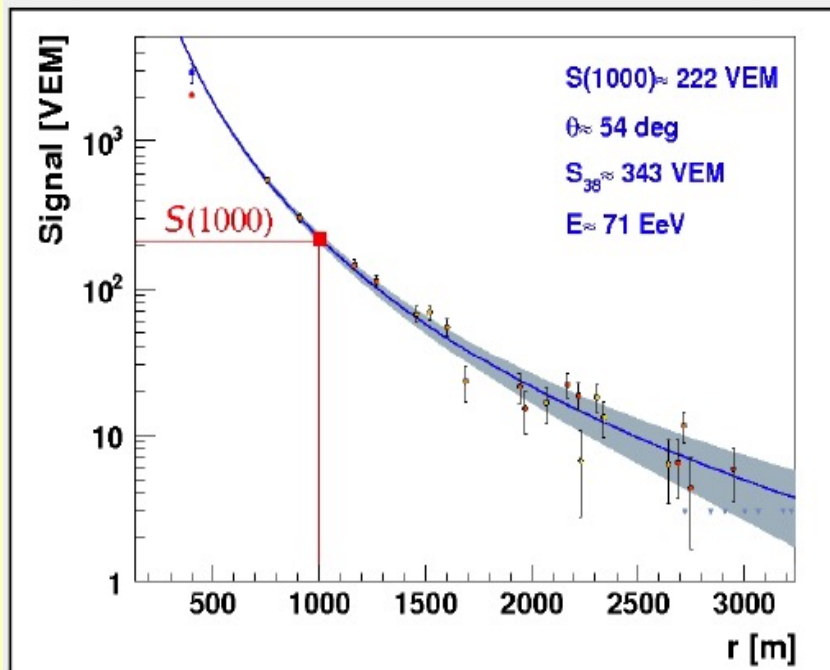
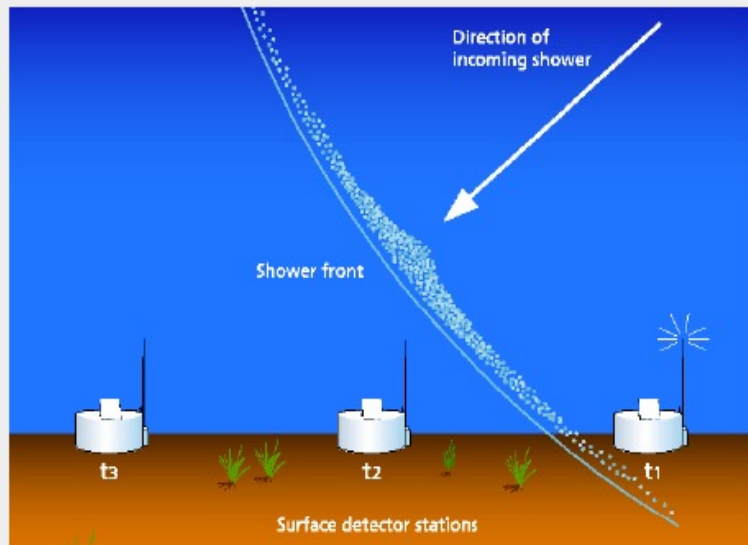
R_p : distance from the telescope to the axis of the shower. Its estimate improves with the measurement of impact time.

The "hybrid detector": SD + FD (2)

Energy reconstruction

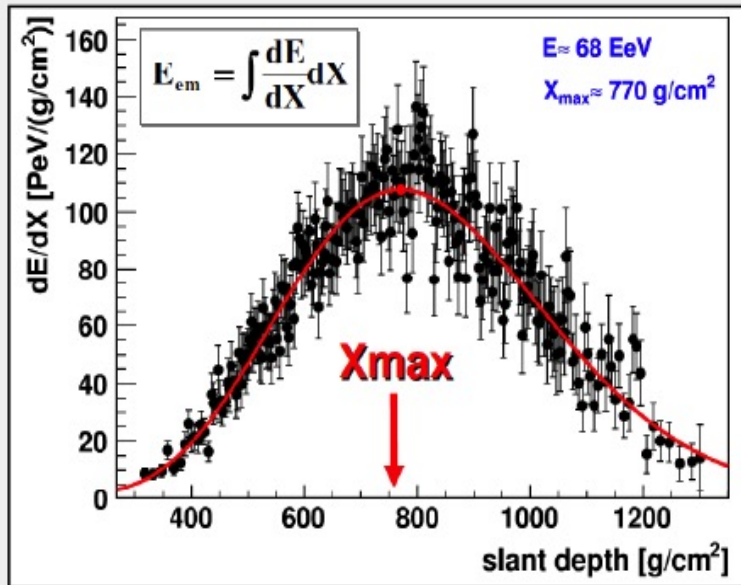
SD reconstruction

- ✓ Energy estimator: $S(1000)$ particle density at 1000 m from shower axis
- ✓ Systematic uncertainties on energy determination 30% (Monte Carlo)

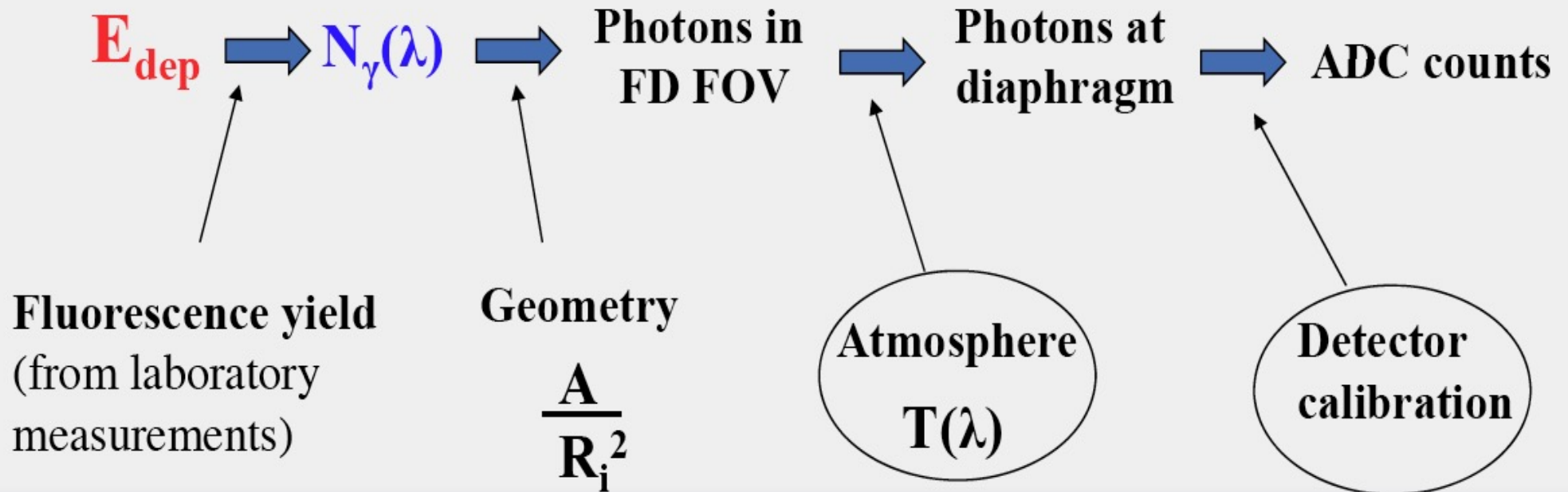
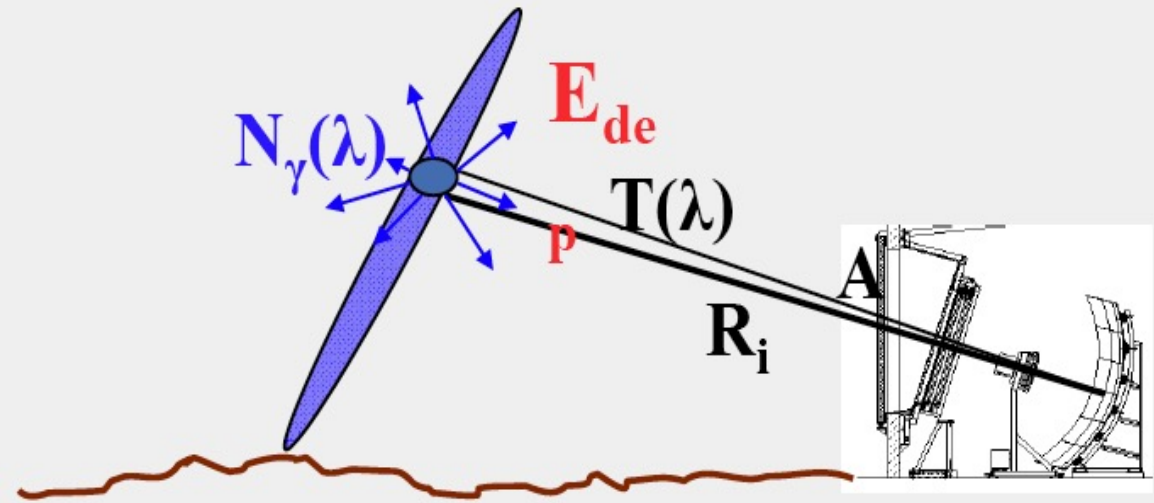


Using hybrid events, the SD energy estimator is calibrated without relying on Monte Carlo

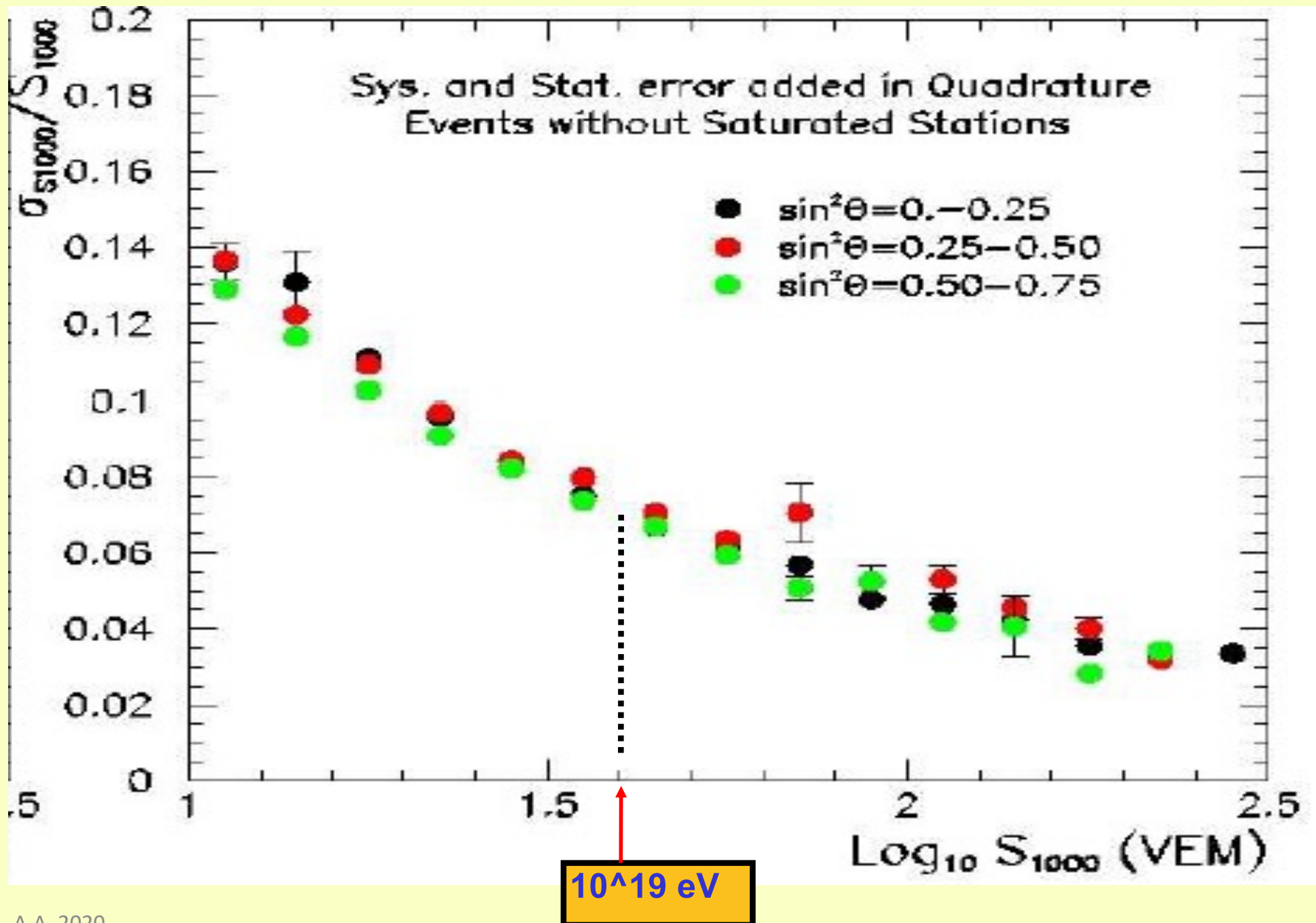
The "hybrid detector": SD + FD (3)



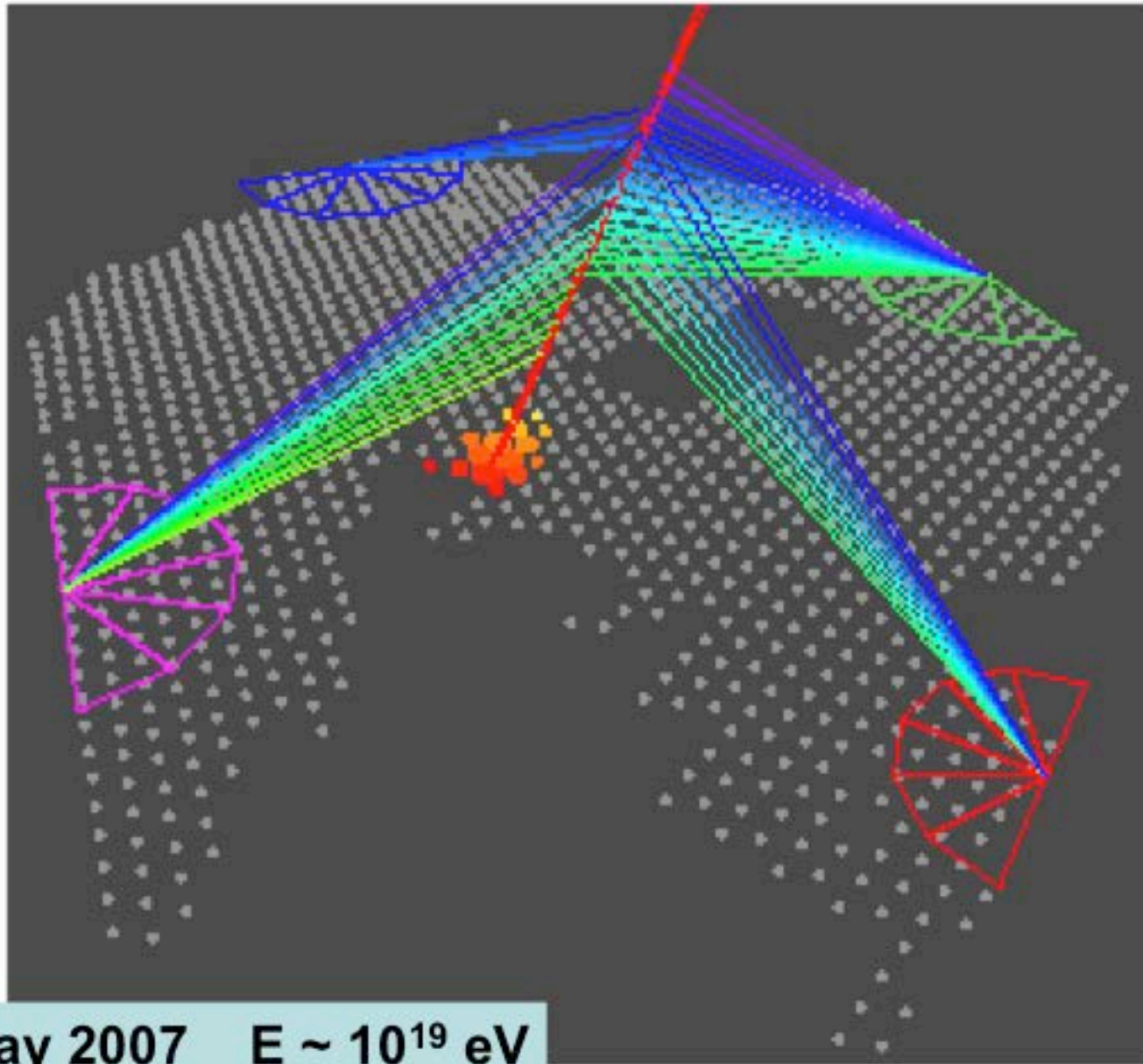
Energy "Calorimetric measurement"



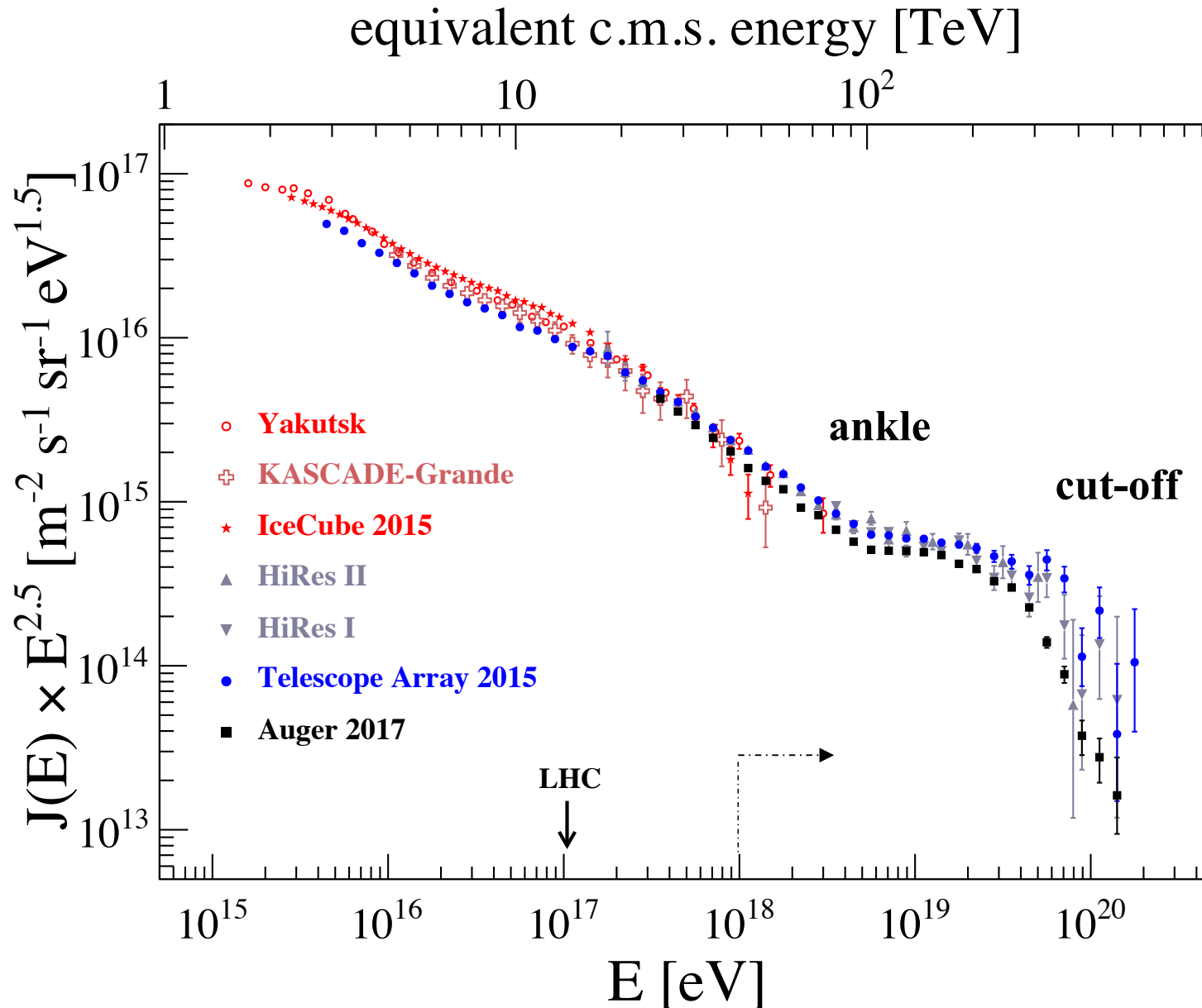
S(1000) the best estimate of the energy



Advantages of the FD "stereo view"



The Energy spectrum



$$\sqrt{s} \cong \sqrt{2m_p E / A}$$

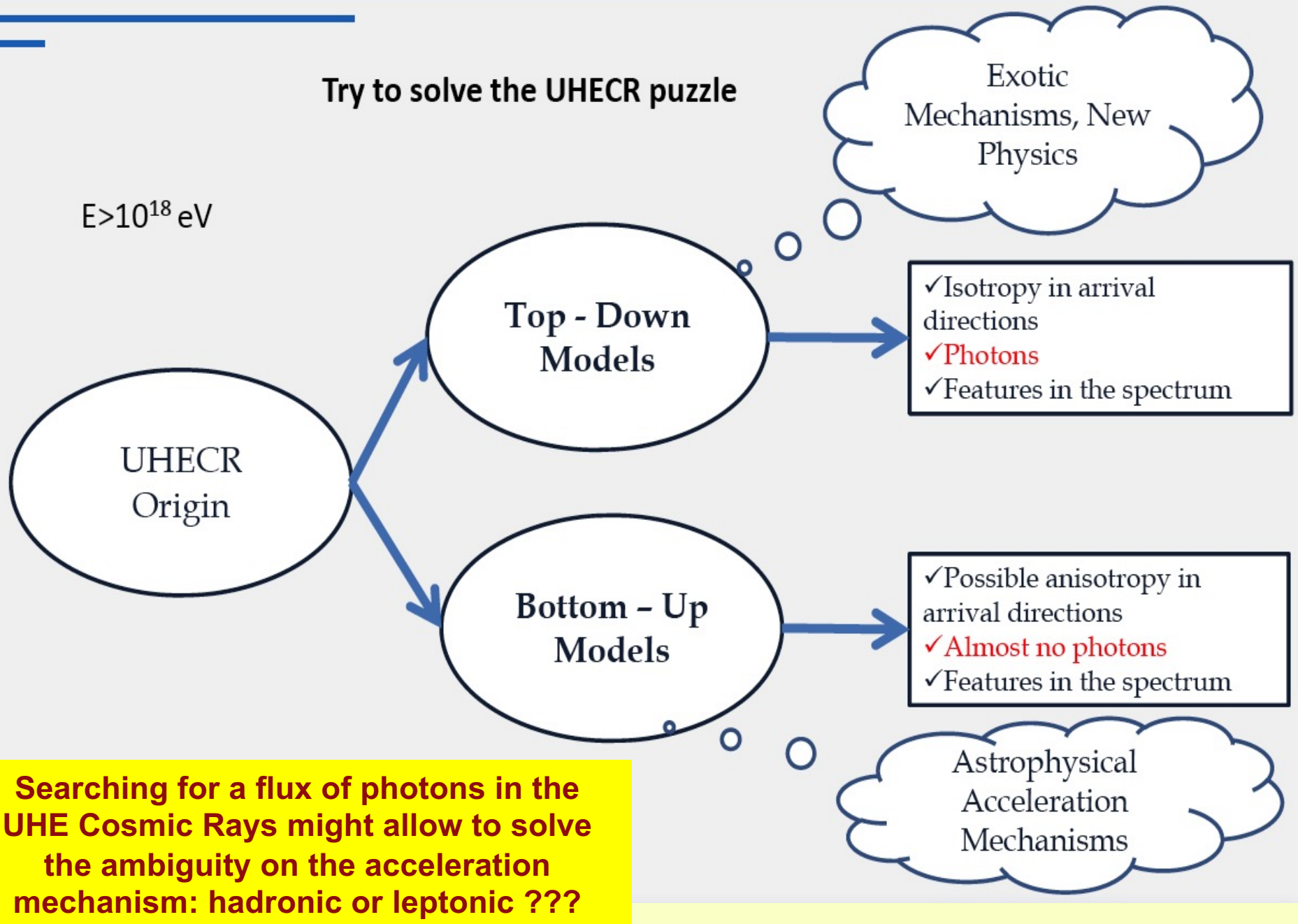
at 10^{20} eV
 ~ 400 TeV

$$\frac{dN}{dE} \sim \frac{1}{E^3}$$

at 10^{20} eV
 ~ 1 part./km²/century

note: at 10^{15} eV
 ~ 1 part./m²/year

The present “puzzle” of UHE Cosmic Rays physics



La fisica dei RC UHE ed il Pierre Auger Observatory

Excluding the hypothesis of the "Top-Down" acceleration we have to accept the hypothesis of "acceleration" of particles in astrophysical sources (bottom-up models).

From the study of:

- **spectrum**
- **composition**
- **isotropy / anisotropy**

we can get info on the sources. We can also study the interaction processes (at energies not accessible to accelerators) of UHE CR with the atmosphere.

The Pierre Auger Observatory today

THE NEW DETECTORS

Muon detector



SD-750 m
61 WCD 750 M SPACING: 25 KM²
ENGINEERING ARRAY OF 7
BURIED MUON DETECTORS
COMPLETED FEBRUARY 2015

3 HIGH-ELEVATION FD
FOV 30-60°

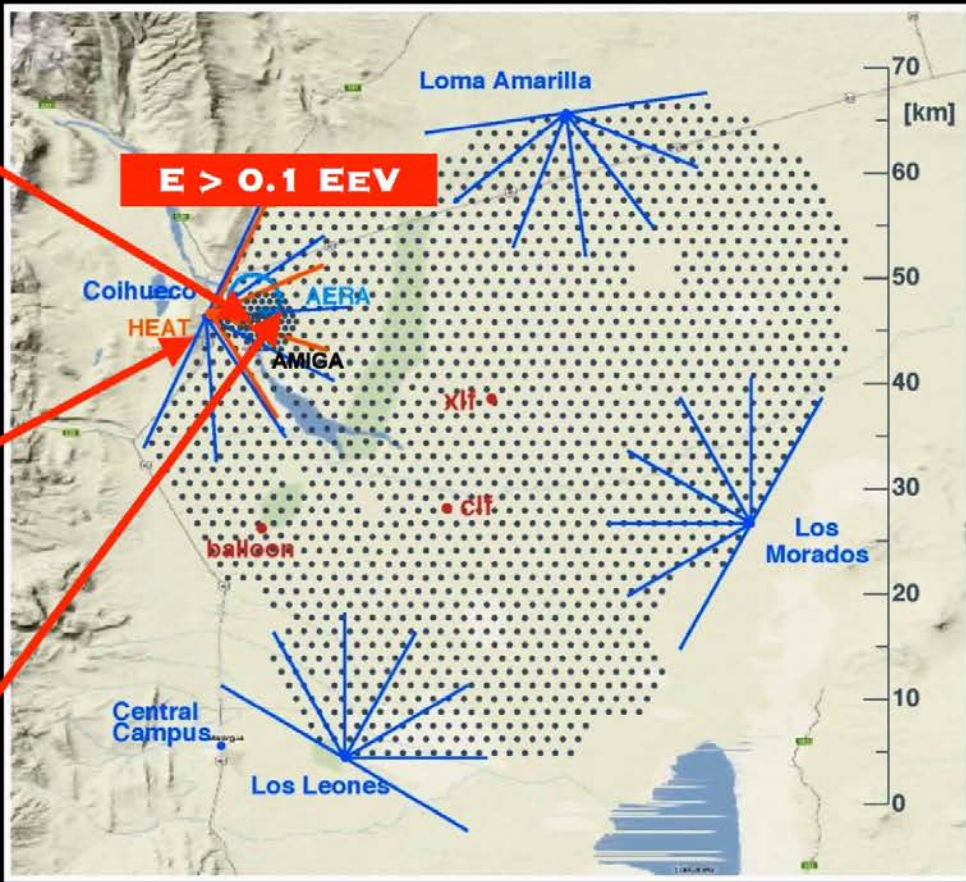


HEAT
153 RADIO ANTENNAS
GRADED 17 KM² ARRAY
COMPLETED APRIL 2015



AERA
Radio detector

The Pierre Auger Observatory, Argentina




E > 0.1 EeV

Map labels: Loma Amarilla, Coihueco, HEAT, AERA, AMIGA, XII, Clif, Los Morados, Los Leones, Central Campus.

THE INITIAL DETECTORS

RPC



A VERY PRECISE
RPC MUON-HODOSCOPE

Tank

RPC

Muon detector

**A COMPLEX DATA-QUALITY
DATABASE FOR 22000 PMTS IN
10 YR OF OPERATION:
50 MILLIONS OF RECORDS**

FD detector

**UPGRADE OF THE LASER
FACILITY: RAMAN-LIDAR**



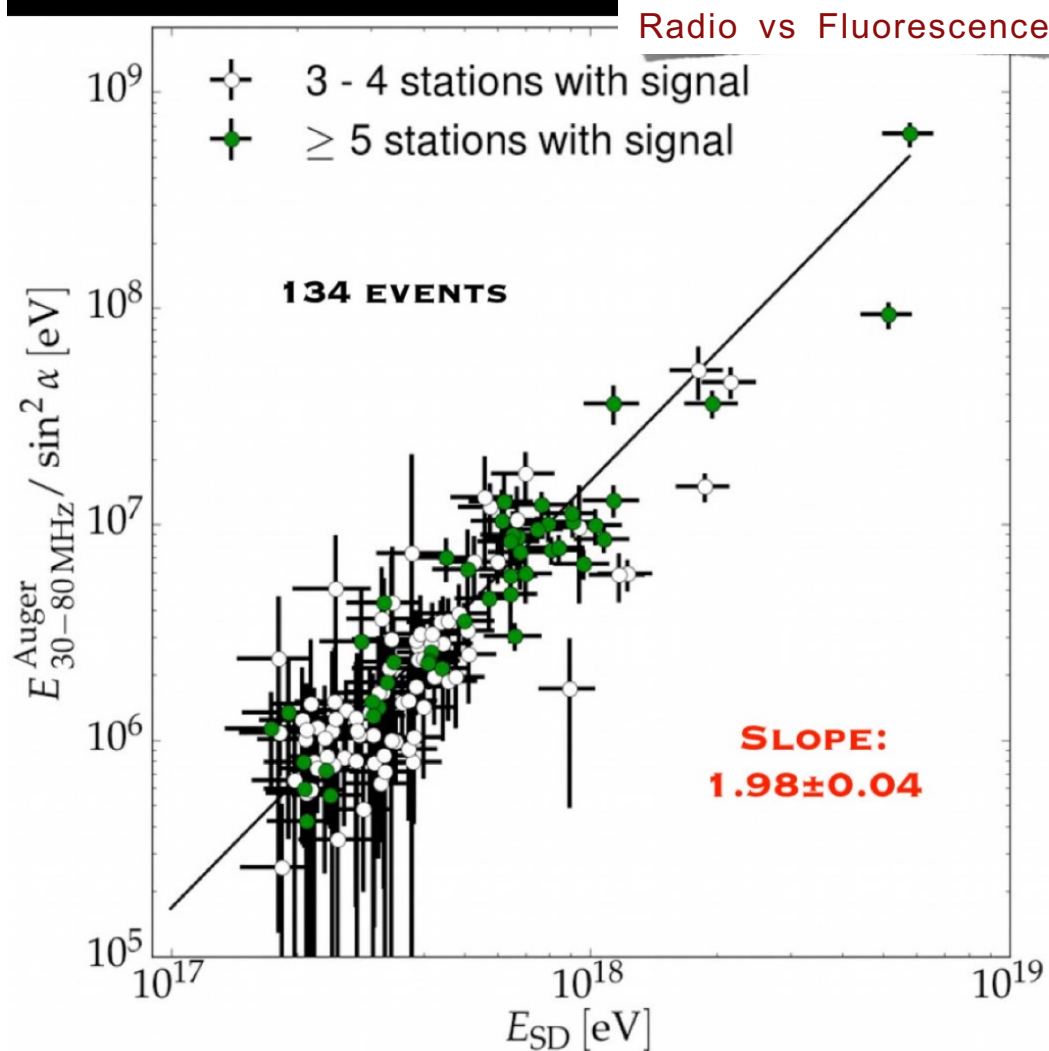
Calibration

HEAT (High Elevation Auger Telescopes) are three tiltable fluorescence telescopes which represent a low energy enhancement of the fluorescence telescope system of the Pierre Auger Observatory in Argentina. By lowering the energy threshold by approximately one order of magnitude down to a primary energy of 10^{17} eV, HEAT provides the possibility to study the cosmic ray energy spectrum and mass composition in a very interesting energy range, where the transition from galactic to extragalactic cosmic rays is expected to happen.

AERA (Auger Engineering Radio Array) is a new antenna system to measure short radio pulses emitted by cosmic ray air showers of the highest energies. It consists of an array of dozens of antennas sensitive in the frequency range of 30 to 80 MHz with signal processing and electronics developed specifically for this purpose. AERA antennas are active 24 hours a day, like the surface detectors of the Pierre Auger Observatory. Radio detection of cosmic rays has been applied first over 50 years ago, but only with the digital signal processing available today it could be implemented on large scales yielding detailed and high-quality measurements.

Using “radio signals” to measure C.R. energy

The energy in the radio signal of extensive air showers



The showers radio-signals scale quadratically with the cosmic ray energy

Radio energy resolution $\approx 17\%$

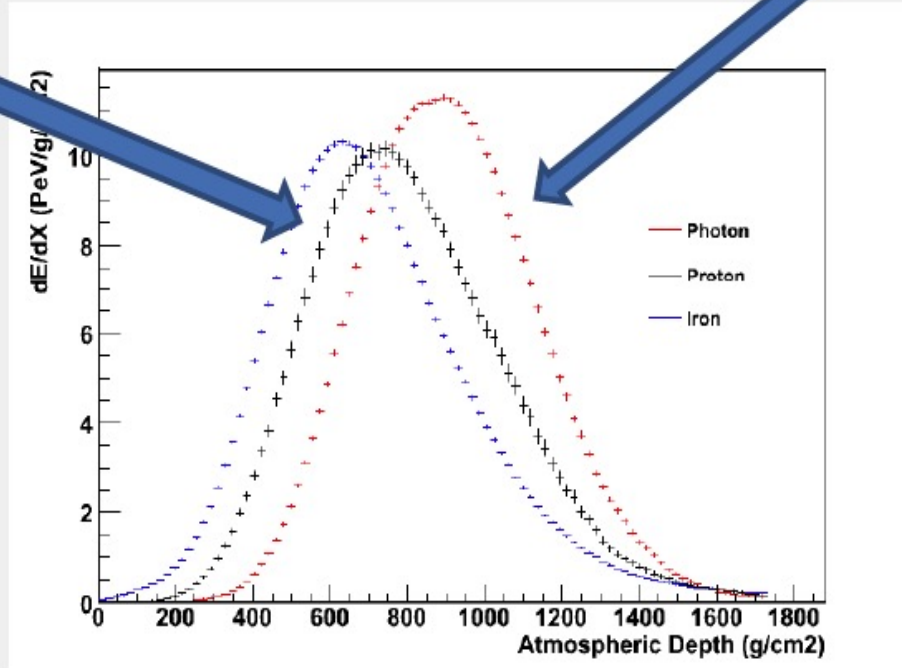
Measurement of the radiated energy (in the 30-80 MHz band):

16 MeV for a 1 EeV cosmic-ray

Independent determination of the energy scale of a cosmic-ray observatory

The method to identify showers induced by UHE γ

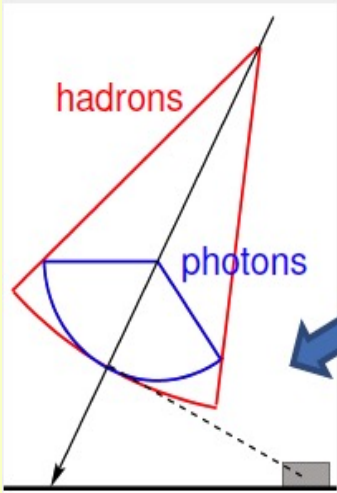
hadrons



Photons

FD photons search based on X_{max} distribution

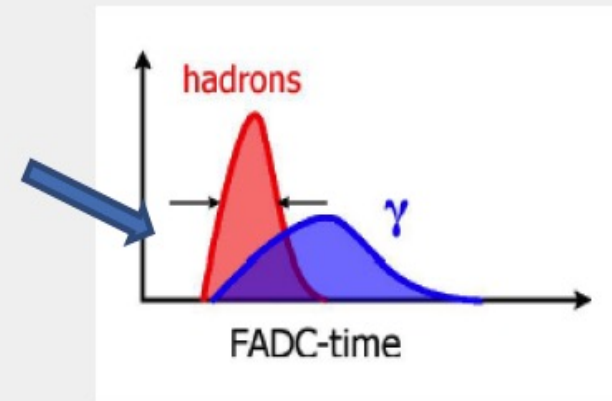
photon-induced showers in general reach their maxima deeper in the atmosphere than showers initiated by nuclei



Deeper showers larger curvature

Slower signal, longer risetime

SD photons search based on signal structure



P. Auger Collaboration, arXiv:0903.1127v2 [astro-ph.HE] (2009).

No UHE γ found \rightarrow set an Upper Limit to the flux of UHE photons

Exotic Mechanisms

- ✓ Decay of topological defects
- ✓ Relic monopoles
- ✓ Etc.

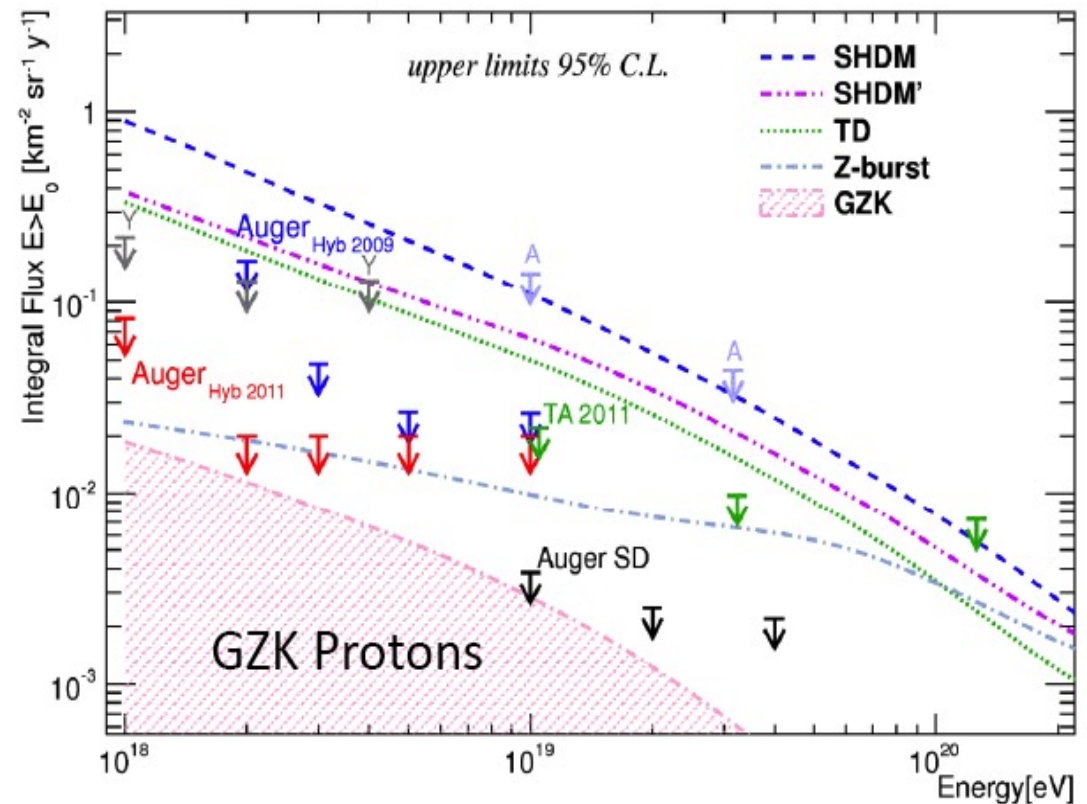
New Physics

- ✓ Supersymmetric particles
- ✓ Strongly interacting neutrinos
- ✓ Decay of massive new long lived particles
- ✓ Etc.

SHDM = SuperHeavy Dark Matter

TD = Top Down models

Z-burst = Ultra HECR da interazioni di neutrino con produzione di Z-bursts



GZK region within reach in the next years

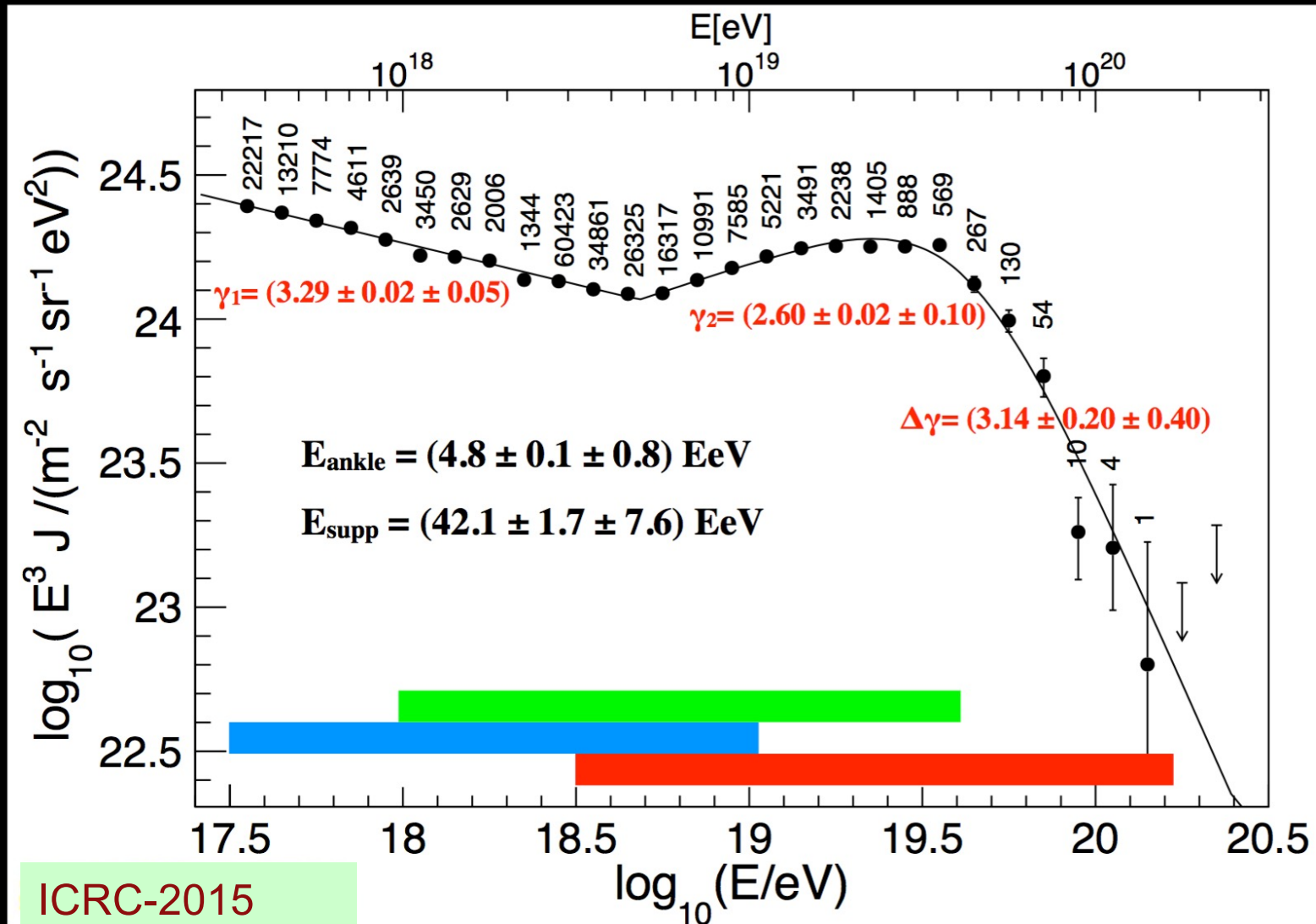
Top-down models severely constrained

Favour astrophysical origin of UHECR

Top-Down model: P. Bhattacharjee, G. Sigl, Phys. Rep. 327, 109 (2000).

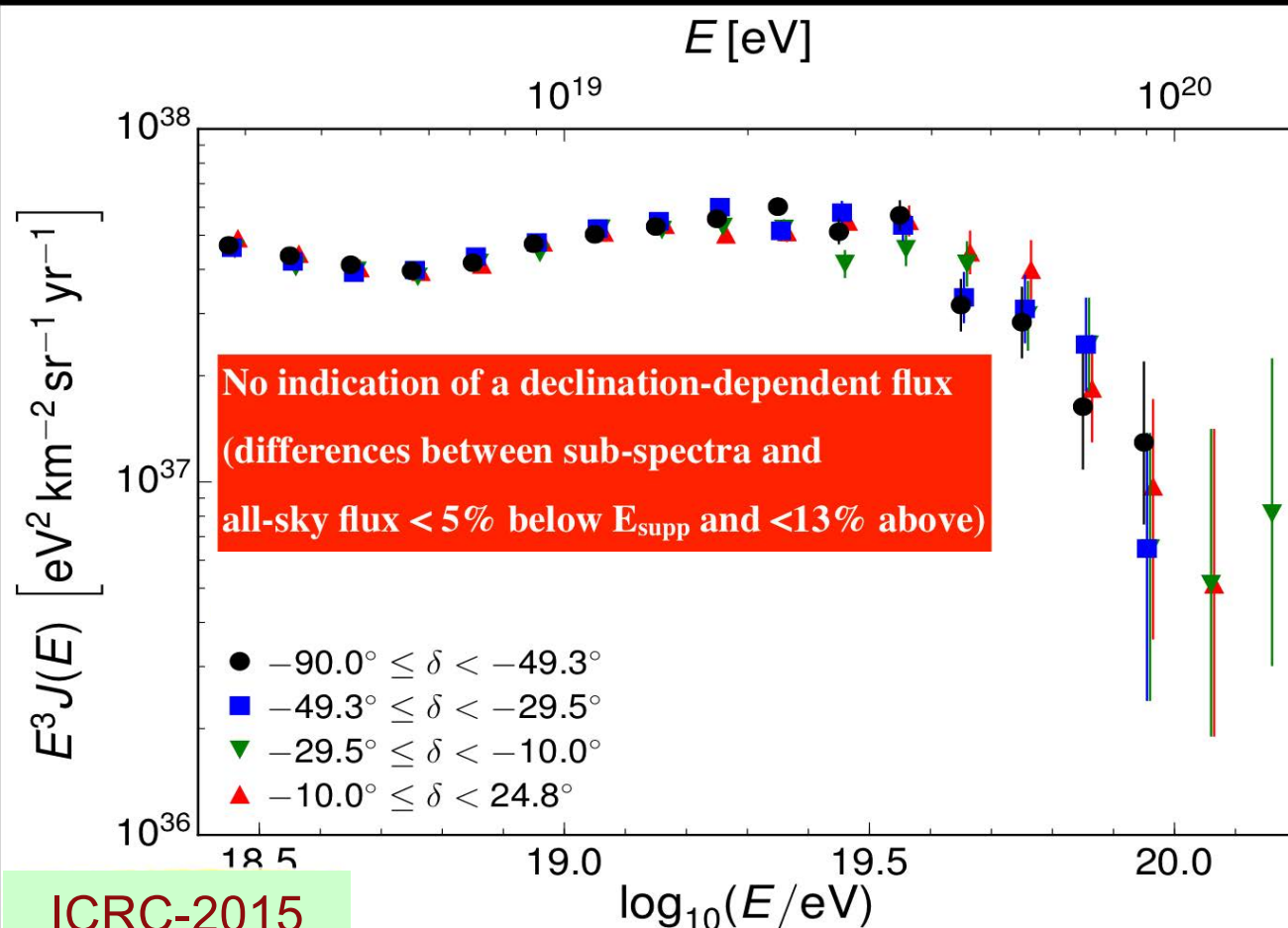
Pierre Auger Observatory: the flux of UHE CR

4 data sets combined: **SD 750 m**, **FD (hybrid)**, **SD 1500 m (0-60°)**, **SD 1500 m (60-80°)**
 ≈ 200 000 events, ≈ 50000 km² sr yr exposure, FOV: -90°, +25 in δ



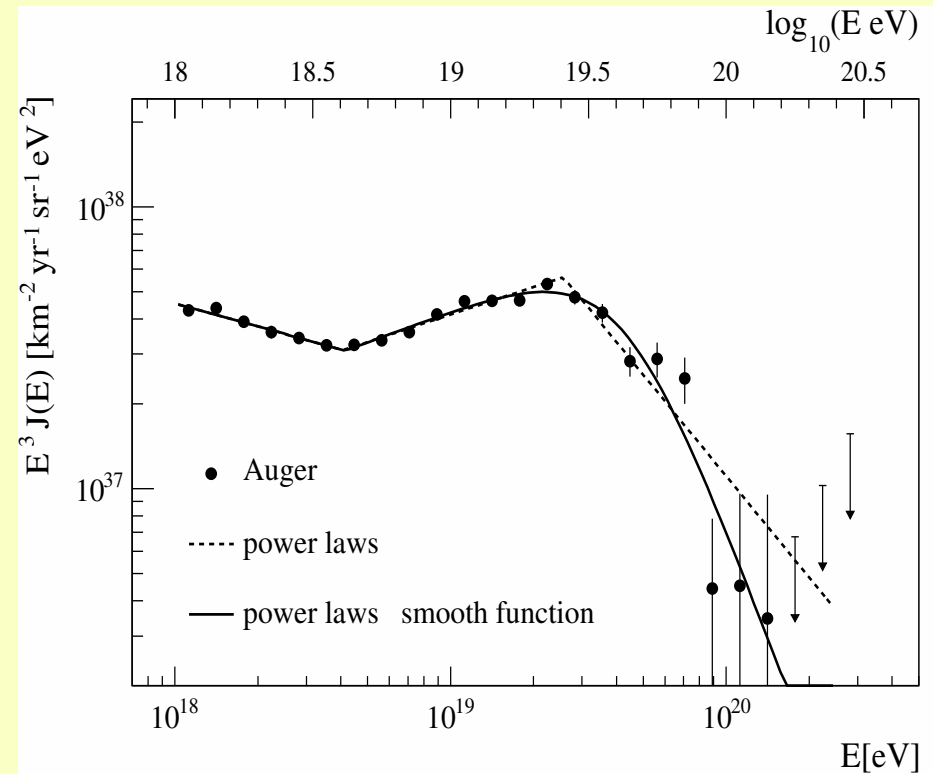
Pierre Auger Observatory: UHE CR spectrum, "all particle", for different declination angles (1)

The large number of events and wide FOV allow for the study of the flux vs declination



Pierre Auger Observatory: UHE CR spectrum (2)

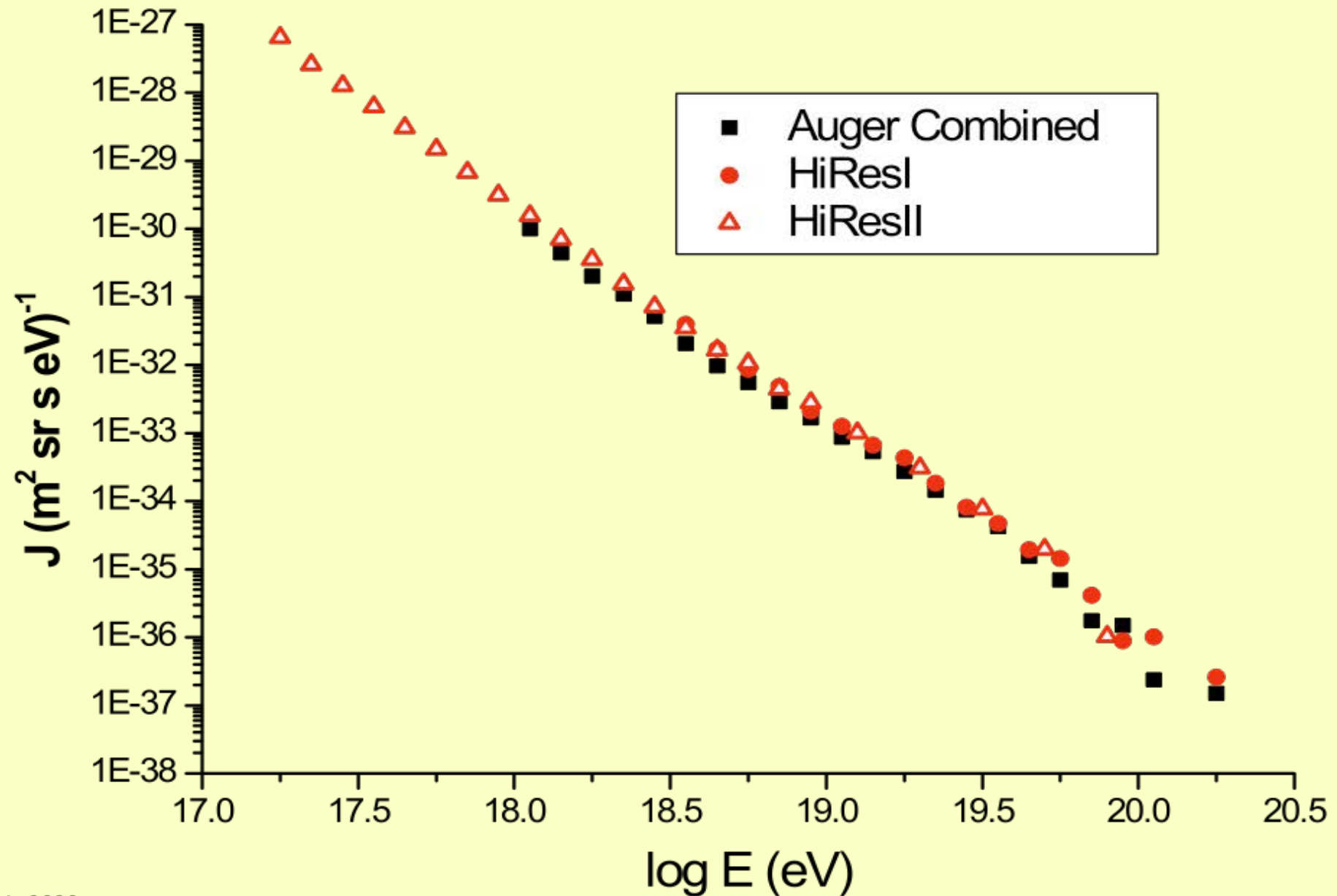
With the present spectrum AUGER reject the hypothesis that the cosmic ray spectrum continues in the form of a power-law above an energy of 4×10^{19} eV with more than 20σ . This result is independent of the systematic uncertainties in the energy scale, the suppression at high energies can be due to the GZK cutoff [GZK] or just that sources are running out of power[Allard].



[GZK] K. Greisen, Phys. Rev. Lett. 16, 748 (1966); G. T. Zatsepin and V. A. Kuzmin, Pis'ma Zh. Eksp. Teor. Fiz. 4, 114 (1966) JETP Lett. 4, 78 (1966).

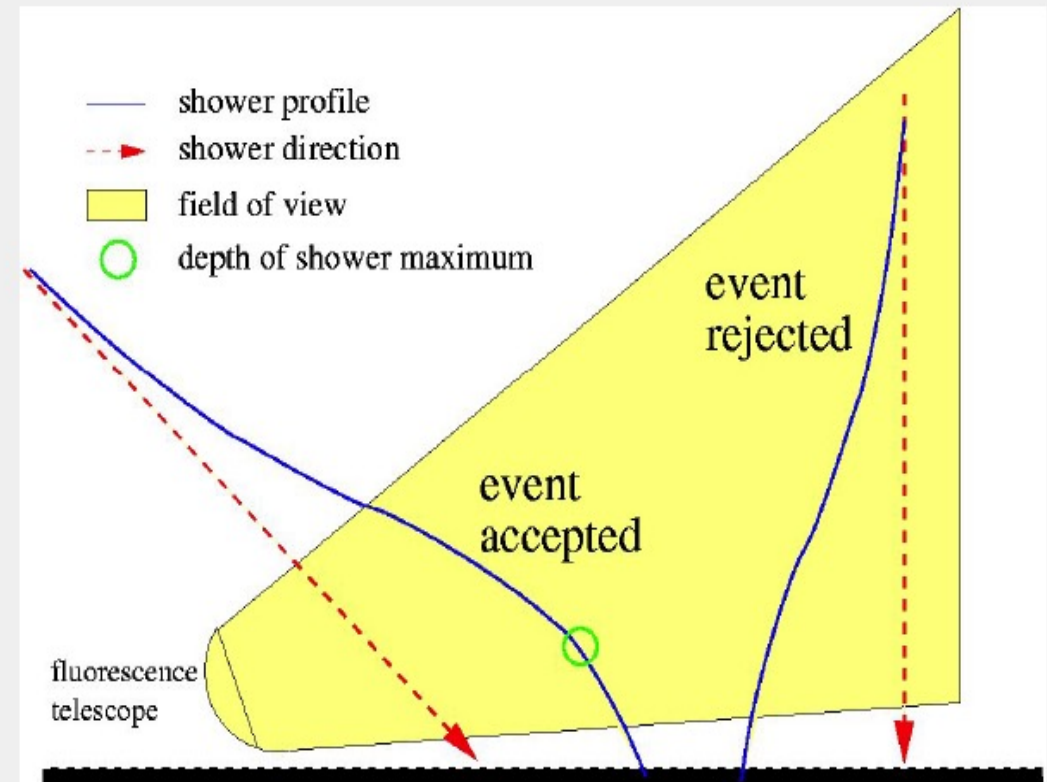
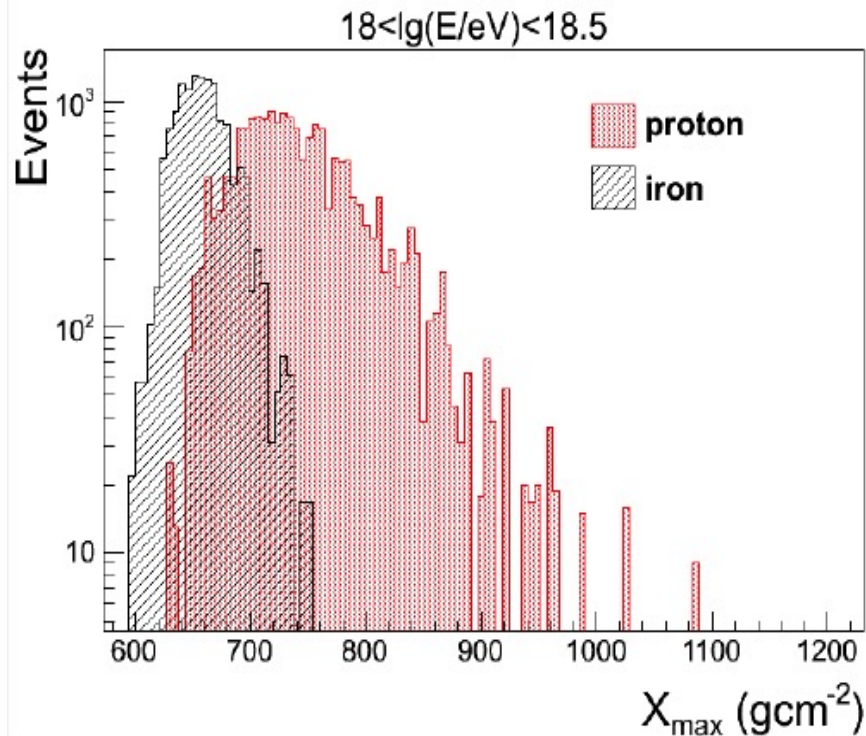
[Allard] D. Allard, Astropart. Phys., 39-40 (2012) 33.

Comparison HiRes-AUGER



Pierre Auger Observatory: the mass composition (1)

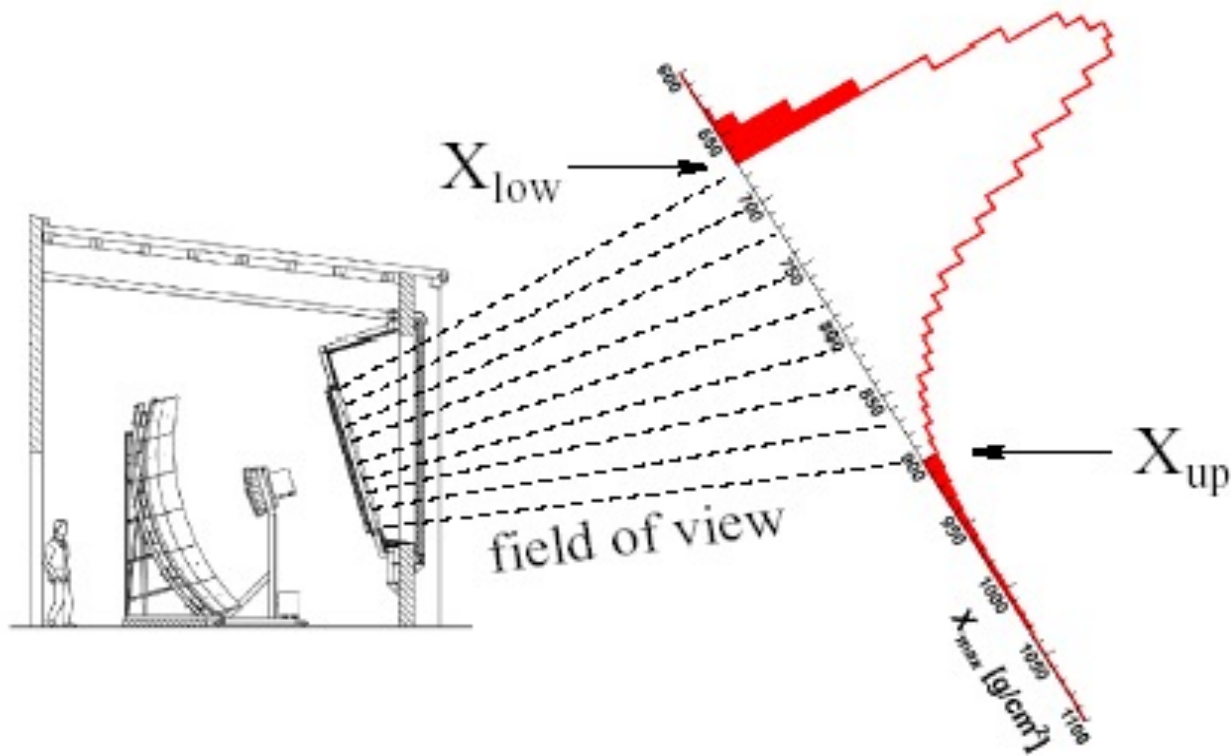
The main instrument of analysis is the Fluorescence Detector, but also the Surface Array can be used.



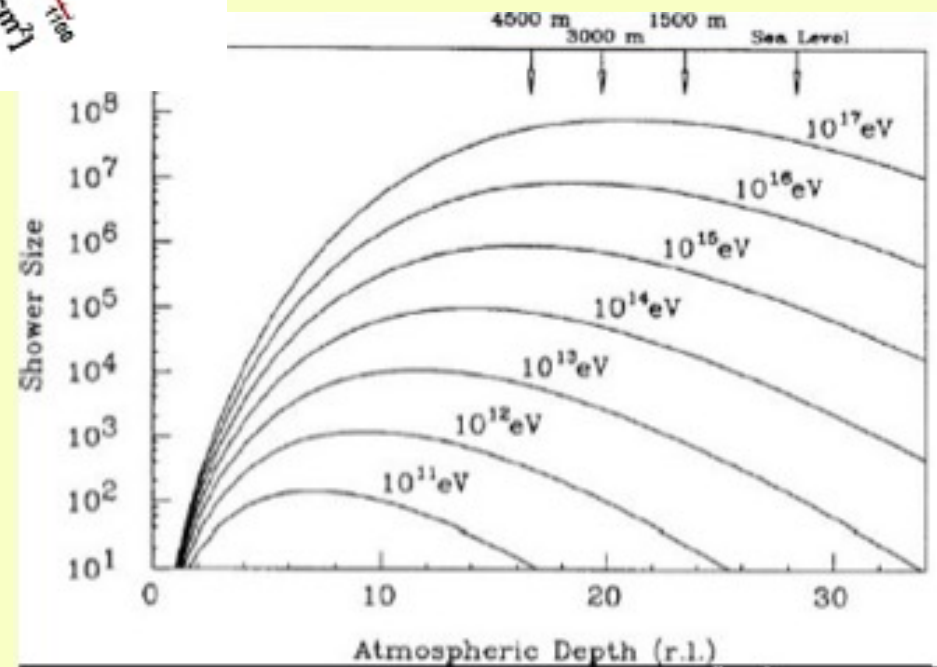
$\langle X_{\max} \rangle$ and its RMS sensitive to mass composition

Key observables for composition studies

Field of View and Anti-Bias cut used to obtain detector independent results



Fluorescence detectors field of view includes heights 1km- 5km above the sea-level: this is sufficient to observe the major part of the showers longitudinal development.

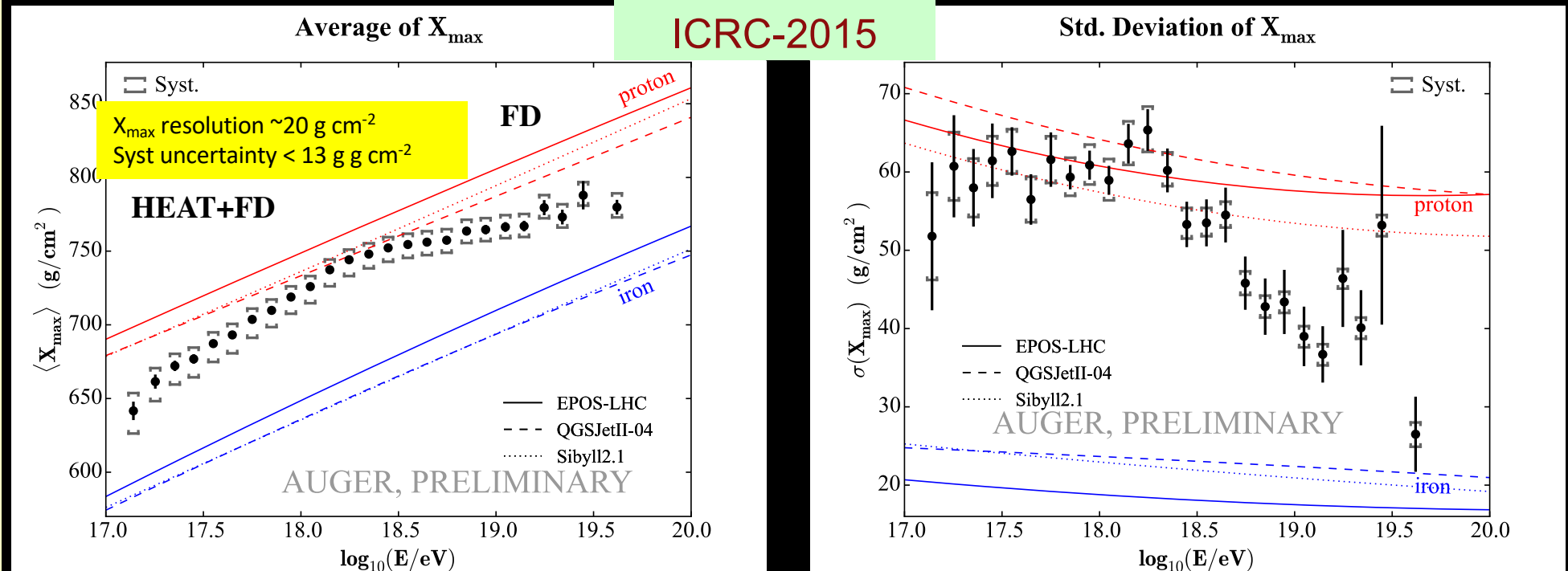


Pierre Auger Observatory: the mass composition (2)

Depth of shower maximum premiere observable for mass composition studies

HEAT data extends the FOV of the fluorescence detector up to 60°

Extension of the depth of shower maximum measurements down to 10^{17} eV



Compared to expectations from **proton** and **iron**
EPOS-LHC, QGSJETII-04, Sybill2.1 as hadronic interactions models

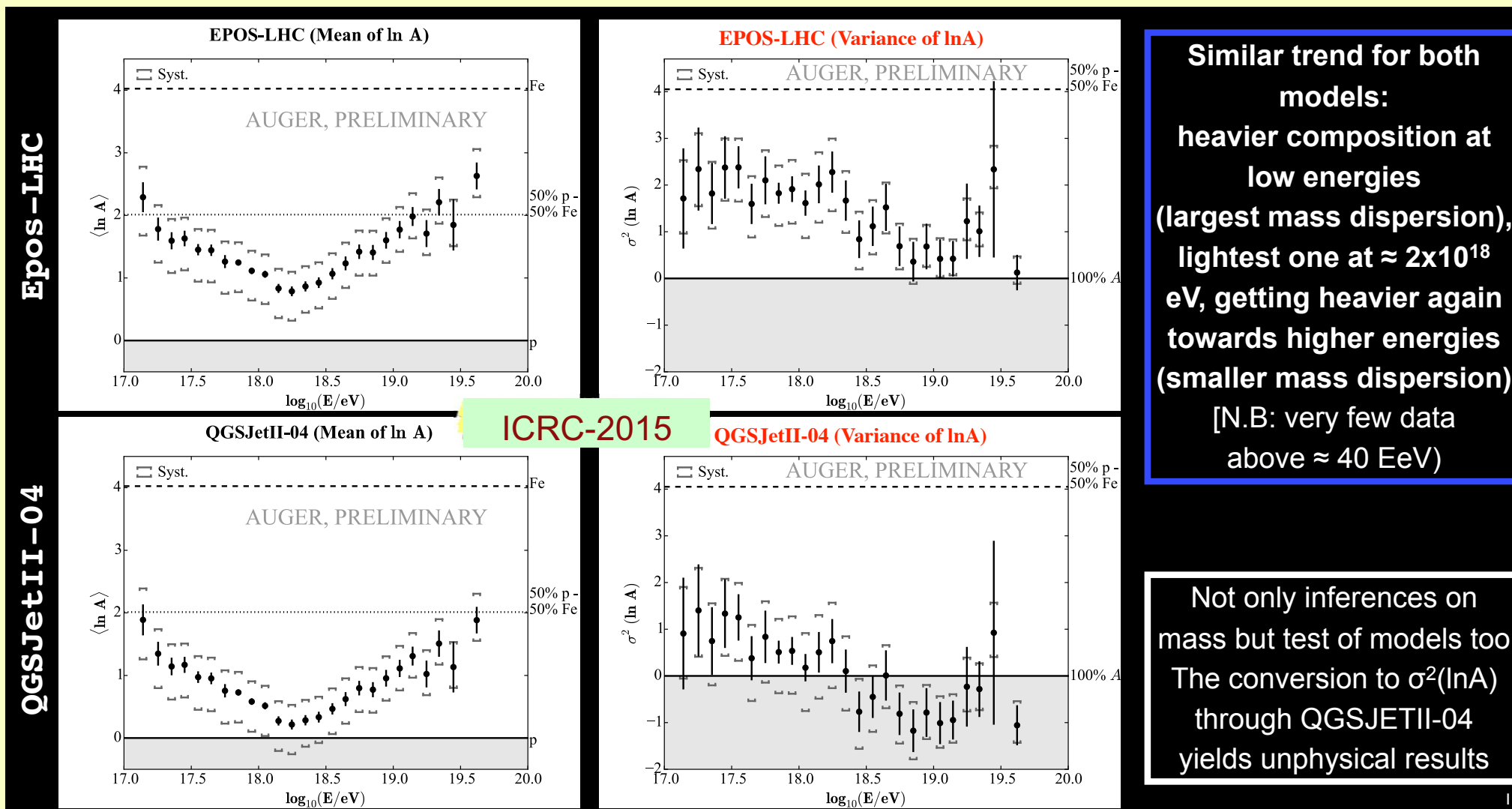
$\langle X_{\max} \rangle$ became lower with E_{CR}

X_{\max} distribution became narrower with E_{CR}

Increase of the mean mass with the energy ?? Inadequate interaction models for the simulation of the CR interaction and shower development in the atmosphere ?

Pierre Auger Observatory: the mass composition (3)

From the depth of shower maximum to primary mass ($\ln A$)

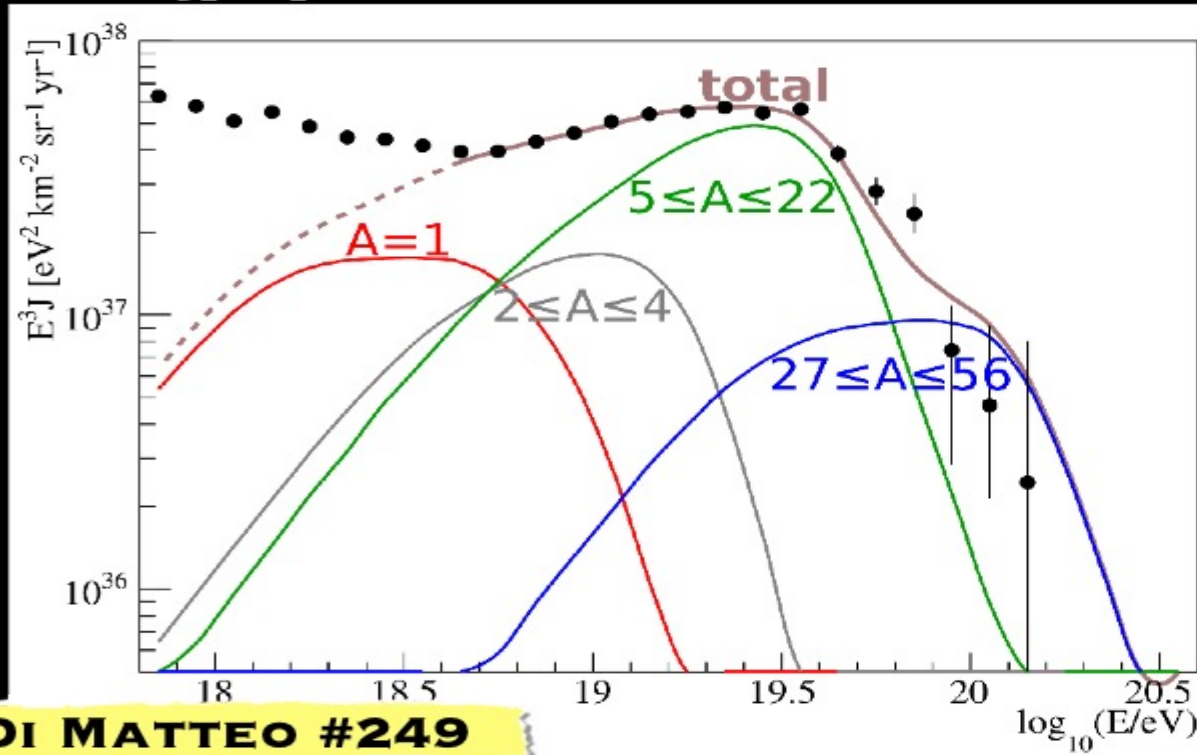


Pierre Auger Observatory: the mass composition (4)

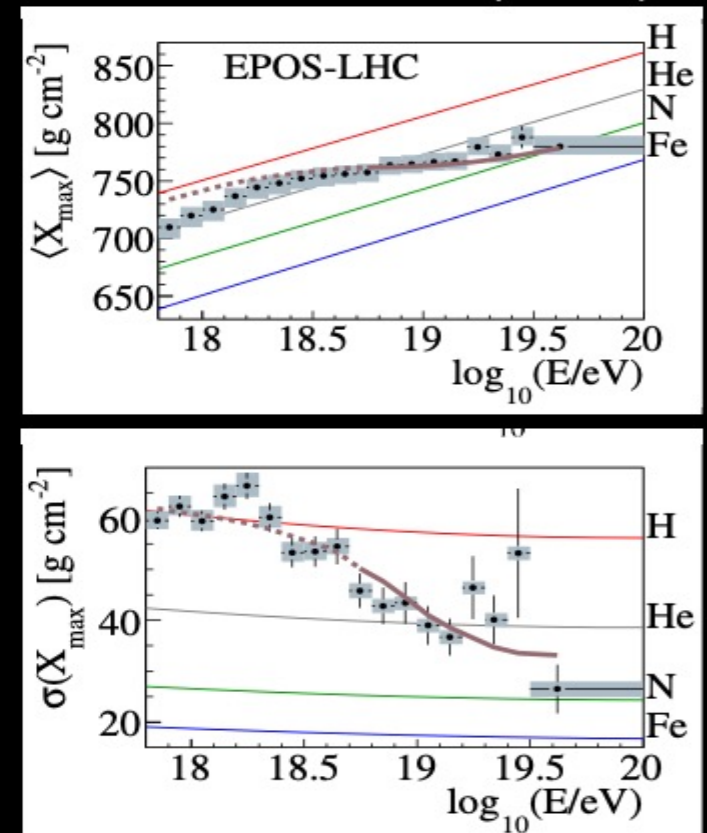
What do spectrum and composition data tell us?

(Simple) Model of UHECR to reproduce the Auger spectrum and X_{\max} distributions at the same time
Homogeneous distribution of identical sources accelerating p, He, N and Fe nuclei.

Energy spectrum and elements fractions



$\langle X_{\max} \rangle$ and $\sigma(X_{\max})$



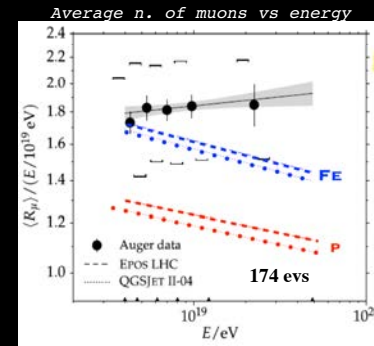
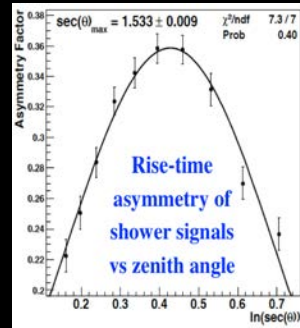
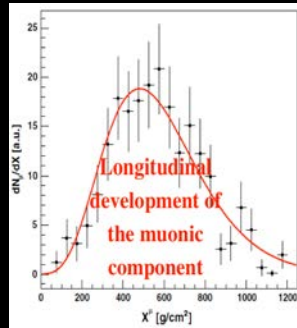
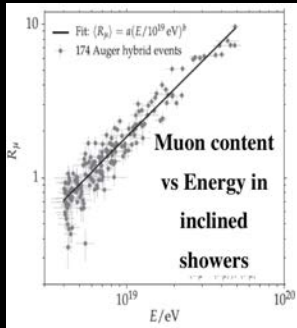
Pierre Auger Observatory: the muon content

2.2 "Shower properties measurements might impose constraints on hadronic interaction models at energies well beyond the reach of accelerator-based experiments..."

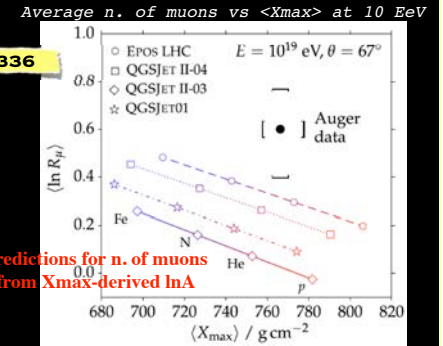
Testing hadronic models: the EAS muon content (FD and SD data)

Horizontal showers ($\theta > 60^\circ$) dominated by muons (em component largely absorbed)
 Estimation of the number of muons vs energy from horizontal showers observed by FD and SD

Shower properties (mass-sensitive) measured with the surface detector



High abundance of muons in data
 Systematic uncertainty inherited from energy scale



Predictions for n. of muons from Xmax-derived lnA

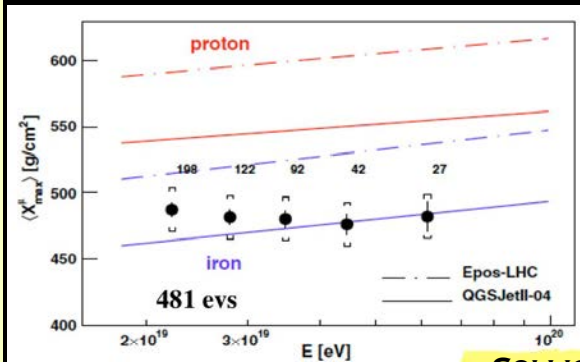
Tension between n. of muons and Xmax
 Deficit of muons in simulations between 30% and 80%

Testing hadronic models: the Muon Production Depth (SD data)

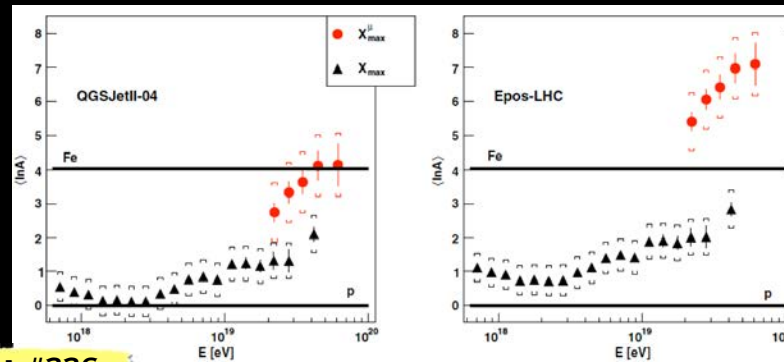
Horizontal showers ($\theta > 60^\circ$) dominated by muons (em component largely absorbed)
 Muon production depth can be reconstructed from the time structure of SD signals in horizontal EAS

ICRC-2015

Max of the MPD distributions vs E



Conversion of the max of the MPD distributions to lnA

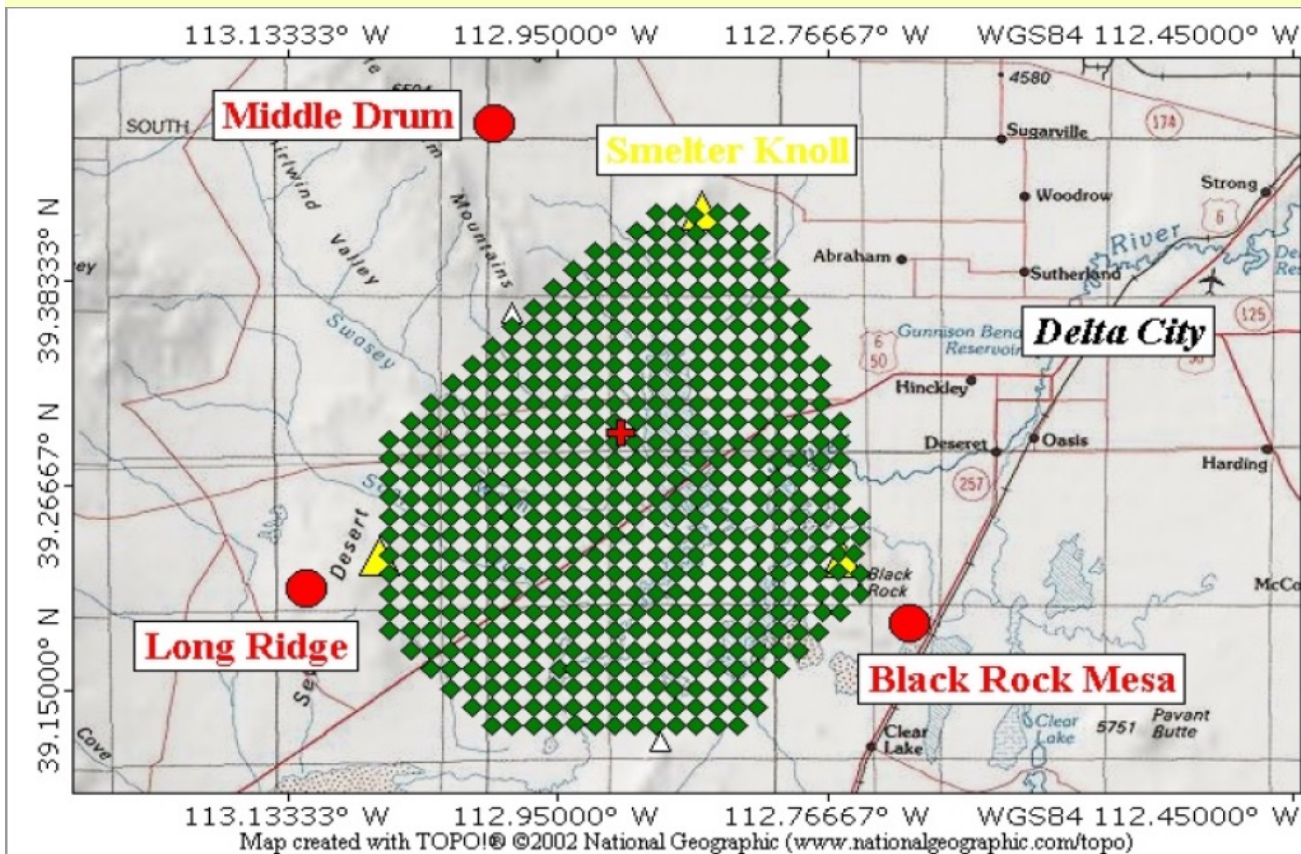


COLLICA #336

Evolution vs E for data flatter than pure p or Fe in both models
 Data bracketed by QGSJETII-04

Comparison with lnA from Xmax data:
 values compatible within 1.5 sigma for QGSJETII-04
 incompatible at > 6 sigma for Epos-LHC

A detector for UHECR in the Nord Hemisphere: the Telescope Array Hybrid Detector



- ▶ Deployed with the spacing ~ 1.2 km
- ▶ Powered by solar panels. Connected by radio.

- ▶ 507 scintillator detectors covering 680 km²
- ▶ 3 fluorescence sites, 38 telescopes
- ▶ Surface detector fully operational from March 2008
- ▶ SD relative size: TA $\sim 9 \times$ AGASA \sim PAO/4

The Telescope Array Fluorescence Detector

Refurbished
from HiRes

Observation
started Dec.
2007

Middle Drum

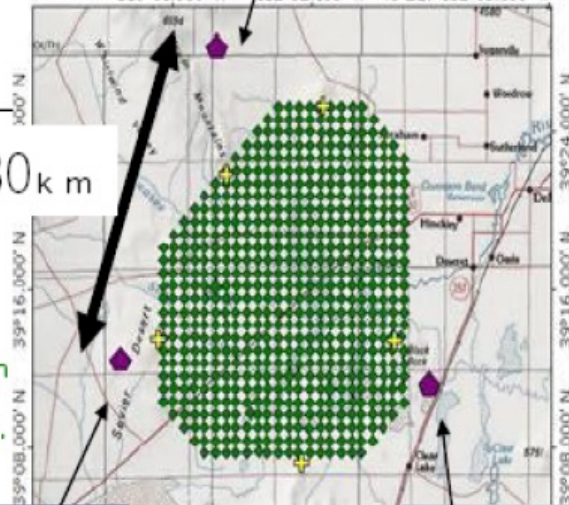


14 cameras/station
256 PMTs/camera



5.2 m²

TOPOI map printed on 07/12/04 from "StakeJun04-01.tpo" and "Untitled.tpg"



~30 k m

Observation
started Nov.
2007

Long Ridge



Black Rock Mesa



Observation
started Jun.
2007

New FDs

256 PMTs/camera
HAMAMATSU R9508
FOV~15x18deg
12 cameras/station

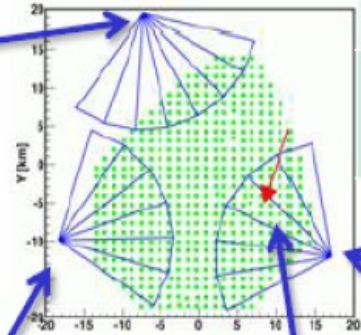
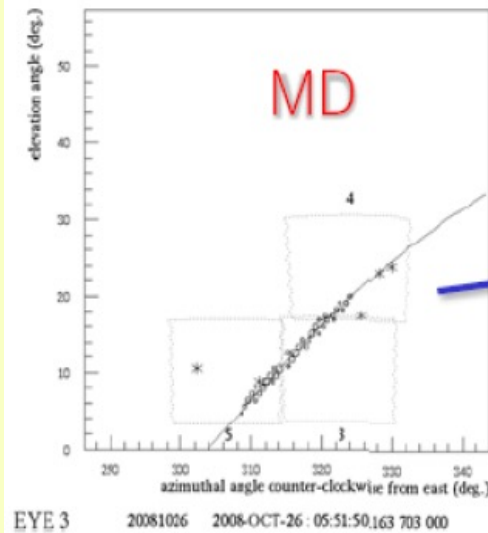


6.8 m²

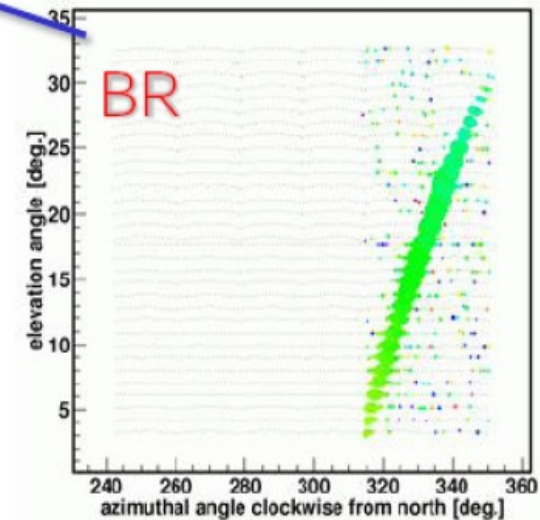
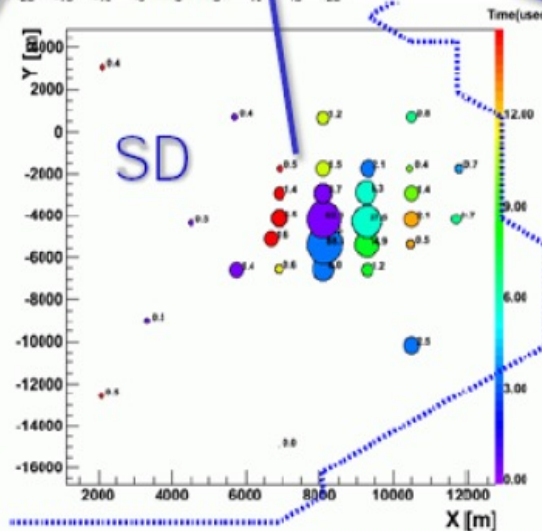
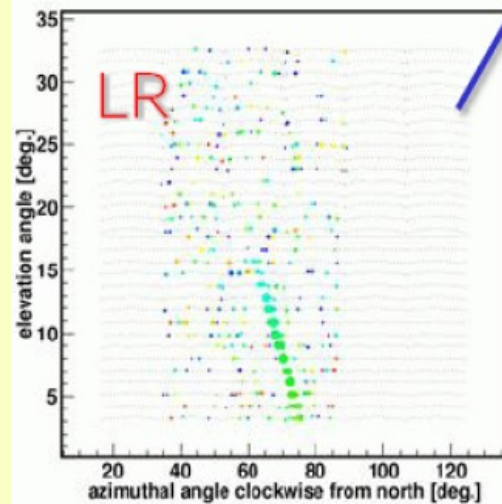
~1 m²

Telescope Array: an event in the Fluorescence Detector

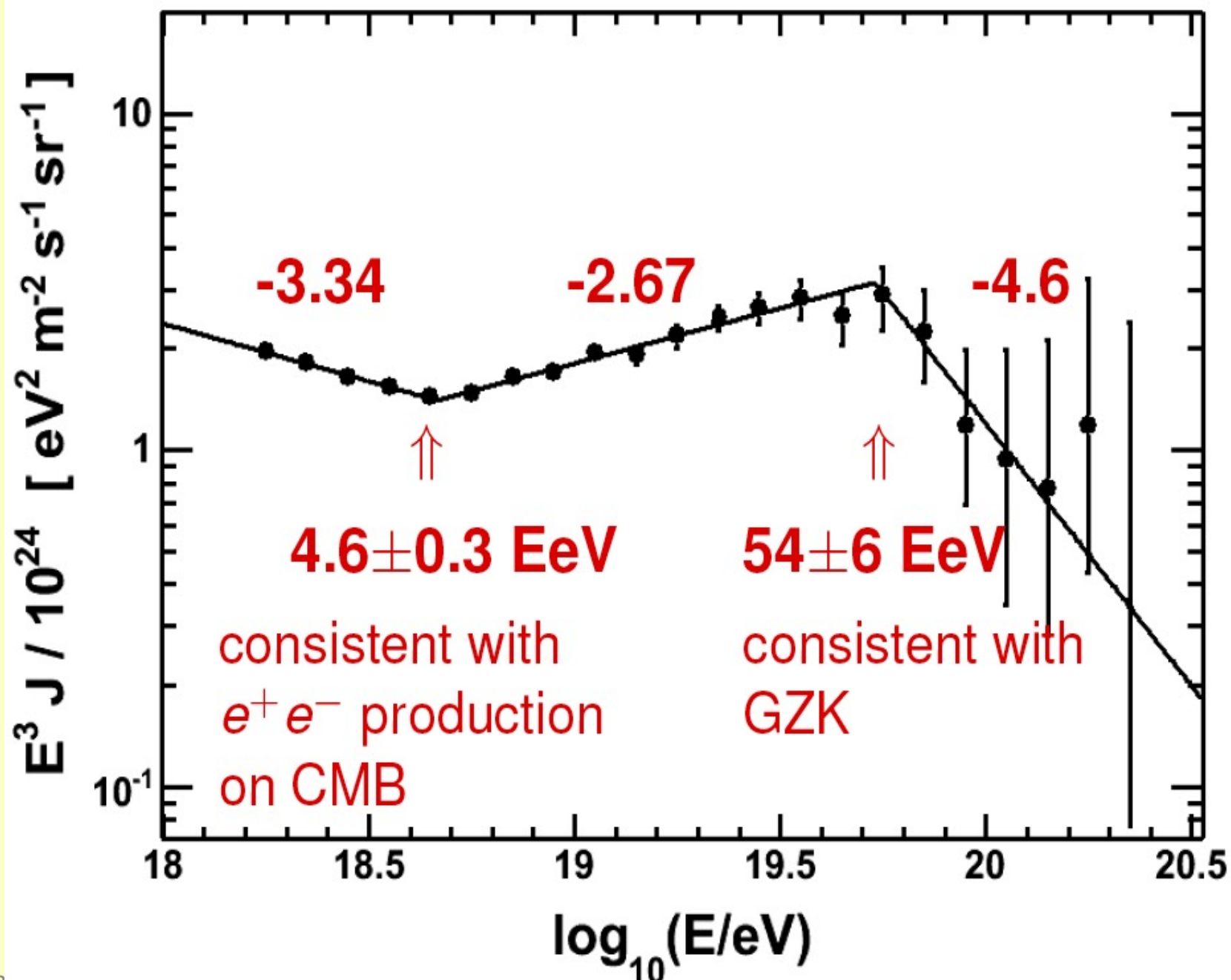
Triple FD Event (2008-10-26)



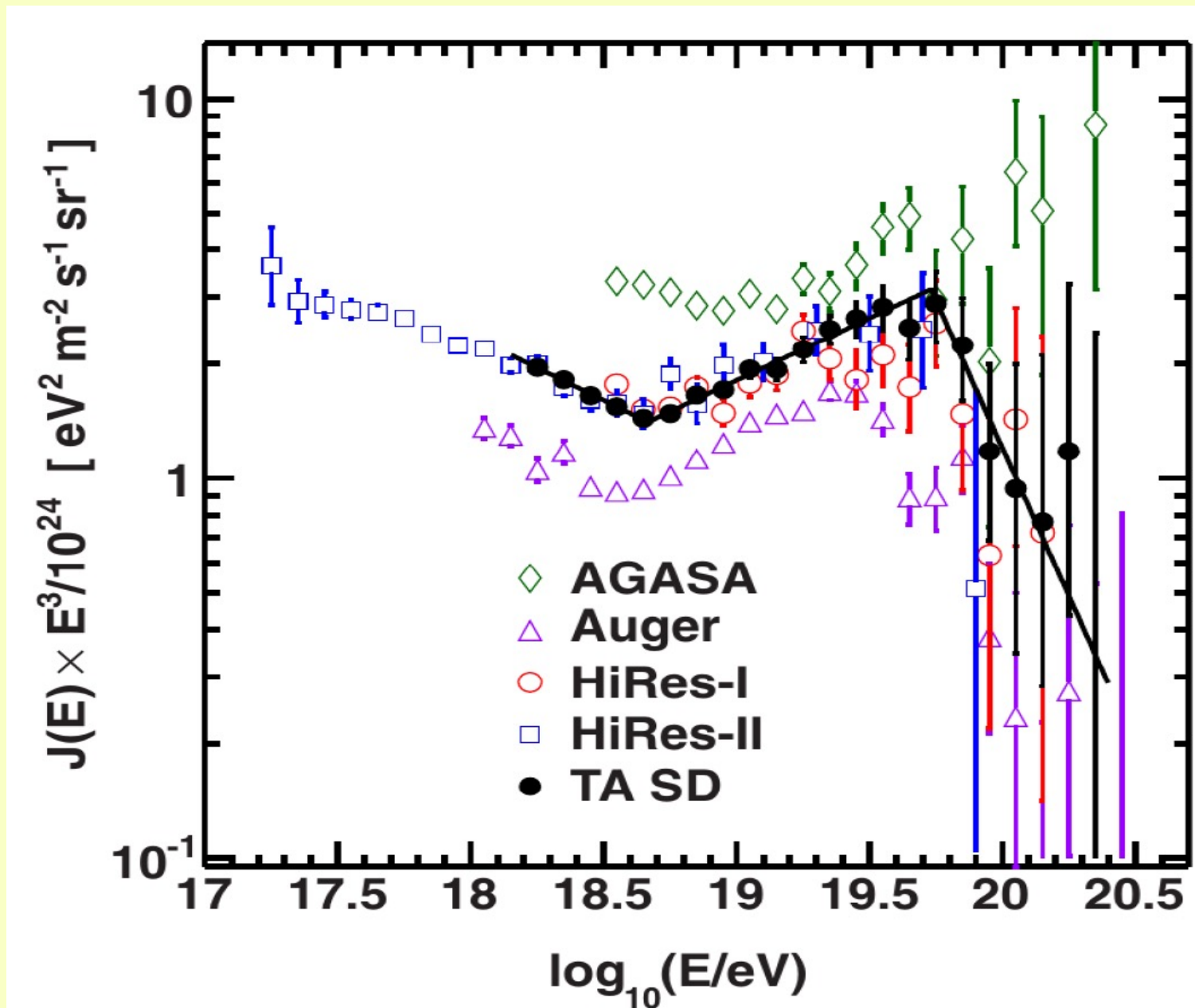
	θ [deg]	ϕ [deg]	X [km]	Y [km]
MD mono	51.43	73.76	7.83	-3.10
BR mono	51.50	77.09	7.67	-4.14
Stereo BR&LR	50.21	71.30	8.55	-4.88



Telescope Array: measurement of the UHECR spectrum - 1

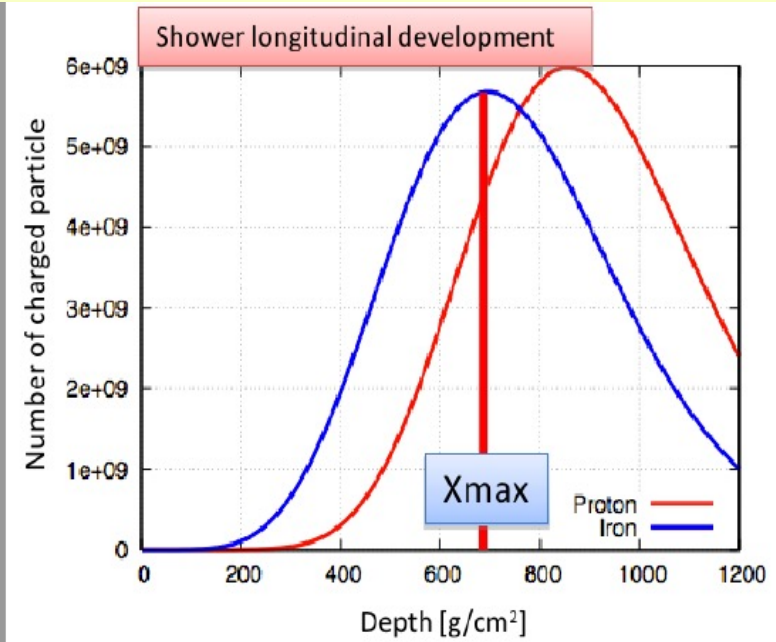


Telescope Array: measurement of the UHECR spectrum - 2

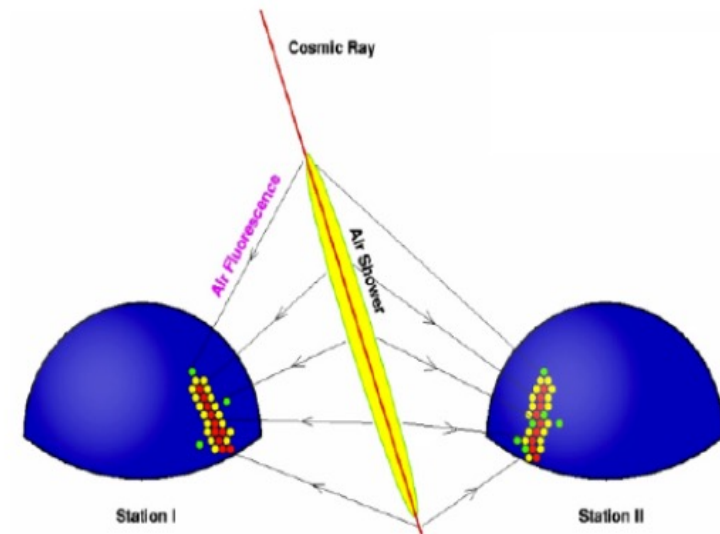


Telescope Array: measurement of the UHECR composition (1)

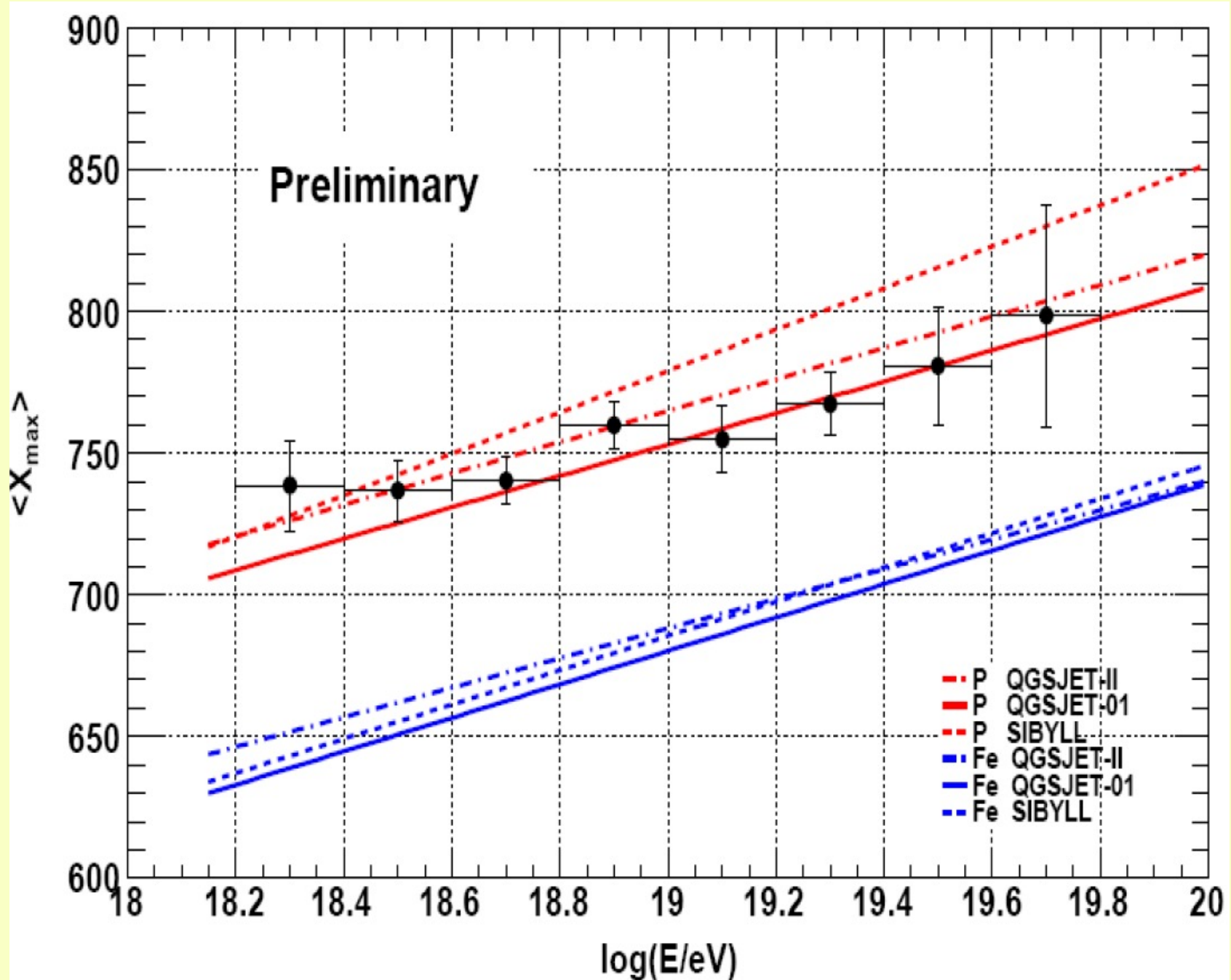
- ▶ Observable sensitive to composition: shower depth X_{\max}
⇒ FD data only
- ▶ Difficult measurement:
 - ▶ large fluctuations
 - ▶ limited statistics
 - ▶ biases in event selection
- ▶ TA strategy:
 - ▶ full MC simulation of the data analysis chain (including event selection)
 - ▶ prediction for different compositions
 - ▶ comparison to data



FD stereo analysis



Telescope Array: measurement of the UHECR composition (2)



Combined PAO and TA measurement of the UHECR spectra and composition – ICRC 2015 (1)

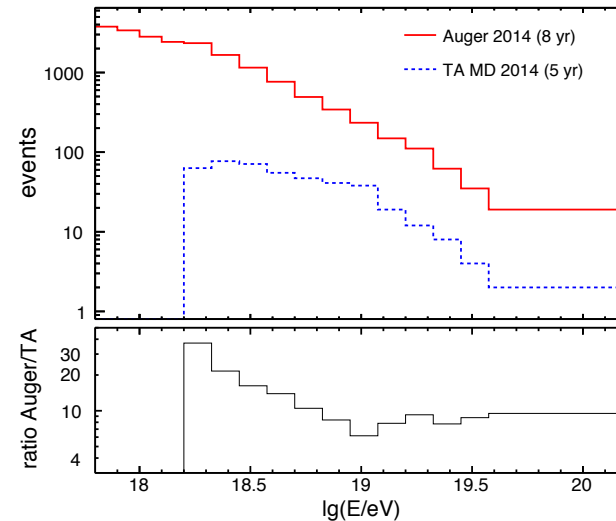
Data Samples

Auger:

- ▶ 8 years
- ▶ hybrid (at least one surface detector station)
- ▶ 24 telescopes
- ▶ 19,759 events above $10^{17.8}$ eV, 7365 events above $10^{18.2}$ eV
- ▶ PRD **90** (2014) 12, 122005

TA:

- ▶ 5 years
- ▶ hybrid (at least three surface detector station)
- ▶ Middle Drum telescopes (MD)
- ▶ 438 events above $10^{18.2}$ eV
- ▶ APP **64** (2014) 49



Telescope Array Collaboration, APP **64** (2014) 49:

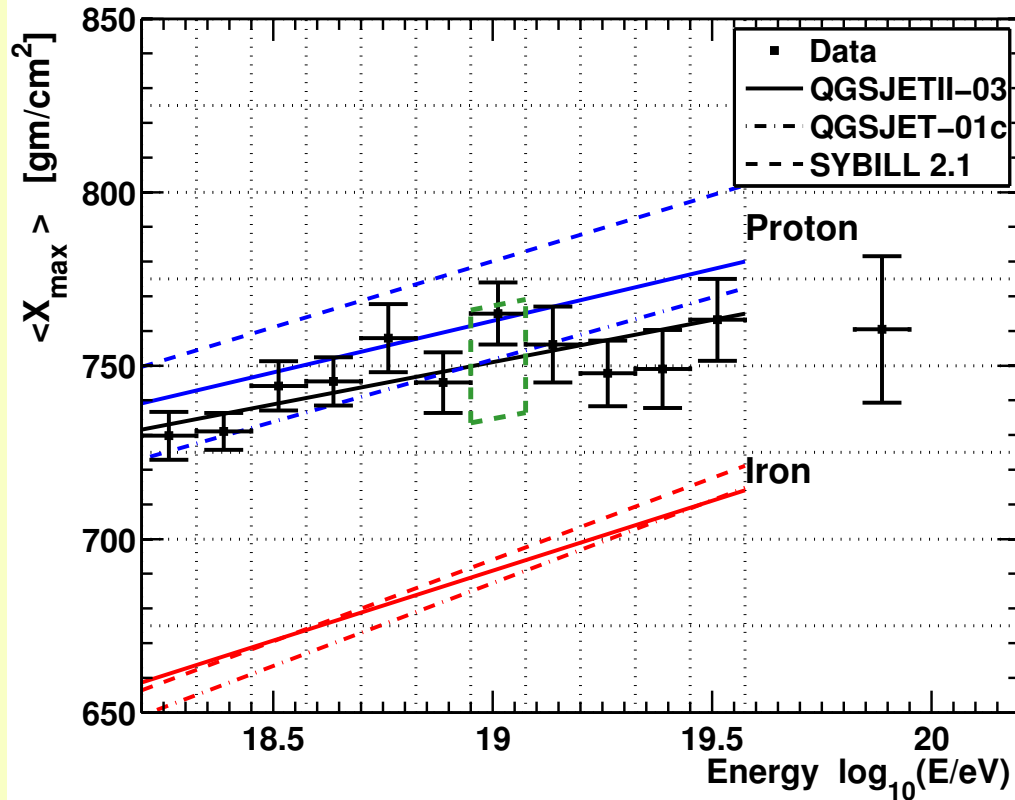
“[...] good agreement is evident between data and a light, largely protonic, composition when comparing the measurements to predictions obtained with the QGSJetII-03 and QGSJet-01c models.”

Pierre Auger Collaboration, PRD **90** (2014) 12, 122005:

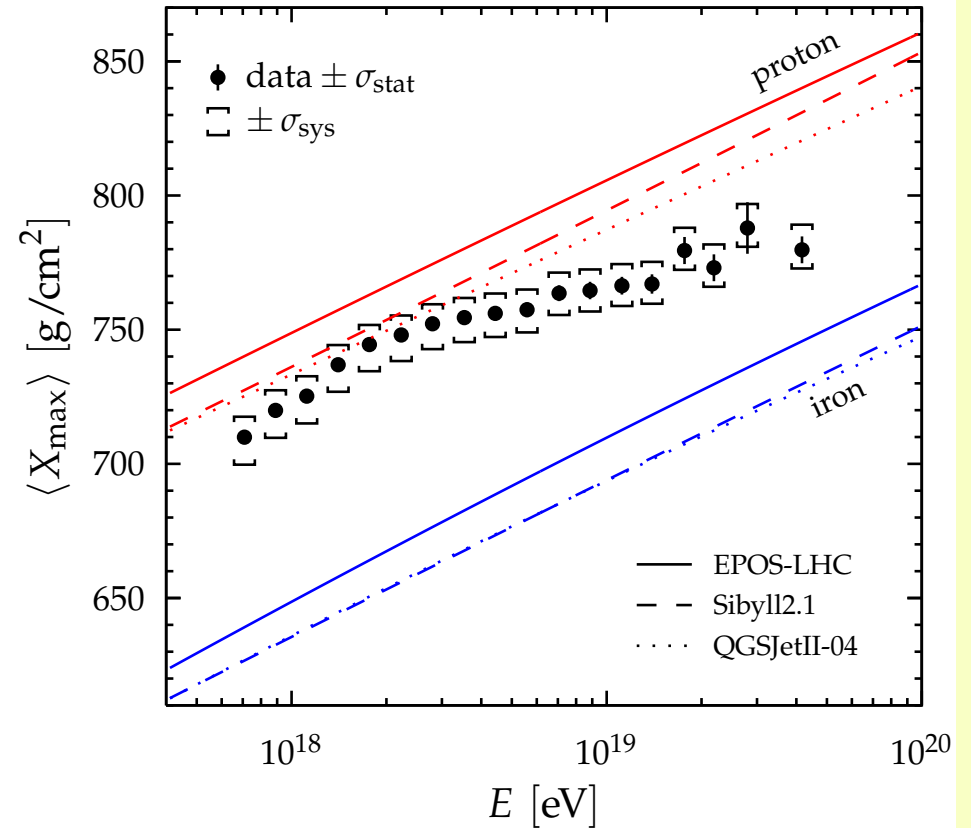
“[...] simulations have been performed using the three contemporary hadronic interaction models (QGSJETII-04, EPOS-LHC, SIBYLL2.1). [...] there is an evolution of the average composition of cosmic rays towards lighter nuclei up to energies of $10^{18.27}$ eV. Above this energy, the trend reverses and the composition becomes heavier.”

Combined PAO and TA measurement of the UHECR spectra and composition – ICRC 2015 (2)

Average Shower Maximum, $\langle X_{\max} \rangle$



Telescope Array Collaboration, APP **64** (2014) 49



Pierre Auger Collaboration, PRD **90** (2014) 12, 122005

Combined PAO and TA measurement of the UHECR spectra and composition – ICRC 2015 (3)

Different Analysis Strategies

Steven Saffi, University of Adelaide



Ben Stokes, University of Utah



Auger:

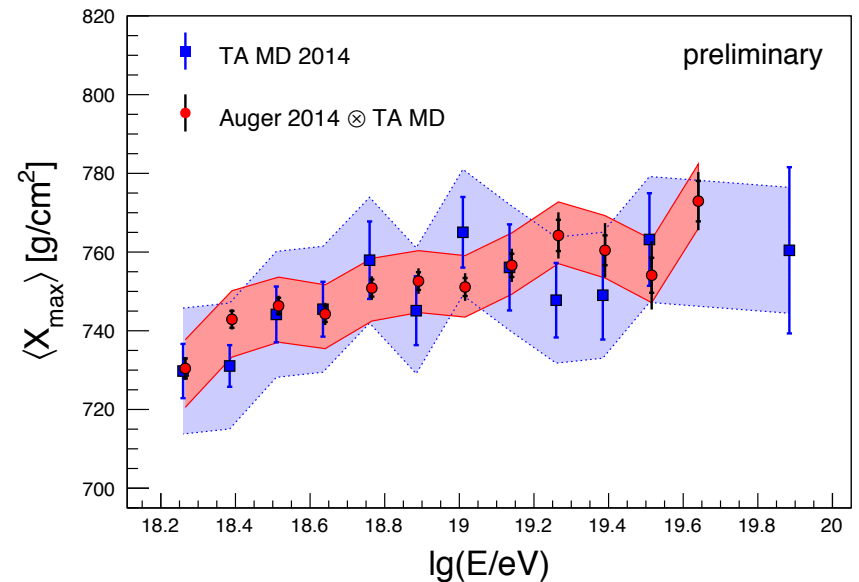
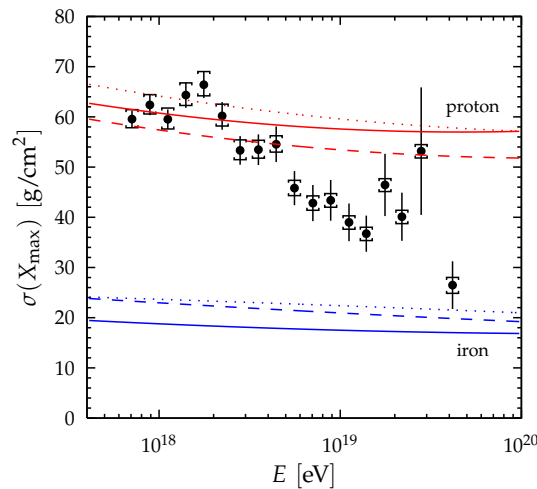
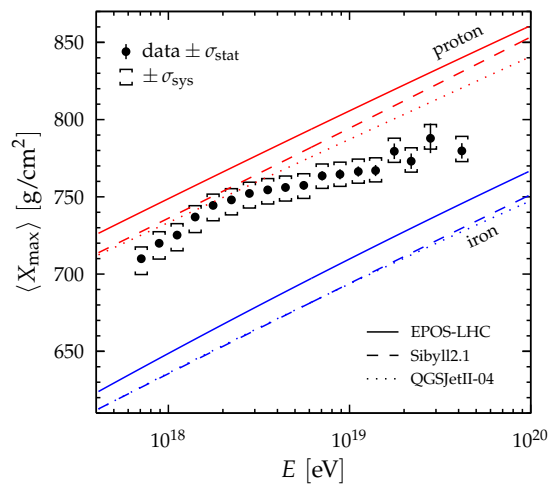
- ▶ minimize measurement bias
- ▶ result: “ $\langle X_{\max} \rangle$ in atmosphere”
- ▶ compare to: simulations at generator level

TA:

- ▶ maximize statistics
- ▶ result: “ $\langle X_{\max} \rangle$ in detector”
- ▶ compare to: simulations including detector effects

Result

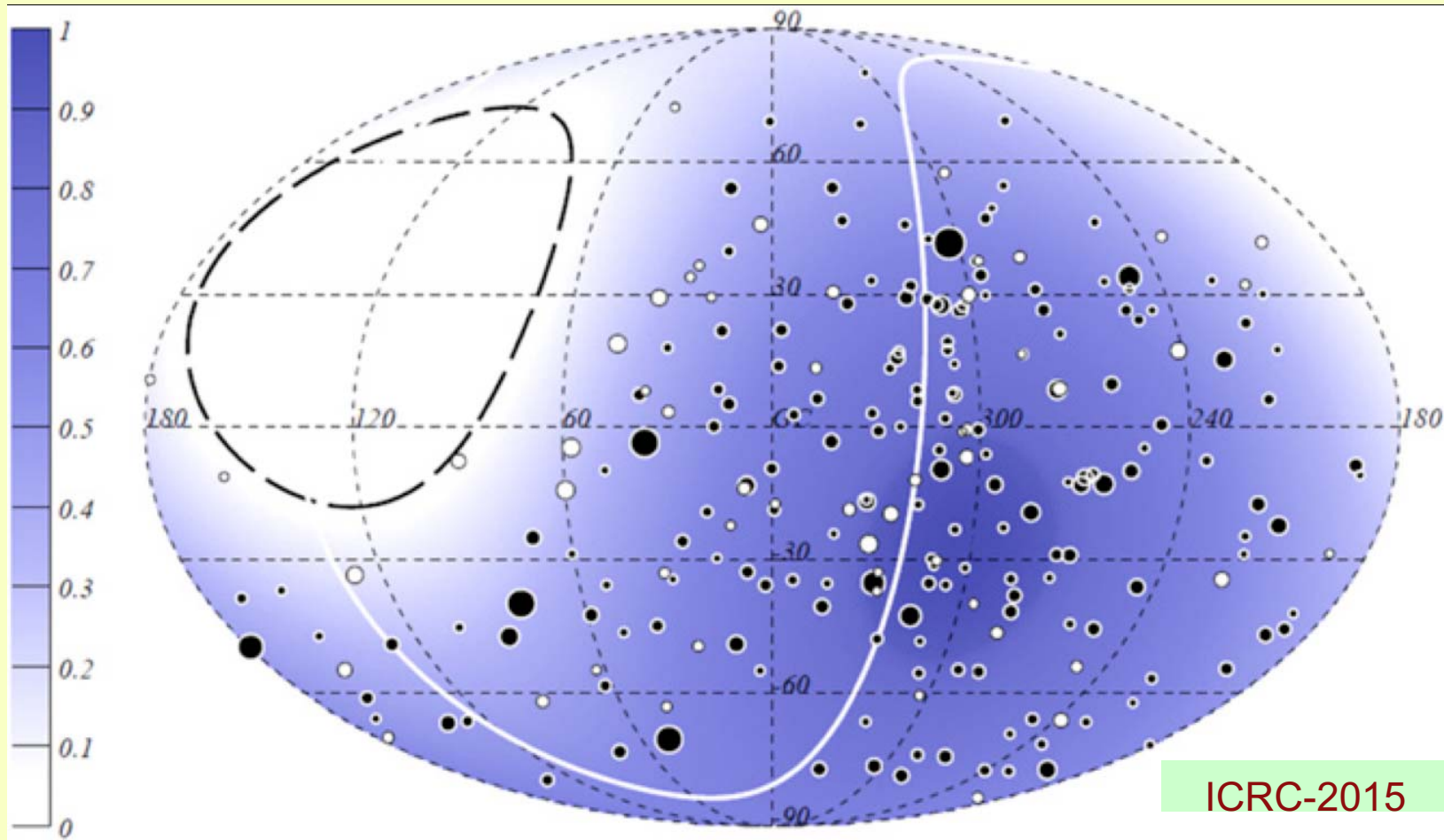
Mean and Standard Deviation of X_{\max} Distribution



average difference: $\langle \Delta \rangle = (2.9 \pm 2.7 \text{ (stat.)} \pm 18 \text{ (syst.)}) \text{ g/cm}^2$

Pierre Auger Observatory: the CR arrival direction

“...a systematic study of the **arrival directions**, that will indicate if there is anisotropy in the distribution and/or clusters which would indicate the existence of point sources...”



No room for anisotropy from these data !

THE END
... for the moment ...